



BINDING SERVICES
Tel +44 (0)29 2087 4949
Fax +44 (0)29 20371921
e-mail bindery@cardiff.ac.uk

CARDIFF UNIVERSITY



**ENERGY CONSCIOUS DESIGN IN ARCHITECTURE:
OPTIMISING THE RECEIPT OF SOLAR RADIATION
BY BUILDING SURFACES WITH THE AID OF
ENHANCED COMPUTER SIMULATION**

**A thesis submitted to the University of Wales, Cardiff
in fulfilment of the requirement for the degree of
Doctor of Philosophy**

BY

**Farzin Haghparast
(M.Arch)**

**Supervised By
Dr. Andrew Marsh**

Welsh School of Architecture

June 2006

UMI Number: U584056

All rights reserved

INFORMATION TO ALL USERS

The quality of this reproduction is dependent upon the quality of the copy submitted.

In the unlikely event that the author did not send a complete manuscript and there are missing pages, these will be noted. Also, if material had to be removed, a note will indicate the deletion.



UMI U584056

Published by ProQuest LLC 2013. Copyright in the Dissertation held by the Author.
Microform Edition © ProQuest LLC.

All rights reserved. This work is protected against
unauthorized copying under Title 17, United States Code.



ProQuest LLC
789 East Eisenhower Parkway
P.O. Box 1346
Ann Arbor, MI 48106-1346

DECLARATION

This work has not previously been accepted in substance for any degree and is not being concurrently submitted in candidature for any degree.

Signed F. Haghparast (Farzin Haghparast)

Date 28/06/2006

Statement 1

This thesis is the result of my own investigations, except where otherwise stated. Other sources are acknowledged by giving explicit references. A bibliography is attached in the thesis.

Signed F. Haghparast (Farzin Haghparast)

Date 28/06/2006

Statement 2

I hereby give consent for my thesis, if accepted, to be available for photocopying and for inter-library loan, and for the title and summary to be made available to outside organisations.

Signed F. Haghparast (Farzin Haghparast)

Date 28/06/2006

Abstract

With the increasing complexity of building design and performance evaluation, computational tools must be reconsidered to facilitate better solar design and application. The aim of this research is to demonstrate how reverse computation can play a significant role in building design. This approach has been used to explore a family of building design problems which deal with solar radiation falling on surfaces in obstructed situations and different locations. It was found that using the selected design tool (Ecotect), optimum solutions could be established for this family of problems based on reverse computation, starting with the performance requirements and leading to either a full range of tested solutions or simple optimum. The findings of this research are a first step in generating the form of buildings from climatic data and environmental performance constraints.

Acknowledgements

First of all I am extremely grateful to the Almighty. This work could not have been completed without the great support and sincere help from many people, to whom I am very grateful.

I would like to express my sincere appreciation to my supervisor, Dr Andrew Marsh, for his invaluable guidance, inspiration, enthusiasm and assistance throughout the course of this research. Also I would like to be thankful of him again for to his agreement and assistance to make parts this thesis able to be published as a guide book in the future.

I also would like to gratefully acknowledge Professor Phil Jones, Head of Welsh School of Architecture and joint PhD student supervisor for his support and guidance all the way through this study. I would like to express my deepest thanks to Dr. Judi Loach for great helps, valuable guidance, annually held school conferences and her non-stop spiritual support. I would like to send my thanks and appreciation to Mrs Sylvia Harris from whom I received much valuable help during entire four years of my study. I am also very thankful to Dr. Mike Fedeski for his great efforts and guidance to get the research done in the right way. I would like to be thankful of Mr. Dylan Dixon and Mr. Simon Lannon for their great helps and supports. My thanks also go to the staff of the Welsh School of Architecture, particularly to Ms Katrina Lewis and Ms Annie Pitchford. My gratitude also goes to Mr. Javad Banaei and Dr. Behzad Rafezi for their cooperation, friendship and valuable discussion.

I also would like to thank the Islamic Art University of Tabriz and the Iranian Ministry of Science, Research and Technology for sponsoring me throughout my postgraduate studies. I thank also the members of the Sahand University of Technology in Tabriz for their support and awarding this PhD scholarship.

My heartfelt gratitude goes to my parents, my sister and brother for their emotional support. My special gratitude also goes to my brother in law; Mr. Jalil Shoarinejad, who was the first interest me in Architecture. Finally, I truly wish to express my special appreciation to my dear wife, beloved son and daughter for their great love, unlimited sacrifice, continuous encouragement and endless help throughout this research.

DEDICATION

To my parents, wife and children

TABLE OF CONTENTS

Declaration.....	2
Abstract.....	3
Acknowledgments.....	4
Dedication.....	5
Table of Contents.....	6
List of Figures.....	14

CHAPTER ONE

1 Introduction	22
1.1 Overview	22
1.2 Problem Statement.....	23
1.2.1 Tightly Defined Design Problems	25
1.2.2 Reverse Computation	26
1.3 Significance of Research	27
1.4 Aim of Research	27
1.4.1 Research Objectives	27
1.5 Research Methodology	28
1.5.1 Literature Review	29
1.5.2 Using Advanced Computer Software	29

1.5.3	Developing Algorithms	30
1.5.4	Utilizing Existing Method	30
1.6	Thesis Structure	30
1.7	Summary.....	32

CHAPTER TWO

2	Literature Review	34
2.1	Introduction	34
2.2	Solar Radiation	35
2.2.1	Sun position	35
2.2.1.1	Image-Base Approach	36
2.2.2	Sky Distribution.....	37
2.2.3	Surface Incidence	38
2.2.4	Solar Collection and Optimization	38
2.2.5	Surface Mapping.....	40
2.3	Performance-Based Design	41
2.3.1	Shading System Design	43
2.4	Available Tools.....	44
2.4.1	Background.....	44
2.4.2	SEMPER.....	45
2.4.3	Ecotect	47

2.4.4	GenOpt and Optimisation Tools.....	48
2.4.5	RADIANCE.....	48
2.4.6	SUNTool.....	49
2.5	Tools Justification.....	50

CHAPTER THREE

3	Solar Radiation Measurement	52
3.1	Solar Radiation	52
3.2	Types of Solar Radiation	53
3.2.1	Visible Radiation	53
3.2.2	Invisible Radiation.....	53
3.2.3	The Term “Solar Radiation”	55
3.3	Direct and Diffuse Radiation.....	56
3.3.1	Solar Radiation and the Atmosphere	56
3.3.2	Direct and Diffuse Radiation.....	58
3.3.3	Daylight and Sunlight.....	58
3.4	The Basics of Solar Geometry.....	59
3.4.1	Solar Azimuth and Altitude`	59
3.4.2	Direct Angle of Incidence.....	60
3.4.3	Diffuse Angles of Incidence	62
3.5	Solar Radiation Values	63

3.5.1	Deriving Direct and Diffuse Values	64
3.5.2	Global Radiation.....	65
3.6	Sources of Solar Data	65
3.7	Sky Luminance Measurement	67

CHAPTER FOUR

4	Predicting Received Solar Radiation on Surface.....	71
4.1	Calculating surface Irradiance	71
4.2	Surface Mapping.....	71
4.3	Details of the Methodology	72
4.4	Instantaneous or Cumulative Skies.....	73
4.5	An Image-Based Approach	74
4.6	An Object-Based Approach.....	74
4.7	An Alternate Approach.....	75
4.8	Incident Radiation.....	75
4.9	Solar Radiation Values	75
4.9.1	Sky Subdivision.....	76
4.9.2	Implementation in Ecotect.....	78
4.9.3	Diffuse Incidence Effects	79
4.9.4	Sky Radiant Distribution	80
4.9.5	Relating Skylight and Radiation.....	81

4.10	The Cumulative Sky	81
------	--------------------------	----

CHAPTER FIVE

5	Shading Masks.....	84
5.1	Introduction	84
5.2	Partial Shading.....	86
5.3	Available Radiation Maps	88
5.4	Reflected Solar Radiation.....	89
5.5	Shading Mask Layers	92
5.6	The Application of Shading Masks	92
5.7	Sky Factors and Sky Components	92
5.7.1	Vertical Sky Component	93

CHAPTER SIX

6	Optimizing Solar Collector Angle.....	97
6.1	Introduction	97
6.2	Collector Efficiency.....	97
6.3	Overshadowing Effects.....	98
6.4	Solar Collector Optimization Techniques	98
6.4.1	Hemispheric Sampling	99
6.5	Solar Collector Optimization Using Shading Mask	100

6.5.1	Optimizing Collector Angle	102
6.5.2	Benefits	103
6.6	An Urban Example	104
6.6.1	The Extent of Variation	104
6.6.2	Potential Efficiencies	106
6.7	Seasonal Comparison	108

CHAPTER SEVEN

7	Irradiance Surface Mapping and Performance-Based Design.....	111
7.1	Introduction	111
7.1.1	Dynamic Effects	112
7.2	Variations in Spatial Solar Availability.....	114
7.3	Evaluating Shading Designs	114
7.4	Section Conclusion.....	116
7.5	Performance-Based Shading Design	117
7.6	Reversing the Calculation Process	118
7.7	Complex Shading Shapes	120
7.8	Further Extensions.....	122

CHAPTER EIGHT

8	Envelope Design in Consideration of Existing Recipient Surface; Reverse Computation	125
---	---	-----

8.1	Simulation and Generation	125
8.2	Simple Preliminary Applications.....	126
8.3	Insolation as a Loosely Defined Problem.....	126
8.3.1	An Analytical Solution	129
8.4	Right-To-Light: A Tightly Defined Problem	131
8.4.1	Daylight Availability	132
8.4.2	Generative Geometry.....	133
8.5	Discussion.....	134

CHAPTER NINE

9	Conclusion and Summary.....	137
9.1	Introduction	137
9.2	Summary.....	137
9.3	Major Contributions	139
9.3.1	Optimizing Angle of a Surface or a Solar Collector	139
9.3.2	Insolation Control Using Reverse Calculation.....	139
9.3.3	Design Influence on Existing Developments	139
9.3.4	Holistic design paradox	140
9.4	Further Steps.....	141

REFERENCES

10	References:	143
----	-------------------	-----

APENDICES

11	Appendices	152
11.1	Appendix A - Stadium Design.....	152
11.1.1	Introduction	152
11.1.2	Methodology, Optimisation and Geometry of stadium design.....	156
11.1.3	The Impact of Shading on Turf	160
11.1.4	Stadium Calculation Results.....	161
11.1.5	Findings	164
11.1.6	Detailed Optimisation of Roof Glazing.....	165
11.2	Appendix B– Papers’ Summary Presented in Conferences Based on the Thesis Investigation.....	168

LIST OF FIGURES

Figure 2-1: Procedure to determine the sun position for the sun and non uniform sky condition from the annually occurring sun positions in 15 minute time step. (Image source: Mardaljevic 2003)	36
Figure 2-2: Total annual irradiation mapping for San Francisco (Image source: Mardaljevic 2003).....	41
Figure 3-1 Spectrum of thermal radiation (Lang 2001)	52
Figure 3-2 The Sun's spectral flux.	53
Figure 3-3 The electromagnetic spectrum radiation from the Sun.....	54
Figure 3-4: Gas proportion of the atmosphere. (Generated in Microsoft Excel by author).....	57
Figure 3-5: The atmospheric influences on solar radiation. (Image source: square1 website).....	57
Figure 3-6: Different lights scattering based on their wavelengths.....	58
Figure 3-7: Solar Altitude and Azimuth.....	59
Figure 3-8: Computer generated Sun-path diagram for the 45° latitude of France (Image source: square one research 1998-2003)	60
Figure 3-9: The effect of incidence angle, illustrating the cos law. (Image source: http://www.sq1.com/)	60
Figure 3-10: The incidence angle is the 3-dimensional angle between the surface normal and the current Sun position. (Image source: http://www.sq1.com/).....	61
Figure 3-11: As the daily Sun-path changes with season, incidence angles increase on vertical windows in summer whilst reducing on a horizontal roof. (Image source: http://www.sq1.com/)	62

Figure 3-12: Different equipment used for solar radiation measurements. (Images taken from <http://www.eppleylab.com/PrdShadingDevices.htm>)..... 63

Figure 3-13: The difference between normal and cosine corrected pyranometers. (Image source: <http://www.squ1.com/>) 65

Figure 3-14: Sun path diagram for the cities of..... 66

Figure 3-15: Daily means of total solar radiation for Tehran and Tokyo (35.60° N). 67

Figure 3-16: Examples of variation in the luminance distribution over the sky dome under different sky conditions. (Image source: <http://www.squ1.com/>) 68

Figure 3-17: The three major CIE sky models. 69

Figure 4-1: An example of the work of John Mardaljevic, using Radiance to map irradiance levels over building surfaces. 72

Figure 4-2: Some examples of different approaches to sky subdivision. (Image source: <http://www.squ1.com/>)..... 77

Figure 4-3: 10° equal-angle subdivision showing bias in accuracy towards the zenith. (Image source: <http://www.squ1.com/>) 78

Figure 4-4: Different areas of the sky dome ‘visible’ to surfaces at various tilt angles together with a map of the effects of incidence angles..... 79

Figure 4-5: An example overcast sky distribution along with different incidence masks. (Image source: <http://www.squ1.com/>) 80

Figure4-6: An example annual averaged hourly direct solar gain cumulative sky distribution..... 82

Figure 5-1: Diagram showing shadow projects at different times of the day. (Image source: <http://www.squ1.com/>)..... 84

Figure5-2: Diagram showing site obstructions projected onto an imaginary hemisphere centred on the point of interest. (Image source: <http://www.squ1.com/>). 85

Figure 5-3: Two example shading masks for a shadowed point – on the left shading polygons for each obstructing surface are projected and drawn in the sun-path diagram whilst on the right the sky dome is divided into sky zones, each either shading or not shading. 85

Figure 5-4: A pseudo-random grid of points distributed over a test surface. 86

Figure 5-5: Examples images showing ray-tracing approach to the calculation of partial overshadowing using rays distributed randomly over each surface. 87

Figure 5-6: An example shading mask for a surface showing actual shading percentages for each sky segment. 88

Figure 5-7: The sequence required to generate a solar availability map for any surface and, from it, the total incident solar radiation. 88

Figure 5-8: The process of tracking the contribution of solar reflections in a shading mask. (Image source: <http://www.squ1.com/>) 89

Figure 5-9: Shading masks can accommodate any number of separate layers of information. The above examples show the effect of an additional reflected radiation layer on the solar availability map. 90

Figure 5-10: The relationship of the reflective surface to the analysis window. 91

Figure 5-11: The effect of a reflective surface is to add an extra fraction of solar radiation. This can be accommodated by simply adding the shading and reflection layers of the shading mask together. 91

Figure 5-12: The sequence required to generate a solar availability map for any surface. 91

Figure 5-13: The two component shading mask layers for an unobstructed Vertical Sky Component. (Image source: <http://www.squ1.com/>) 95

Figure 6-1: Half hemisphere with 351 facets. 99

Figure 6-2: Average daily direct solar incidence on a faceted dome – in this case calculated using Moscow weather data and location. 100

Figure 6-3: Comparison of solar availability mask with the insolation falling facets of a sphere.	101
Figure 6-4: A range of incidence angle effects for surfaces at various azimuth and altitude angles.	103
Figure 6-5: An example of a highly overshadowed urban development site.	104
Figure 6-6: The location of test points distributed over the central development site.	105
Figure 6-7: The distribution of solar radiation over the surfaces of each test sphere, relating to the location indicated by the number immediately beneath.	105
Figure 6-8: The distribution of incident solar radiation over a completely unobstructed sphere.	106
Figure 6-9: Analysis Dome Number (7) for Summer.	108
Figure 6-10: Analysis Dome Number (7) for Winter.	109
Figure 7-1: Examples of incident solar radiation (insolation) mapped over a range of different buildings and surface elements.	112
Figure 7-2: The differences in average daily solar radiation taken over the month of June (left) and December (right).	113
Figure 7-3: Average daily solar radiation levels over the three months of summer (left) or the three months of winter (right) – note the different value scales.	113
Figure 7-4: Examples of distributed insolation over areas of open urban space.	114
Figure 7-5: Using insolation as a measure of shading device performance.	115
Figure 7-6: The relative performance of different shading strategies.	116
Figure 7-7: The six basic sun tracks reduced to generate a simple shading device based on time and date constraints.	117

Figure 7-8: The process of projecting a simple window towards the sun at a particular time and onto a shading plane. 118

Figure 7-9: The changing location of the intersected polygon at different times of an example day..... 119

Figure 7-10: The image on the left shows a rectangular window projected onto a horizontal shading grid at set time intervals. The direct solar radiation at each time is then added to each shading cell. The centre image shows a single-day result whilst the image on the right shows the daily average taken over a whole year..... 119

Figure 7-11: An example of shading shapes based in this case on 75, 150 and 250 W/m² instantaneous solar gains on a window..... 120

Figure 7-12: An example of a shading potential calculation for a curvilinear shading surface in which the effect of external site obstructions are considered. 121

Figure 7-13: An example of a shading potential calculation in which the cumulative solar access of multiple windows is considered. 122

Figure 7-14: The optimum location of roof glazing panels can be quickly determined using projections of the playing surface onto the roof area over the three months of winter. 123

Figure 7-15: The optimum location of roof glazing panels can be quickly determined using projections of the playing surface onto the roof area over Winter. 123

Figure 8-1: Stadium model showing the distribution of solar radiation over the playing surface with an unglazed roof..... 127

Figure 8-2: If incident solar radiation is the only criteria, then the entire roof glazed is the ‘optimum’ solution. 128

Figure 8-3: For the same capital and maintenance cost ratios, the left image shows the result when considered over 10 years and the right image over 50 years. 128

Figure 8-4: The optimum location of roof glazing panels can be quickly determined using projections of the playing surface onto the roof area over Winter. 129

Figure 8-5: The optimum location of roof glazing panels can be quickly determined using projections of the playing surface onto the roof area over Winter.	130
Figure 8-6: Swansea (Morfa) stadium built based on the reverse computation technique introduced by the author.	130
Figure 8-7: Example urban site showing existing site and the windows in surrounding facades whose right-to-light must not be adversely impacted.....	132
Figure 8-8: An example shading mask calculated for an east-facing window in the site, showing the resulting VSC in the bottom-right corner.	133
Figure 8-9: The site was divided into grid segments whose height could be independently incremented or decremented.	133
Figure 8-10: The resulting maximally compliant development envelope on the given site.....	134
Figure 11-1: The Geometric Model Used for the Solar Analysis.....	153
Figure11-2: Alternate Configurations Used to Examine Effects of Glazing Area on Pitch Insolation.....	154
Figure11-3: The two extreme ratios within the EQUAL Configuration.	154
Figure 11-4: The two extreme ratios within the BIASED Configuration	155
Figure 11-5: Overshadow masks generated from the centre of the southern 'D'.....	156
Figure 11-6 21st November daily direct and diffuse radiation for Wales	157
Figure 11-7 21st December daily direct and diffuse radiation for Wales	158
Figure 11-8 21st January daily direct and diffuse radiation for Wales	158
Figure 11-9 21st February daily direct and diffuse radiation for Wales	159
Figure 11-10 21st March daily direct and diffuse radiation for Wales	159

Figure 11-11: The Distribution of Annual Average Incident Solar Radiation over the Playing Surface..... 162

Figure 11-12: The relationship between roof glazing ratio and par for each configuration, both annually and over winter..... 163

Figure 11-13: The relationship between roof glazing ratio and incident solar radiation for each configuration, both annually and over winter..... 163

Figure 11-14: Stadium model showing the distribution of solar radiation over the playing surface with an unglazed roof..... 165

Figure 11-15: If incident solar radiation is the only criteria, then the entire roof glazed is the 'optimum' solution..... 166

Figure 11-16: For the same capital and maintenance cost ratios, the top image shows the result when considered over 10 years and the bottom image over 50 years..... 167

CHAPTER ONE
INTRODUCTION

1 Introduction

1.1 Overview

When architecture is created, the inter-relationship between the fabric of the design and its surrounding external space is often not well considered due to the focus on individual building design. Basically, the proportions of buildings have a significant influence on their effectiveness as components in the dynamic urban environment. In modern cities this interaction between buildings and the urban space is a defining characteristic of the urban environment due to the increasing volume occupied by the buildings. For instance, high rise glazed buildings can easily be seen in big cities more often than before, and usually they have little regard for environmental effects and the impact due to their high energy demands. Thus urban form, in particular for vertical growth, has become the concern of this thesis - to look at possible problems that may be invisible to many designers.

The urban environment's characteristic feature is the large variation in solar access over small spatial scales. An apartment or an office may receive bright daylight, whilst a few storeys below may be in complete shade. A walking pedestrian in a city centre may likely experience both good and bad daylight areas during the shortest of walks. Domestic or non domestic buildings, when the main windows see little sky, may be considered gloomy and dull (Mardaljevic 2005).

In other locations, solar radiation provides a tremendous amount of unwanted radiation and the resulting heat must be protected against. Buildings need to be protected from heat using a large amount of energy with artificial air conditioning systems to cool down the spaces. For example in a class room in Saudi Arabia, pupils often have to block the view of the window using opaque curtains to protect from unbearable glare (Abanomi 2005). As a result, a huge amount of energy is wasted and air pollution is sharply increased. A large amount of energy can be saved in the early stages of the design process by using an increased awareness of environmental design principles (Givoni 1994; Perry and McClintock 1997; Salmon 1999).

From the above inference, the concern in this work is solar radiation received at a surface. The common theme is how to design to control solar radiation received by

building surfaces. This may seem to be a simple task to follow, but the author has seen great potential within this point.

Consideration of overshadowing in urban blocks is not a new issue. However controlling, predicting and simulating the prevailing daylight/sunlight condition in urban blocks as a dynamic parameter is capable of novel scholarship.

1.2 Problem Statement

During the rapid economic growth around the globe in the recent decades, the fossil fuel crises and pollution problems underline the significance of using freely available solar energy.

However, putting this freely available solar energy to use has its problems for building designers. These problems are of two kinds. The first concerns the timely and appropriate collection of solar radiation at the surfaces of buildings, and the second the way that buildings utilise the solar energy they have collected. This thesis is concerned only with the former.

The amount of solar radiation received at building surfaces is affected by the obstruction caused by other building volumes in the urban environment, as discussed above. It is also affected by shades and openings placed by designers to control the arrival of radiation at building surfaces, particularly at windows. And it is affected by the inclination and orientation of the collecting surfaces themselves. These issues are not independent. The appropriate orientation for a surface, for example, is affected by the obstruction of surrounding buildings. In controlling the radiation reaching building surfaces so that they receive the amount that they require for optimum environmental performance, designers face a complex problem. In order to achieve a satisfactory solution, they require the assistance of computer simulation.

The thesis is not concerned with what lies behind the surface. Once received, the radiation will be in part reflected back to the urban environment, absorbed by the material behind the surface, or transmitted into the building. The proportions following each route depend on the properties of the building materials, and this matter will be relegated to the class of problems concerning the utilisation of solar energy which are not being considered.

The thesis nevertheless needs to differentiate between different building elements receiving the radiation. Consideration of the quantity of radiation reaching a building surface is most commonly given to windows or other openings in the building envelope. But other surfaces of special interest are, for example, solar collectors and surfaces intended for plant growth.

This makes it clear that the thesis has to consider the purpose for which the radiation is intended or the effect the radiation might have on the environment within the building. Some surfaces require maximum radiation, some minimum, others an optimum between. If the consideration is for the thermal environment, then the requirement will depend on the climate. In hot seasons the intention might be to limit the amount of radiation received by surfaces. In cold seasons it might be to allow as much as possible to reach the surfaces. On the other hand, the radiation might be intended to light the interior of the buildings rather than to warm them. In this thesis, the term “solar radiation” includes both solar heat and light, with each defining a specific set of design problems; more is said about definitions of types of solar radiation in Chapter Three.

A choice has been made from the many possible design problems that could be considered. The reason for the choice is to illustrate a wide range of problems, and to discuss the manner in which computer simulation can be employed in their solution. The principal theme of the research has been to consider how computer simulation can best aid designers in solving problems of this kind.

This range of design problems that will be considered begins with the surface itself. As just explained, the material properties of the surface are not part of this research. But the angle that the incident radiation makes with respect to the surface makes a very great difference to the amount received. So the surface itself makes a huge difference to the effect of solar radiation for a given condition. This raises the question ‘what is the optimum inclination of a surface?’

Another design problem may be a surface that is needed to be in shade - for example in the summer time. To design the desirable shade over surface for a given period, the optimum form of obstacle(s) needs to be designed. In a practical sense, the design process is not only for a single window, but usually for many windows such as in an

office or a residential building. Thus, shading device design is an essential design consideration at all stages of the design process. This question may then rise ‘what is the minimal area of shade that will do this?’

Another problem can occur while designing a new block in a region affecting the light received by windows in the surrounding existing surfaces. It can be a very complex task to measure and evaluate how much influence the new project may have on surrounding buildings. The project being designed is the new block, not the surrounding buildings whose windows are at risk. Nevertheless, the designer is responsible for conserving the amount of light received by the surrounding windows, so the problem is of a kind analogous to the previous two: “what is the maximum volume that can be designed whilst conserving this light?”

All the above can be recognised as a family of problems to investigate solar building design as controlling solar incidence over surfaces. All deal with building surfaces - as solar collectors, as windows to be shaded and as windows whose daylight is to be conserved.

1.2.1 Tightly Defined Design Problems

In this research, a problem is described as *tightly defined* if all its dependant parameters can be fully quantified and there are clear and quantifiable criteria against which possible solutions can be tested. Whilst a simple pass/fail test is the most efficient to apply, a problem can still be tightly defined if there are clear boundaries between which the criteria must fall.

Therefore, a *loosely defined* problem has parameters whose values cannot be unequivocally calculated or range-bounded. They may be quantifiable, but the criterion for selecting any particular value is essentially arbitrary. Thus, even if there are quantifiable criteria against which possible solutions can be tested, the validity or applicability of the basis on which the solution was generated will always be questionable. This uncertainty can limit the usefulness and impact of the information such solutions provide the designer as the extent to which the results depend on the specific values chosen for the input data is usually unclear.

This is an important distinction in this work as the time taken to define and generate solutions for each type of problem is the same, if not longer for loosely defined problems. However, the solution to a tightly defined problem has greater potential to provide meaningful information and real design insight as it can result in a tightly defined solution. (Haghparast 2004).

1.2.2 Reverse Computation

Let us refer to the criteria against which the possible solutions can be tested as performance requirements. In the problems considered above, whether they are tightly or loosely defined, the designer wishes to move from the requirements to the solution. In using computer simulation, the difficulty that faces the designer is generally that the computer program moves in the opposite direction – it needs a proposed solution before it can evaluate whether the requirements have been met.

This thesis presents a set of computerised procedures for solving problems which start with the performance requirements and then guide the designer to a solution. In one case, the computerised procedure generates a solution to the problem. This is a tightly defined problem, and also a very specific problem beyond which such a procedure cannot be readily extended. In the other cases, the procedure does not generate a tightly defined solution, but rather investigates a range of solutions from which the optimum can be selected.

Procedures of this kind will be referred to in this thesis as “reverse computations”.

The three problems in the family discussed above can be succinctly summarised as follows, to bring out the requirements with which the reverse computation is to begin and the problem to be solved:

- 1) requirement: to collect the maximum amount of solar radiation on a surface in a given period: design problem: the optimum inclination of the surface;
- 2) requirement: for a window to be shaded for a given period: design problem: the minimal area of shade that will do this;
- 3) requirement: to conserve a percentage of daylight received by a window; design problem: the maximum envelope for any obstructions that allow this.

1.3 Significance of Research

This research is about designing to control the solar radiation received by the building envelope, as pointed out in the previous section. This control can not be applied unless current computer software application allows the real complexities of urban situations to be taken into account instead of designing for simple conditions. A real urban condition can be very complex and dynamic by shading in a particular period of time rather than designing for idealised unobstructed situations. In such complex situations, it may be possible to use software to actually suggest design solutions.

1.4 Aim of Research

The main aim of this research is to allow designers to apply reverse computation to normal design cycle in relation to solving problems for buildings. This may be possible by making an evolutionary or iterative process from many possible answers to the requirements. If design problems can be clearly defined, then solutions are straight forward by setting appropriate algorithms and testing for the right solutions. The family of problems introduced in section 1.2 can be examples of such complex design problems. To deal with these, current computer analysis software is needed for evaluation in advance. In order to achieve the aim the setting objectives must be considered.

1.4.1 Research Objectives

Consequently, for the purposes of achieving the aim of this research, a number of objectives were derived as follows:

- To develop improved methods of solving selected design problems falling into a general class in which solar radiation reaching a surface is to be optimised.
- To configure these methods so that the computation suggests solutions to the design problem, adapting the software as necessary to achieve this.
- For these methods to take into account any complex obstructions to the flow of radiation whose profile can be modelled, in terms of both blocked and reflected radiation.

- To examine a family of three cases of problem, as described above, in which the object to be designed is removed successively further from the surface whose requirements for solar radiation are to be satisfied.

The novelty of the research rests in the second and third of these four objectives.

The family of problem cases is restated below.

- 1- To evaluate solar collector angle and orientation. That is, to collect the maximum amount of solar radiation on a surface in a given period, there is a way of finding the optimum angle and orientation of the collector.
- 2- To deal with a surface designed to protect another surface, the surface or window must be in shade for a given period, so the possible problematic issue would be determining the minimum area of shade that provides the best protection for desired period of time.
- 3- To focus on existing buildings adjacent to the development site, which is termed as right-to-light in the UK. In other words, it is about the influence of the new design concept on preserving the percentage of daylight/irradiation received by existing windows. With these criteria, the design problem is determining the maximum envelope for any obstructions that allow this percent daylight/irradiation for existing window(s).

These three objectives are common in their need for developed techniques that include a detailed consideration of solar radiation in the early design process. The reverse computation approach would need comprehensive advanced computer software to figure out this required technique. This technique will be elaborated in the research methodology section below.

1.5 Research Methodology

1. *To review the literature dealing with the analysis and prediction of incident solar radiation on building surfaces. This review will be broad-based, but the aim is to catalog techniques used by researchers and/or practitioners for the prediction/measurement of: solar radiation values; solar incidence on*

surfaces; the effect of overshadowing and obstructions; the optimization of solar collector angles; and daylight availability and rights-to-light.

- 2. From the literature review, the cataloged techniques are assessed for their applicability to the family of problems outlined above. These will include adapting the capabilities of each tool to analyse the metrics at the core of each problem and strategies by which they could be used interactively.*
- 3. Where necessary, the techniques have been, modified or enhanced to facilitate solving this family of problems – to allow their use in reversing the design process and suggesting potential solutions. This may require the development of new techniques, scripts or plug-in modules for the tools found.*
- 4. The resulting techniques/tools have been applied to (set) of problems/ examples in which potential solutions are suggested presented in detail. The advantages/disadvantages of the various techniques will be discussed.*

What will be covered in detail are four methods which have been applied to approach the investigation of the research problem. These are also categorized as: literature review; advanced computer software calculation and simulation; developing algorithm for applying in the software; and utilizing some existing methods.

1.5.1 Literature Review

The literature has been reviewed to establish the theoretical foundation of the research related to conceptual building design and evaluation, optimizing angle and orientation of solar collectors, intelligent shading device design, and the use of solar radiation in design process sky illuminance, solar radiation data, overshadowing /shading, right to light /daylight analysis, Radiance, solar access, performance based reasoning and techniques for alternative design solutions. Having read and judged all those related categories in literature, the outcome assists the build up of the research body.

1.5.2 Using Advanced Computer Software

For the past two decades, the fast growth on information technology and evolving awareness of building constraints stimulated a stream of intelligent technology

development, and raised suddenly the demand for intelligent building. However the gap between building designers and computer applications was not very handy technique particularly in performance building design rather than drawing and tracing a layout. Thus, this research has attempted to use the most advanced computer software in conceptual building design not only for simulation and calculation but also for utilizing it for some new approaches.

1.5.3 Developing Algorithms

Two different algorithms have been developed by author to implicate toward the aim. These algorithms could manage the process of design to write some scripts that computer software can run and act over some models understanding and evaluating the performance of design concept whether requirements have been met. For instance, design alternatives need to be evaluated and go to out put point or go back to design cycle after some amendments this algorithms used to put the concept onto the cycle.

1.5.4 Utilizing Existing Method

Mapping solar radiation over surfaces has not a very long history as the author's supervisor has developed the software to map solar radiation over any surface to interactively visualize the amount of solar energy falling on surface to take advantage and reverse this process from solution to met requirements. Even some other potential for utilizing existing methods is to use other software such as Radiance to calculate incident solar radiation at points and for centre of surface (Mardaljevic and Rylatt 2003).

The data obtained from the above four methods successfully represent the dimensions of the research problem its justification and the possible solutions of the research problems.

1.6 Thesis Structure

Mainly this thesis comprises nine chapters. The author has tried to integrate the entire thesis to form a coherent body of research.

Chapter one is an introduction of the research presenting the research background, problem/questions, aim and objectives, significance of the study, the research methodology and the outline of the thesis.

Chapter two assists by the clarification of the aim and objectives. In particular it looks for other scholarships on deriving building form from an analysis of solar radiation. There are also some reviews on preference-based modeling which is relevant to the revised focus on design requirements. It also to provide, through the literature review, a background of different used software, their advantage and why Ecotect one of environmental design software is much more suitable for this research.

From chapter three to chapter five is to review aspects of standard approaches to working with solar radiation that will be used or adapted in this research. In fact it is to supply the necessary background to the work has been done in the research by other words.

Chapter three explains the types of solar radiation as this research deals with wide range of solar radiation wavelength, visible and non-visible solar radiation, sunlight, skylight and reflected radiation. Also measurement of received solar radiation, measurement of sky luminance as well as source of solar data has been illustrated in the chapter.

Chapter four is mainly about prediction of solar radiation received by surfaces of alternative inclinations under open skies. There is some sections to show the problem of the inclined surface, mapping the sky vault, mapping the direct and diffuse components, and cosine correction.

Chapter five is an extended method to take solar radiation obstruction into account. The chapter also demonstrates shading masks, reflected radiation masks, calculation of solar incidence on surfaces, daylight availability at surfaces and absorbed and transmitted of radiation.

Next three chapters demonstrate application for the tools toward the aim.

Chapter six aims to optimize solar collector angle and orientation that is in other words intending to optimize inclination of the recipient surface. The overall theme of this research tries to solve design problems whose deals with a surface as a collector or a surface as a protector for received radiation. This theme leads the thesis to control the amount of solar radiation collected over a period of time by a surface.

Chapter seven shows a reverse ray tracing method to trim a shade or an opening in front of the recipient surface. Thus, controlling the irradiation over a surface over the proposed period is his chapter's main concern.

Chapter eight investigates on placing a building development in front of the recipient surface. As it presents a method which has a great potential to begin to generate form with requirements of maximising the amount of solar radiation collected over a period of time by a surface. This is applicable for daylight and right-to-light.

Chapter nine discusses conclusion of the thesis and the main findings with the purpose of answering the main questions of the research. Major contribution, summary of the work and further research potentials are shown at this chapter.

1.7 Summary

New technology involving intelligent building design shifted the author's interest to do research in the methods which controls solar radiation over surfaces. This allows designers to get control on environmental building design problems more technically. The problems are specified here more about solar radiation recipient depending on the situation for maximize/minimize its effect. Another problem which recognized as a family problem is the envelope design and rights for light of surrounding buildings. Also problem's type definitions were explained here briefly.

Above build foundation lets to establish the research's main aim testing the reverse computation that the research is aimed to reach. Then the research objectives have been clarified and also the techniques which will be used to approach them explained here.

The thesis structure and the content of its nine chapters were traced showing how this research is going to built up its evidences and supports to contribute in the body of knowledge.

CHAPTER TWO

LITERATURE REVIEW

2 Literature Review

2.1 Introduction

The potential of performance-based simulation design helped the author searching for the other similar or probably parallel works have been done or being done in the other parts of the scientific world. The major similar aims and approach was found in a conference called IBPSA 2003 (International Building Performance Simulation Association) held in Eindhoven, Netherlands. One of the closest researches could be fit in the research field has been done by Professor Ardeshir Mahdavi in Technical University of Vienna, Austria. An extended explanation is presented here in the literature review to show how chronologically and technically his work can play a fundamental role for this research. His publications have been considered carefully to investigate the matching point of aims and objectives as well as methods and techniques he has developed to approach to his aims.

As a result of above bases this research is created from a hybrid method that is an amalgam of methods which have been cast before, plus a significant part of knowledge has been added by the author. These routes have come together to carry on a road extended by outcomes of this thesis.

Therefore, the aim of this literature review is to explore earlier research that shares parallel/similar research aims. For this purpose the related research results have been reviewed including established methodologies and terminologies under consideration of this research field. Accordingly, a clear structure has been built for the reviewing literatures.

Thus, three main categories can be defined to look at the related literatures. These categories have been recognized based on defined aim and objectives introduced earlier in the introduction chapter. These categories are as follow:

1. Solar Radiation
2. Performance-Based Design
3. Available Tools

These categories are the main point of view, to the literatures to support involving parameters of the goal. First of all, for controlling solar radiation over surfaces knowing characteristic solar radiation, physics and behavior become essentials. Then performance-based designing approach must be carefully studied, to see who has looked at it before and what did they approach. Finally, knowing how tools have been used, what tools are available now and which one must be used as well as the reasoning of their usage is discussed below.

2.2 Solar Radiation

Solar radiation as a free source of energy is used in buildings much more widely, to help to save energy and environment as well as better performance of buildings. However, this research intends to focus on solar radiation as a design analyzing tool. Then, first step would be explaining characteristics solar radiation itself and calculations.

2.2.1 Sun position

The Sun's position over the sky equals the coordinates of the Sun in relation to the Earth's movement in its orbit around the Sun. This involves some different trigonometric calculations which mainly has been tried to reduce the calculation's uncertainty. The accuracy of solar positioning has becomes an important task to research. For example a report by Jean Meeus described an algorithm is written in a step by step format for implementing the algorithm to calculate the solar zenith and azimuth angles in the period from the year -2000 to 6000, with uncertainties of $\pm 0.0003^\circ$ (Meeus 1998).

Therefore, fundamental to any form of solar radiation analysis is having an accurate knowledge of the position of the sun at any time and date. Many methods to calculate solar position have been published in the literature. However, when referring to the work of Blanco-Muriel (Blanco-Muriel et al. 2001), Reda and Andreas (Reda and Andreas 2004) suggested that their accuracy in most cases were no greater than $\pm 0.01^\circ$ and that they were only valid for certain time spans. Reda and Anderas summarise the work of Iqbal (Iqbal 1983) to produce a more accurate but quite laborious calculation procedure requiring multiple steps and several look-up tables. Roy, Carruthers look in detail at a wide range of more simple trigonometric formula

and showed reasonable correspondence with recorded solar angles, proposing their own method based on statistical analysis of historical recordings (Carruthers et al. 1990). Furthermore, Diasty has revealed the importance of the time duration of the sun at a given sky element and atmospheric conditions other than clear sky (Diasty 1998).

2.2.1.1 Image-Base Approach

A new approach has been published by Mardaljevic and Rylatt (Mardaljevic and Rylatt 2003) for mapping solar radiation over surface. This new approach they called irradiation mapping. The sun positions are shown in Figure 2-1(a) for the location of Leicester, UK. The distribution in altitude and azimuth is divided into 'bins' using of 8° grid as an arbitrary resolution. The number of sun positions that occurred in each bin are counted, and the bin mean sun position evaluated Figure 2-1(b). The number of bins $B = 179$. Annual totals of irradiation are the most uncomplicated to derive using this method. However the total can easily be amended to produce a summation for any preferred fraction of the year, e.g. seasonal totals, monthly totals, am and pm totals etc.

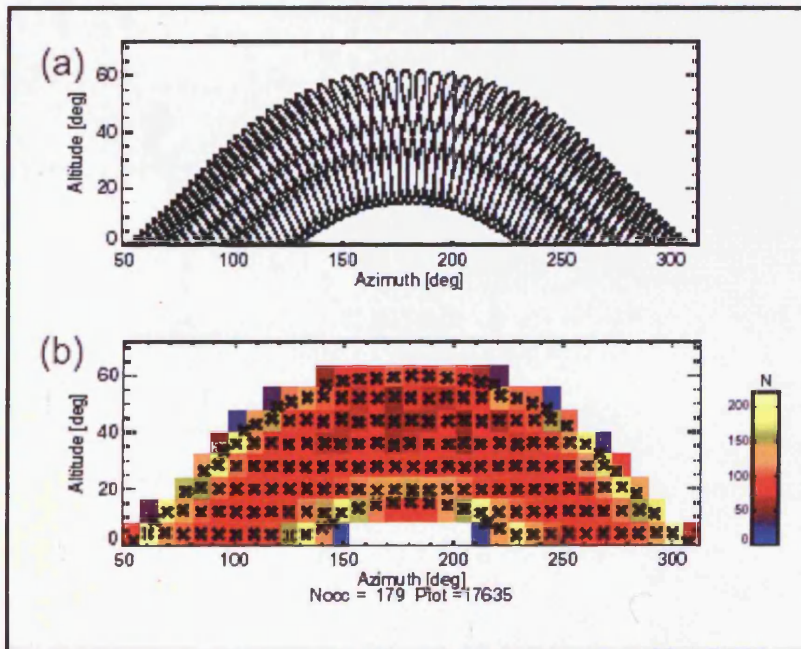


Figure 2-1: Procedure to determine the sun position for the sun and non uniform sky condition from the annually occurring sun positions in 15 minute time step. (Image source: Mardaljevic 2003)

Having done the position of the sun its distribution over sky vault is the next step that radiation has to pass through the atmosphere, obviously.

2.2.2 *Sky Distribution*

Since modeling sky luminance distribution has been the aim of many researchers, first standardization of luminance distribution on clear skies has been introduced by CIE (Commission International de l'Eclairage) in 1973 ((CIE) 1973). Also luminance distribution for overcast skies was presented by CIE based on a model by Moon and Spencer (Moon P and Spencer DE 1942). Many attempts have been focused on modeling of partly cloudy skies as those luminance distribution models could not be applied in satisfactory level. For their improvement or the development of new ones many efforts have been made. As a result Perraudeau and Chauvel introduced a cloudiness index and created five types of sky luminance distribution (Perraudeau and Chauvel 1986). A zenith luminance developed model has been done by Perez and colleagues for all sky types. It was tested for ten different places in the United States and three sites in Central Europe with the result of site and time dependent (Perez et al. 1990). The ratio of zenith luminance to diffuse illuminance and the luminance turbidity has been introduced by Kittler (Kittler and Darula 1998; Kittler et al. 1997). Kittler also introduced the notions of 'relative gradation' and 'relative scattering indicatrix' defining fifteen standard sky types (Kittler 1994; Kittler and Darula 1997; Kittler et al. 1998).

These elements combination resulted in fifteen realistic sky types (standards) for luminance distribution. By using their methodology Tregenza did the examination of the influence of daylight conditions in interior spaces (Tregenza 1999). Also Bartzokas evaluated the daylight at one site in Central Europe and a second one in the Eastern Mediterranean using same methodology for sky distributions (Bartzokas et al. 2003). A recent research work has been used the same methodology presented by Kittler to study the daylight climate in Sheffield, Central England, during winter. The study showed that the most frequent winter sky types in Central England as well as their frequency of occurrence in percentage indicating that the sun is obstructed by the clouds most of the time. Therefore, the direct normal-incidence irradiance will be under 120W/m^2 (Markou et al. 2005).

2.2.3 Surface Incidence

Having different sky distributions, solar radiation will reach on any surface passing through one of the classified skies. To collect maximum amount of available solar radiation some different parameters are involved. The incidence angle is one of the most important involving parameters that obviously indicates normal incidence angle as the maximum possible amount of received energy; however it is not always possible to get all due to sun's dynamic condition over the sky in addition to the skies dynamic conditions discussed in the previous section. Thus, available collection methods and how can collect optimally, is going to be discussed here.

2.2.4 Solar Collection and Optimization

One of the most comprehensively covered areas in solar collection is the optimization of solar collector angle and orientation. The effects of collector angle and orientation on solar energy availability are highly significant. For instance Bari has published a paper for optimum orientation of domestic solar water heaters for the low latitude countries. It was observed that the majority of collectors installed in Malaysia were incorrectly installed and they are receiving 10-35% less radiation than a optimized installed collector (Bari 2001).

As a result, if looked at over solar collection, chronologically some papers can be found having fundamental ideas of optimizing and solar collection estimation methods. For example Tiris has cited in a 1998 paper, which Liu and Jordan used a simple method for estimating the average daily radiation on each month over surfaces facing directly towards the equator in 1966. Also the paper's author mentioned an estimation of the monthly values of total radiation from sunshine hours on vertical and inclined surfaces which have been done by Klevien in 1977 (Klein 1977) and Page 1964 (Page 1986). According Tiris's statistical comparison between measured data and the equation derived by Liu, Jordan and Page, they do not give accurate results (Tiris and Tiris 1998). Over time and with the opportunity to use new equipment, technology and simulation, more and more accurate solar data prediction over surfaces are becoming possible. Computer simulation of incident solar radiation over surfaces in any angle and orientation has made it possible to compare results and optimize surface collection. For example Kundu has done a performance analysis and optimization of absorber plates for a flat-plate solar collector under a comparative

study (Kundu 2002) and also Gunerhan and Hepbasli determined the optimum tilt angle of solar collectors for building applications based on experimental data measured for Izmir in Turkey much recently (Gunerhan and Hepbasli). However, none of their methods were based on computer simulation dealing with the effects of complex overshadowing and they seem too complicated in terms of being used by architects and designers.

Additional to the above publications, if looked at the subject based on location a lot of researches have been done on the optimum tilt angle and orientation for the collection of solar radiation in different parts of the world. For example, Chow found for numerical study of desirable solar collector orientations, a solar collector facing the south-west direction in the costal region of south China could be the most desirable for a wide range of tilt angles and for maximizing the annual yield (Chow and Chan 2004). Also Adnan Shariah has studied optimum inclination angle for the maximum solar fraction in Amman. The result showed the relationship between latitude and the collector angle is 10° - 20° additional to the latitude angle from the northern region to the south would be the optimum (Shariah 2002). Mohd Azmi bin Hj Mohd Yakup achieved used a mathematical model for estimating the total (global) radiation on a tilted surface, and to determine the optimum tilt angle and orientation for the solar collector in Brunei Darussalam. The results showed that changing the tilt angle 12 times in a year increased the maximum value of solar radiation. This achievement made 5% more solar radiation gain than the case of a fixed collector on a horizontal surface (Mohd Azmi bin Hj Mohd Yakup and Malik 2001).

It is worth also to mention a paper about the accuracy of the put in data and simplification of the use of data, according to the paper published by Hartley under the title of "*The optimization of the angle of inclination of a solar collector to maximise the incident solar radiation*" the method involving monthly averages was more accurate and easier to work with (Hartley and Martinez 1999).

In the over all of the above researches, any of them have *again* not considered overshadowing and obstructions effects over the collectors. This has been shown to cause a huge difference in collector performance in the period of time. The evidence for this; the research has been done by Robinson and Stone indicating ignoring

obstructions to the sky vault leads to considerable error in predicting surface irradiance (Robinson and Stone 2004).

2.2.5 Surface Mapping

Several approaches to the irradiation prediction over surfaces have been described in the literature. Notable examples are a simulation-based approach by Kovach and Schmid using a ray tracing technique (Kovach and Schmid 1996); Irradiance calculations on shaded surface as a manual projection-based method by Quaschnig and Hanitsch (Quaschnig and Hanitsch 1998) and Snow have described a computer based simulation approach in a building integrated Photovoltaic (Snow et al. 1999). All of the techniques referenced above, calculate solar radiation in a point-based manner. In fact the point-based methods do not support any anisotropic distribution of solar radiation over surfaces and also have some other limitations. More recently Mardaljevic and Rylatt have formulated another approach to overcome the problem of the point-based methods. His approach was more accurate than previous methods as the used weather data were more accurate test reference year (TRY) was used and there was not any practical limitation for the site complexity. As an example Figure 2-2 shows total irradiation map by this method over a complex site in San-Francisco U.S. Additionally, shading and inter-reflection between buildings have been accounted including realistic sky radiance patterns to model non-overcast sky.

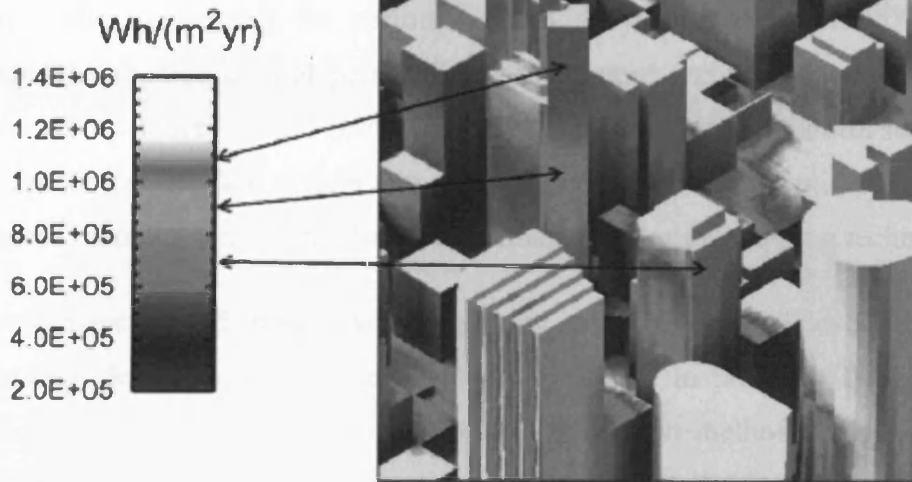


Figure 2-2: Total annual irradiation mapping for San Francisco
(Image source: Mardaljevic 2003)

This approach used physically-based rendering and data-visualization technique called Irradiation mapping for Complex Urban Environment or ICUE (IQ) (Mardaljevic and Rylatt 2003). More will be said about this research in section 4.2.

2.3 Performance-Based Design

Using buildings performance as the starting point for design will generally lead to different solutions in the hands of different designers. This is due to their differing world-views and objectives. To achieve the desired shared understanding among designers, they can modify the solution for the purposes of improving the overall performance of the project, it is necessary to test the results the disciplinary valuations among the requirements, in a manner that will be readily understandable by all levels of designing knowledge. Furthermore, the performance design process must convey not only the parametric value of the performance (e.g., energy use), but also the satisfaction amount of which designer views the results and the degree of flexibility to which the performance may vary before that amount of satisfaction is greatly affected.

The method have been used by some researchers for this purpose is based on the concept of satisfaction functions, first introduced by Kunz and Rittel (Kunz and Rittel 1972), and more recently applied by Mahdavi as part of the SEMPER system. SEMPER system is an active, multi-aspect prototype design environment (Mahdavi

1996; Mahdavi et al. 2001; Mahdavi et al. 1997; Mahdavi and Ries 1998). These are mappings that express, in functional form, the supposed relationship between some parameter value, indicating the performance of a system (as predicted by some performance evaluation tool, or personally by the expert) and the subjective measure of its desirability under specific circumstances. Therefore, active junction support via a multi directional interface system that provides not only the conventional design-to-performance mapping option but also a performance-to-design mapping technology.

Thus performance-based mechanism developing at an operational level lets use of computational design generation and evaluation method in practice. This also is a proof of concept for amalgamation of detailed simulation methodologies within an active, multi-aspect computational environment to effectively support performance-based reasoning in building design.

For performance evaluation in building design, some efforts for computational implementation in comprehensive scale have been made. Much of these efforts have focused on the computational design support system "SEMPER", with four major aims:

1-Flexible performance modelling throughout the entire building design and engineering calculations with consistent methodology.

2-Performing a multi-domain building evaluation support.

3-Proper dynamic communication between the general building representation and the simulation model in an environment which relies on space as the base and is object-oriented.

4- Achieving a full support for active convergence through a bi-directional inference mechanism providing both preference-based performance-to-design mapping technology and the conventional design-to-performance mapping technique.

Since many simulation modules are dynamically well linked to a shared space-based object-oriented architectural representation, changes in design are dynamically mapped into corresponding modifications in the inherently homologous domain

representations of the simulation models. This is achievable with no dependency on user intervention, geometry interpretation, or translational routines. Consequently, as a proof of concept for incorporation of detailed elaborated simulation methodologies within an active, computational environment with multiple aspects is provided to effectively support performance-based reasoning in building design (Mahdavi 1999).

There is also a constant challenge for the computational performance-based building design support to face. Providing building performance feed back to the designer at the earliest possible time is of significant importance in the design process. Many aspects of building performance are noticeably affected by the building technical systems design, which are typically brought into consideration in detail only in the final stages of design. Thus, the challenge is to adopt a method via which employment of detailed simulation tools even in the early stages of design when values for many of the variables for the technical sub-systems of the building are yet unavailable is practically possible.

It can be demonstrated how this problem may partially be solved by combining two different levels of automation. The first level indeed is formed by differential building representation containing a number of domain (application-specific) object models which are automatically derived from a shared object model. In the second level, generative agents that create reference designs for the technical sub-systems of the building are applied. To display the level of feasibility for the proposed approach, one can focus on the building energy systems domain (heating, cooling, ventilation, and air-conditioning (Mahdavi et al. 2001).

By adapting this approach, detailed computational building performance assessment tools may become even further more available to any general user.

2.3.1 Shading System Design

The application of performance-based design to shading devices has been considered by a number of previous researchers. This work has been particularly influenced by that of Kaftan (Kaftan 2001) in his work to establish the extents of shading requirement by matching solar position against recorded hourly data for direct and

diffuse solar radiation. This allowed him to map the amount of solar radiation passing through the surface of a potential shading device before striking a particular window, calculated using a spreadsheet model. His approach included the consideration, in a relatively simple way, of the heating and cooling requirement of the room behind the window and reconciles this with the solar availability.

Another research to influence this author was that of Marsh (Marsh 2003) using solar geometry to generate optimum shading device shapes based on cut-off dates and times. As part of research work undertaken with the author, Marsh has extended this approach with a more performance-based method using reverse ray tracing, tracking the movement of the sun from the perspective of a surface and mapping each ray as it passes through potential shading devices.

2.4 Available Tools

According to U.S. Department of Energy, Energy Efficiency and Renewable Energy, building energy software tools directory has published all available building design tools (U.S. Department of Energy 1996). This is a valuable directory for the valid existing software in efficient building design. Some of that software, which was relevant to performance design and the research area, has been chosen to compare. The next are their explanations and justifications.

2.4.1 Background

In 1991 Mahdavi and Lam stated that any performance simulation tools had not been integrated effectively in the architectural design process. The current tools of operational or functional characterize them as verification tools rather than design support tools (Mahdavi and Lam 1991). Especially in the early stage of design, where many important decisions are made, lack of computational environments represented a serious weakness. In 1992 Mahdavi and Berberidou introduced identifiable of the 'mono-directionality' of many conventional tools as one of the parameters responsible for that circumstance (Mahdavi and Berberidou-Kallivoka 1992). The majority of available computer simulation tools did not directly provide information on design configurations that would meet the desired performance criteria, however instead require a computationally unsupported focus toward the solution through extensive parametric studies. The conventional simulation procedure was based on the

transformation of applicable design data e.g. geometry, materials, environment into a set of performance indicators for a given context. The procedure produced theoretically unique results for a given algorithmic formulation.

Mahdavi also stated by the concept of an "open" simulation environment for performance-driven design exploration as a multi-directional approach to computer-aided daylight modeling has been the center of attention for the designers. Prototypical realizations of a Generative Simulation Tool for Architectural Lighting (GESTALT) for simultaneous treatment of daylight-related design and performance variables have been introduced (Mahdavi 1993).

Earlier findings have exhibited that GESTALT by virtue of a fast-response computational module can operate in a rather "explicit" mode. Further refined "implicit" mode of operation which employs a comprehensive simulator and investigative projection techniques are introduced. Illustrative sequences of design explorations with this new GESTALT version have been presented and discussed.

There have been a number of scenarios for using GESTALT in design exploration through which the feasibility of flexible and multi-directional design to performance mapping operations have been vividly displayed. Based on a series of preference functions extracted from numerous information sources GESTALT has actively been proven to enable the designer in dealing with the struggle to obtain the desired answers. One should keep this point in mind that preferences must not be viewed as the sole rigid and unchangeable set of constraints and this indeed is an outstanding feature of GESTALT (mahdavi and Berderidou-Kallivoka 1995).

2.4.2 *SEMPER*

Mahdavi describes SEMPER as "a prototype of an active multi-aspect prototype design environment". He has written widely on the application of high-end simulations techniques to the earliest stages of the design process, and SEMPER is the product of this research. Whilst of significant interest to the author, it is unavailable for detailed analysis and, even though an approach has been made to Professor Mahdavi for more information, only references to published papers were received.

Thus, a computational environment (SEMPER) designing bi-directional, multi-domain is performed by Mahdavi (Mahdavi et al. 1997). The necessity of a computational environment arises and intensifies further as there is a lack of active design support which is mono-directional. Rather, SEMPER provides two functionalities: first, it enables the designers to make changes in performance variables and, second, it allows the designer to observe the results of changes in other design variables whilst one or more relevant variables are kept constrained.

SEMPER incorporates seven performance modules for simulation:

Thermal analysis, with grid-based nodal heat-balance as modelling technique and heating, cooling, electrical loads and space temperatures profiles as performance indicators.

HVAC system, in which modular, component-wise approach is employed for modelling and the HVAC system energy consumption and fuel consumption are performance indicators.

Air flow, for which hybrid multi-zone and CFD by use of grid-based nodal network form the basis of modelling and the air flow patterns and quantities act as the performance indicators.

Thermal comfort, with algorithmic routines for numeric indicators and knowledge-based system for expert advice as modelling technique and thermal comfort (PMV-PPD, SET, TSENS, and DISC) as performance indicator. [Predicted Mean Vote, Predicted Percentage of Dissatisfied]

Lighting (including both the daylight and electric light), which employs discretized sky model and inter-reflection based on radiosity and take the advantage of spatial distribution of luminance and illuminance levels as performance indicators.

Acoustics, with the application of hybrid stochastic approach combining features of sound particle models and statistical energy distribution analysis. In this module sound pressure level distribution and parameters of the reverberant field perform the role of indicators.

Life-cycle assessment which relies on comprehensive eco-analysis comprising production, construction, operation and decommissioning phases of building as well as eco-balance methods as modelling method and first and life-cycle costs, payback periods and loads to natural resources as the performance indicators.

The possibility of deriving the design implications of desired performance objectives, using a preference-based approach has been described. However bi-directional tools do not model the design process (Mahdavi 1997).

2.4.3 *Ecotect*

This software has a unique approach to conceptual building design. It matches an initiative three dimensional design interface with a comprehensive set of performance analysis function and interactive information display.

Ecotect is a conceptual stage building modeling and analysis tool that deals directly with all aspects of building's performance. It is included the thermal, acoustic, lighting and solar design issues. Ecotect includes conformity testing functions for local building regulations such as the new UK Part-L. The software has about 3000 licensed users around the world. It has been taught at about hundred universities mainly in Australia, USA and the UK. It has supporting tools such as solar tools, psycho tools, terrain tools, weather data tools, sound tools, life cycle analysis tools, conversion-equation tools and lumen tool. The flexibility's of Ecotect lets the model be assess in the wide range of features that add to its accuracy of solar radiation prediction and the fact that the model can be easily import or exported to other programs such as Auto Cad, WINAIR4 (CFD) and Radiance without any re-modeling. The programming is written in C++.

The incident solar radiation analysis in Ecotect which can be used in this research for incident solar radiation prediction also refers to the availability of incident solar radiation on points and surfaces within the model. Ecotect for solar radiation calculations uses hourly recorded direct and diffuse radiation data from the weather file. Overshadowing requires only the geometry of the building and its surroundings. The latitude and longitude of site must be set and selects the right weather data file before performing any calculations(Marsh 1997).

2.4.4 *GenOpt and Optimisation Tools*

Much work is being done on design optimisation algorithms and their application to building systems. Tools such as GenOpt from Lawrence Berkeley Laboratories (Wetter 2004), and others such as DOT (Vanderplaats 2001) and SimuSolv (Struub 2005), allow for low level optimisation of multiple numeric parameters by linking and invoking different analysis tools as part of an iterative solution.

The work presented here is not looking at the application of complex mathematical solutions or genetic algorithms. Rather, the primary consideration is the mechanism for translating analysis results into geometric decision-making and the computational generation of building form to meet specific performance criteria. The integration of more efficient optimisation techniques can follow as part of future work; however, as this is intended as a proof-of-concept stage, a much simpler brute-force approach has been taken to solution.

2.4.5 *RADIANCE*

RADIANCE is a highly accurate ray-tracing software system. Radiance is a set of programs for the analysis and visualization of lighting of designing. Input files identify the geometry, materials, luminaries, time, date and sky conditions in case of daylight calculations. Radiance simulation results can be displayed as colour images, numerical values and contour plots.

Radiance similarly to Ecotect has no limitation over simpler lighting calculation and rendering tools on the geometry or the materials that may be simulated. Radiance can be used by all kind of designers like architects and engineers to predict illumination, visual quality and appearance of innovative design spaces. It can be used by researchers to evaluate new lighting and daylighting technologies.

Radiance is intended to aid architects and lighting designers by predicting the light levels and appearance of a space before construction. It is included programs for modelling and translating scene geometry, luminaries' data and material properties as input data to the simulation. The lighting simulation uses ray tracing techniques to compute radiance values for example the quantity of light passing through a specific

point in a specific direction that they are typically arranged to form a photographic high quality image. The resulting image may be analyzed, displayed and manipulated within the software, and converted to other popular image file formats for export to other programs. In overall Radiance is a powerful lighting analyser tool.

2.4.6 *SUNTool*

SUNtool (Sustainable Urban Neighborhood modeling tool) is for use at the conceptual stage of the master-planning process offering comprehensive information in a non-technical way regarding resource use, costs, emissions etc to support optimization of the site layout, mix of uses, range of sustainable technologies etc. all the while shielding the user from the associated modeling complexity. In fact it is a new approach for an integrated architectural design and environmental simulation tool. This tool is also for supporting the user through the process of optimizing the sustainability of master-planning proposals. Hence the user is able to quickly sketch the form of the neighborhood involving based on some simple descriptions such as building use and age, a set of default constructional and operational attributes is associated with these. Therefore at this preliminary level the user may call for energy, water and waste flows to be simulated or alternatively project may be defined in more detail. A type of graphical results analysis facilities would be available, however the intention is to support the rapid identification of the key performance characteristics of the project and means for further improvement. Thus SUNtool leads to a range of innovations as follow:

- 1- An urban-sensitive daylighting and solar radiation modeling system
- 2- Thermal microclimate model
- 3- A generation of stochastic models to emulate human behavior
- 4- Procedure to rapidly attribute buildings
- 5- A parametric engine to automate the execution of sensitivity studies

It has announced that SUNtool is due to completion early 2006 (Robinson et al. 2003), thus it was not completely available to be used in current research.

2.5 Tools Justification

There are several criteria that must be considered for choosing an analytical and simulation program seriously. They should be taken into account to achieve the main aim of a building design or research. First of all the information type needed from the model then the validity and accuracy of the program, third is the accessibility and familiarity to the model, and last one the accessibility to technical support staff (Hanafi-Rifai 1990). Based on the above criteria Ecotect have been chosen for performing the simulation and analysis toward the aim. This program is among the modelling programs that have been widely used in the field of architecture and building science research within the UK and other countries.

As it has been explained in section 2.4.3 Ecotect is a building analysis application that was compiled by Square One research and Welsh School of Architecture at Cardiff University (Haghparast 2002). It is a designing tool as well as simulation program which can provide users with a comprehensive range of performance analysis and simulation functions by a user-friendly three dimensional modelling interface. This program is very helpful for architects especially in conceptual stage to test alternative design parameters at any stages of a building design.

Additionally, this program, as mentioned above and in the abstract, has been developed by Dr Andrew Mash who works at the Welsh School of Architecture assisted by the author in some cases. Therefore, working closely with the program developer who was kindly available to answer any questions and was able to solve any problems faced during any stage of this research made the Ecotect incomparable to use beside the other explained software. However the advantage of knowing the other programs like Radiance or SEMPER is unavoidable. In fact they had great influence to think about their abilities and take the idea to set the subject and carry on the right way toward this research.

CHAPTER THREE

Solar Radiation Measurement

3 Solar Radiation Measurement

3.1 Solar Radiation

Obviously, solar radiation from the sun carries energy in all directions. Radiation behaves like wave trains when moving in space, also called photon; it has both electrical and magnetic properties and is therefore known on electromagnetic radiation. All radiation travels in empty space at a constant speed of 300,000,000 m/s the speed of light. Sunlight takes about 8 minutes to get to the earth surface through the average distance between the sun and the earth (150,000,000 km). Electromagnetic radiation emerges in differing wavelengths but propagating at the same speed. As Figure 3-1 indicates while the intensity of thermal radiation is outstretched as a function of wavelength, the resultant spectrum is most intense in a band of wavelengths that depends on the temperature. This happens at visible wavelengths when the temperature is about 6,000 degrees Kelvin. This emits radiation at longer wavelengths at a lower intensity. On the other hand, non-thermal radiation is more intense at longer radio wavelengths as high-speed electrons emit non-thermal radiation in the company of a magnetic field (Lang 2001).

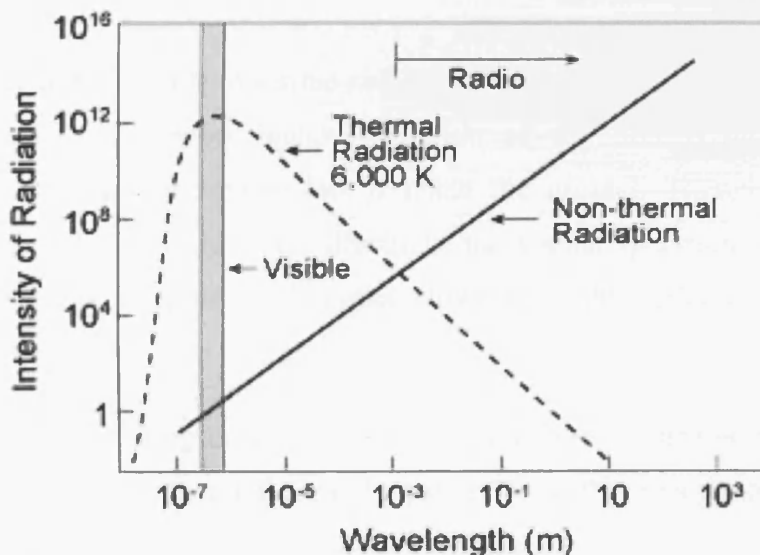


Figure 3-1 Spectrum of thermal radiation (Lang 2001)

Types of solar radiation distinguished by electromagnetic spectrum are subject for more explanation.

3.2 Types of Solar Radiation

The Sun's spectral flux at the Earth can be mapped as a function of the wavelength. At all wavelengths the amount of received solar energy on the ground is less than outside the atmosphere. This is due to absorption in the Earth's atmosphere none monolithic, varyingly by absorption of molecules of oxygen O₂, Water H₂O and carbon dioxide, CO₂ as Figure 3-2 shows that the attenuation is much greater at certain wavelengths than at others (Lang 2001).

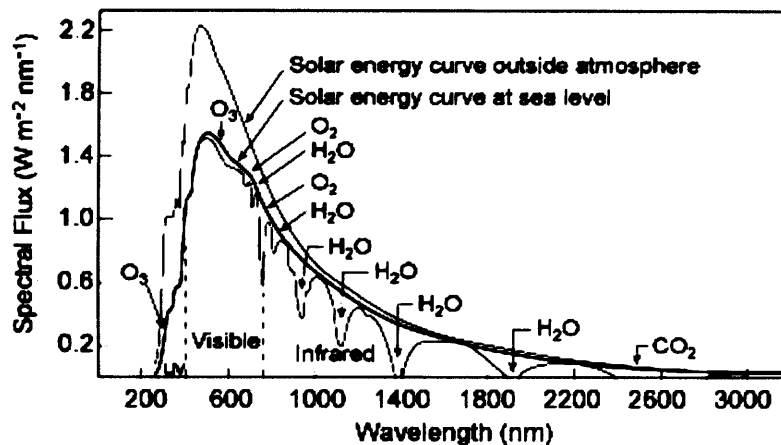


Figure 3-2 The Sun's spectral flux.

(Image source: The Cambridge Encyclopedia of the Sun)

3.2.1 Visible Radiation

The human eye responds just to visible radiation. Radiation in this wavelength band is known as “light”. The most intense radiation of the Sun is emitted at these wavelengths, and our atmosphere lets it reach the ground. Therefore our eye is matched to the tasks of vision. As illustrates the visible spectrum is a very small portion of the entire range of wavelengths. However visible radiations contain most energetic photons compare to the others.

The amount of light falling on a unit area of a particular surface is its Illuminance. The amount of light leaving a unit area of a particular surface in a particular direction, whether emitted, diffused or reflected, is its Luminance

3.2.2 Invisible Radiation

In addition to visible radiation, there is invisible radiation. The solar spectrum extends over an enormous range in wavelength, and different wavelength contain different names as seen in Figure 3-3. The invisible domains include the infrared and radio

waves, with wavelength longer than the red light, and the ultraviolet (UV), X ray and gamma (γ) rays that are shorter than violet light. They are all electromagnetic waves and they all move in empty space at the velocity of light, but can not be seen by human eye. However, electromagnetic radiation at short X-ray and Ultra violet wavelengths is absorbed in our atmosphere so the Sun can be observed in these regions from above the atmosphere. The only kind of invisible radiation does not absorbed in the Earth's atmosphere are radio waves. This wave contains only small portion of photon energy compare to the photons of visible light.

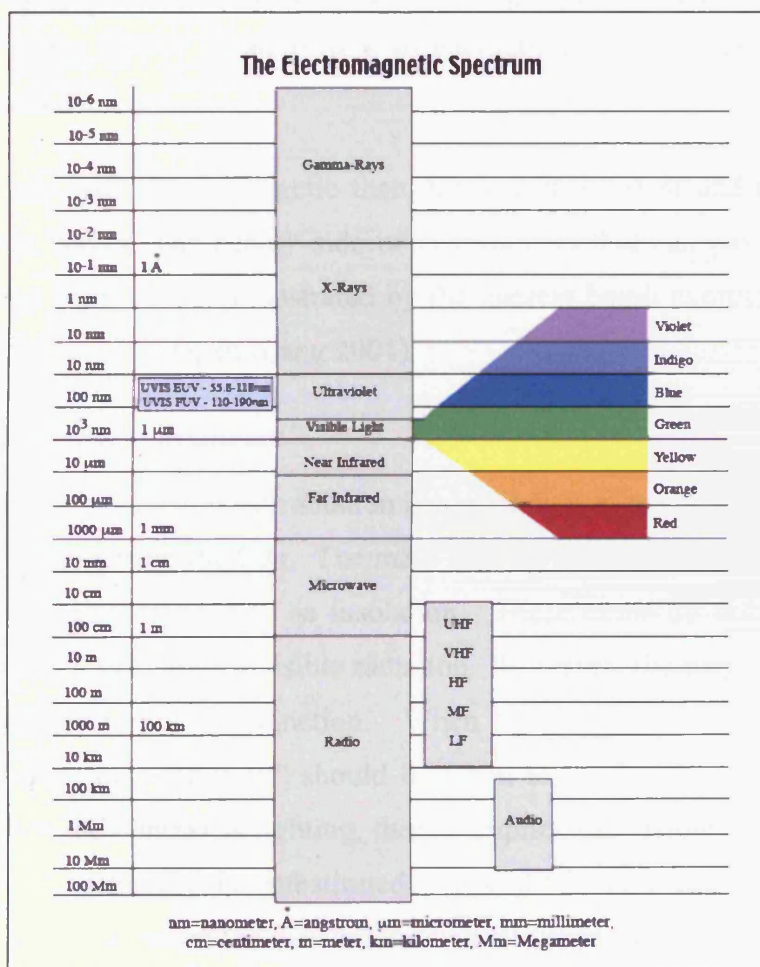


Figure 3-3 The electromagnetic spectrum radiation from the Sun and other emitted cosmic objects. Image source: (www.images.google.com/Electromagnetic%20Spectrum.htm)

As can be seen in the above Figure the infrared part of the electromagnetic spectrum is located between the radio waves and visible area. Infrared radiation is absorbed by

the Earth's atmospheric particles and molecules, such as water vapour and carbon dioxide.

Beyond violet light there is a short-wavelength called ultraviolet (UV). This part of the electromagnetic spectrum has sufficient energetic photons to tear electrons or atoms off many of the molecular constituents of the Earth's atmosphere, particularly in the ozone layer. These energetic photons cannot reach the ground; however the ultraviolet radiation that reaches the ground can damage our eyes and skin.

In the short wavelength side of ultraviolet radiation the X-ray region of the electromagnetic spectrum extends from a wavelength of one-hundred-billionth of a meter almost in the size of an atom. It is so energetic that it is usually described in terms of its carried energy.

Gamma rays are even more energetic than X-ray with shortest and most energetic electromagnetic waves. The deadly side of gamma rays that can pass through a 20 centimetres iron plate were demonstrated by the nuclear bomb explosions tragedy at Hiroshima and Nagasaki, Japan (Lang 2001).

3.2.3 *The Term "Solar Radiation"*

In this research, reference to solar radiation is to radiation of any wavelength received at the Earth's surface from the Sun. The main interest is in solar radiation reaching a surface, which is also referred to as insolation. These terms do not in themselves distinguish between visible or invisible radiation. However, the particular context of the discussion may imply a distinction. When the context is thermal heating or cooling, the term "solar radiation" should be taken to imply the whole of the solar spectrum. When the context is lighting, then it implies the visible spectrum and the term "light" will generally be substituted. The distinction can be important in practice. For example, when the discussion is about the exclusion of sunlight, that is of direct light, the aim of design may or may not be to exclude the heat in this direct radiation, depending on the thermal climate.

3.3 Direct and Diffuse Radiation

Knowing all variation of radiation emitted from the Sun, Solar radiation usually known as thermal radiation despite of its lighting. However this research has been considered both energetic potential of visible (light) and invisible (heat) the spectrum.

Incident solar radiation refers to the wide spectrum electromagnetic energy radiating from the Sun which then strikes a surface. After passing through the Earth's atmosphere, insolation includes both a *direct* component from the Sun itself and a *diffuse* component comprising radiation reflecting off moisture vapour and particulates within the sky. It can also include a reflected component from the ground and other surrounding objects. A wide explanation included in terms of reflected radiation from objects in the section 5.4 next.

3.3.1 Solar Radiation and the Atmosphere

“When the sun's rays hit the atmosphere, more or less of the light is scattered, depending on the cloud cover. A proportion of this scattered light comes to earth as diffuse radiation. On the ground, this appears to come from all over the sky. Without it, the sky would appear black”
(Boyle 1996).

Radiation first has to penetrate into the atmosphere and reach sea level by filtering through the atmosphere. The atmosphere consists of several hundred different gases in different layers. In fact it is a relatively thin layer of gas that surrounds the earth. This gas is held in place by the earth's gravity and has about 5.5×10^{15} Metric tons of mass. With the exception of water vapour, all gases exist in similar proportions, up to around 80 kilometres.

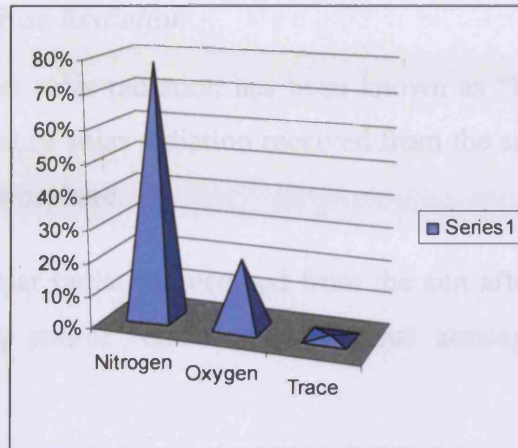


Figure 3-4: Gas proportion of the atmosphere.
(Generated in Microsoft Excel by author)

Figure 3-4 shows proportion of existing gases in the atmosphere - the majority of which are Nitrogen (78%), Oxygen (21%), Argon (0.93%) and a small amount of trace gases. Some parts of the atmosphere also contain water vapour which depends on local weather conditions. This water vapour has a very important role in the creation of clouds and delivery of water in its different forms; rain (liquid), hail (solid) or snow (Streete 1996).

Figure 3-5 shows what happens to radiation entering the atmosphere. Each layer in the atmosphere plays an important role in alleviating harmful radiation reaching the earth's surface. For instance, ultra violet radiation, which potentially causes eye damage and skin cancer is absorbed by the ozone layer also harmful X-ray and γ -rays are absorbed in the upper layer of the atmosphere. (Lang 2001)

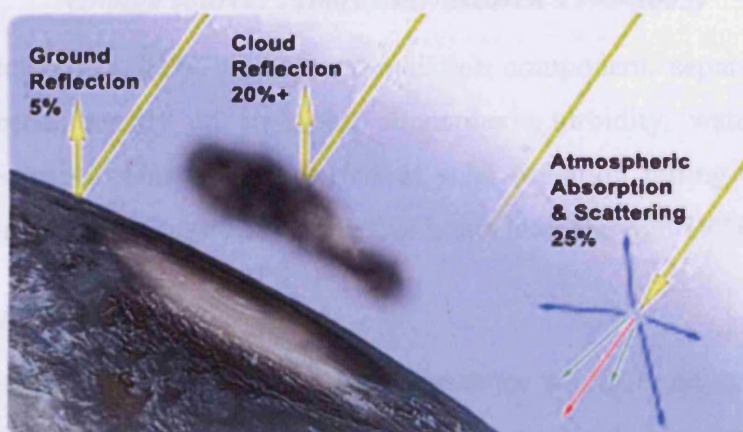


Figure 3-5: The atmospheric influences on solar radiation.
(Image source: square1 website)

3.3.2 Direct and Diffuse Radiation

The definition of direct solar radiation has been known as “Beam Radiation”. Beam radiation is that amount of solar radiation received from the sun without any direction change through the atmosphere.

Diffuse radiation is solar radiation received from the sun after its direction has been changed by scattering and/or reflection by various atmospheric particles (Duffie 1974).

Figure 3-6 indicates how the atmosphere scatters radiation of different wavelengths. Also it shows that blue light arrives from all surrounding space after scattering while other colours arrive almost directly from the sun and that is why we see the sky dome in blue colour (Chauliaguet 1977).

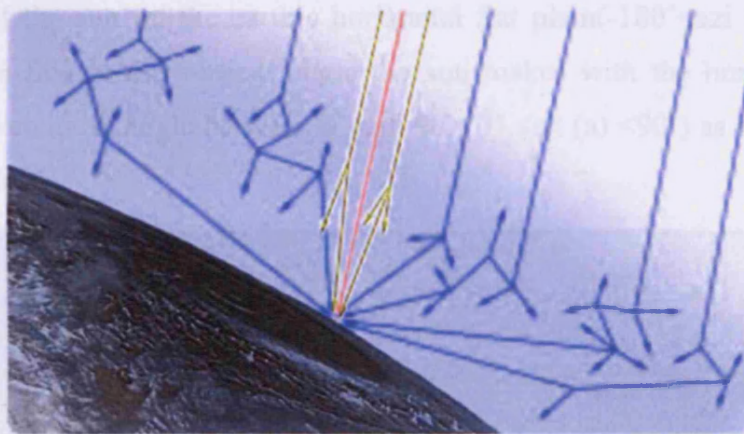


Figure 3-6: Different lights scattering based on their wavelengths.
(Image source: square one research 1998-2003)

As Sayigh declared in 1979, the diffuse radiation component, separated from solar radiation, depends mostly on air mass, atmospheric turbidity, water vapour, dust content and aerosols. This is almost 16% of solar radiation falling on a horizontal surface at noon, it may rise to 25% some five hours later (Sayigh 1979).

3.3.3 Daylight and Sunlight

When referring to visible radiation, or light, the terms sunlight and daylight are often used to distinguish between direct and diffuse radiation. Daylight refers to the amount of available skylight or diffuse radiation in the entire sky dome, which directly affects

illumination in buildings. Illumination is a function of available skylight or diffuse radiation and the size of window through which natural light can penetrate.

3.4 The Basics of Solar Geometry

3.4.1 Solar Azimuth and Altitude`

Successful solar building design also requires knowledge of site location, orientation and solar geometry. It is necessary to match design values with this knowledge to make the right decisions for conceptual building design. Although other climatic factors are very important, site and solar geometry play key roles for environmental building design.

From a site perspective solar position mainly concerns the solar azimuth and altitude. The azimuth of the Sun is the horizontal angle from true north to the line of observation of the sun on the earth's horizontal flat plain ($-180^\circ < \text{azi} (e) < 180^\circ$). The altitude of the Sun is the vertical angle the sun makes with the horizontal ground plane. It is given as an angle between 0° and 90° ($0^\circ < \text{alt} (a) < 90^\circ$) as shown in figure Figure 3-7 below.

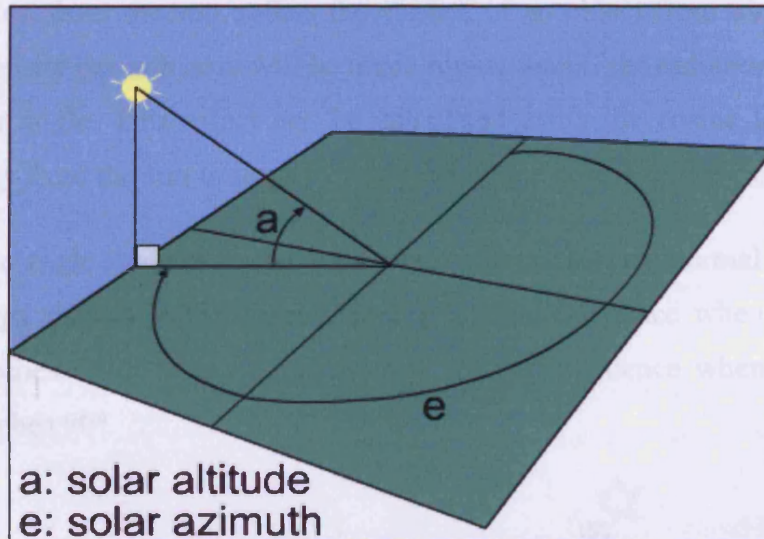


Figure 3-7: Solar Altitude and Azimuth

(Image source: <http://www.jelsim.org/content/applets/solar/>)

As the Sun's position in the sky is not fixed, the position of the sun at any specific date and time has to be calculated. The Earth's axis of rotation and its orbit around the Sun are the basis of the calculation, which for normal design use need not be

complicated. However one can rely on solar tables or computer generated sun-path diagrams to predict the Sun's position, as shown in Figure 3-8.

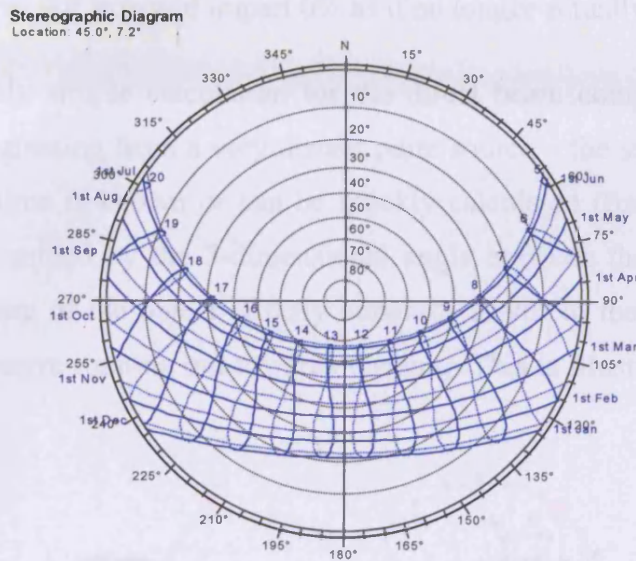


Figure 3-8: Computer generated Sun-path diagram for the 45° latitude of France (Image source: square one research 1998-2003)

3.4.2 Direct Angle of Incidence

When radiation from the sun strikes the surface of an object from directly front-on, the energy density per unit area will be much higher than if the radiation struck from a much greater angle. This effect can be calculated using the cosine law, where the radiant energy from the sun is simply multiplied by the cosine of the incidence angle.

The incidence angle is always calculated relative to the surface normal of each plane. Radiant energy density is at its maximum at normal incidence when the incidence angle approaches 0°. It is at its minimum at grazing incidence when the incidence angle approaches 90°.

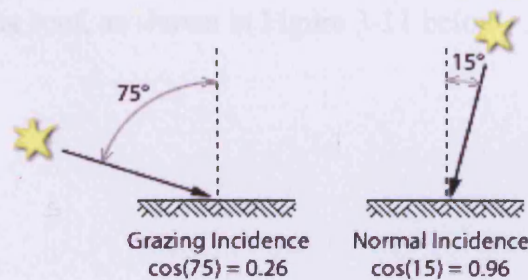


Figure 3-9: The effect of incidence angle, illustrating the cos law. (Image source: <http://www.squ1.com/>)

In the examples shown above, when the radiation strikes at 75° it imparts only 26% of its energy to the surface. At 15° it imparts 96% of its energy. Obviously at 0° it would impart 100% and at 90° it would impart 0% as it no longer actually strikes the surface.

This is a relatively simple calculation for the direct beam component as it can be considered as originating from a very distant point source – the sun – whose position at any date and time is known or can be quickly calculated (Szokolay 2004). Thus incidence is determined by the 3-dimensional angle between the surface normal (a line from the centre of the object directly outwards at 90° to the surface) and a line from the object centre running out towards the sun. This is illustrated in Figure 3-10 below.

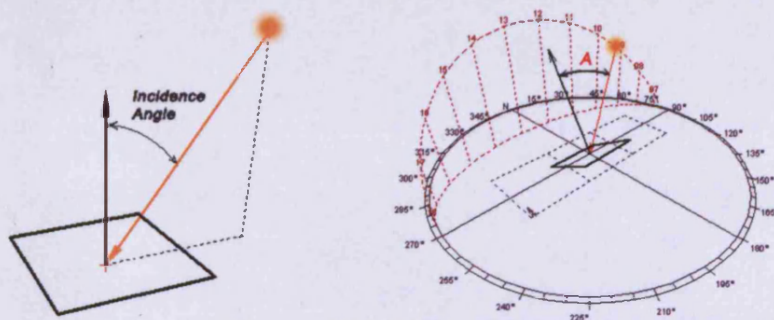


Figure 3-10: The incidence angle is the 3-dimensional angle between the surface normal and the current Sun position.

(Image source: <http://www.squ1.com/>)

This is an important concept as diurnal and seasonal changes in sun position will affect surfaces at various orientations quite differently, especially at mid-latitudes. For example, if a vertical equator-facing window is compared to a flat roof, at noon in winter the sun is lower in the sky – thus closer to normal incidence for the window but closer to grazing incidence for the roof. In summer when the sun is much higher in the sky, at noon it is closer to grazing incidence on the window and closer to normal incidence on the roof, as shown in Figure 3-11 below.

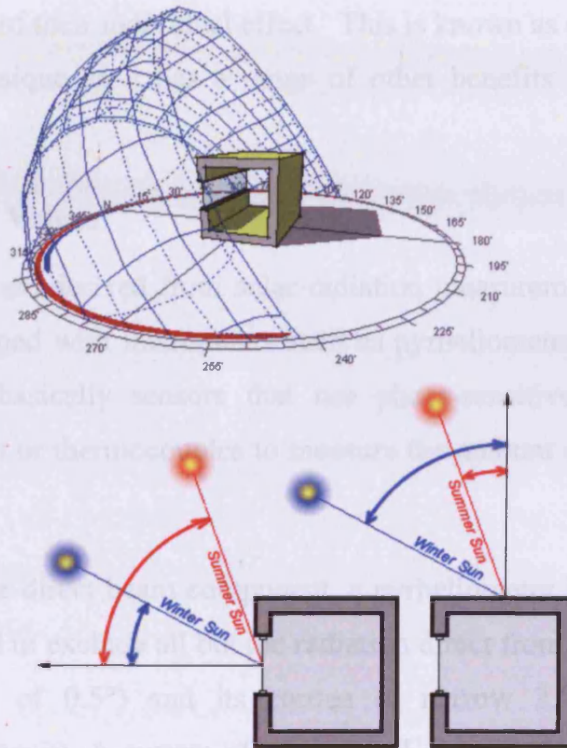


Figure 3-11: As the daily Sun-path changes with season, incidence angles increase on vertical windows in summer whilst reducing on a horizontal roof.
 (Image source: <http://www.squ1.com/>)

This is only a simple example, however it does illustrate that surfaces at different angles will be more sensitive to some parts of the sky than others.

3.4.3 Diffuse Angles of Incidence

Unlike direct radiation, which comes from a very specific part of the sky, diffuse radiation arrives from the whole sky. As shown in Figure 3-11, the angle of the surface will mean that, irrespective of the distribution of radiation over the sky dome, some parts of the sky will contribute more than others simply due to incidence effects.

For a horizontal surface under a uniform sky, the diffuse radiation arriving from a segment at the zenith of the sky will impart greater energy than a segment of equal area at the horizon. This is simply because the light from the zenith arrives close to normal incidence on a horizontal surface whereas that from the horizon is closer to grazing incidence.

Whilst it is possible to generate a calculus equation for any given surface for the continuous integral of the diffuse contribution from each part of the sky, it is usually much quicker to simply break the sky up into a large number of small segments, and

then calculate the sum of their individual effect. This is known as sky subdivision and is a widely used technique as it has a range of other benefits which will also be explained.

3.5 Solar Radiation Values

Solar radiation values are derived from solar radiation measurements available from weather stations equipped with instruments such as pyrheliometers, pyranometers or solar colorimeters – basically sensors that use photo-sensitive material, charge-coupled devices (CCD) or thermocouples to measure the amount of radiation coming from the Sun.

To directly measure the direct beam component, a pyrheliometer is placed at the end of a long tube designed to exclude all but the radiation direct from the Sun (which has an apparent diameter of 0.5°) and its corona (a narrow 2.5° annulus of sky immediately surrounding it). A system of motors and gears is then used to keep the tube pointing directly at the Sun throughout each day. Because of their moving parts, such systems can be expensive and prone to malfunction.

A pyranometer on the other hand is used for measuring solar irradiance from the entire sky falling on a flat planar surface. When mounted and horizontally facing upwards, it measures *global horizontal* solar irradiance, the sum of the direct beam radiation and the diffuse horizontal. This is the simplest and least expensive value to measure; so many weather stations simply use two horizontal pyranometers - one fully exposed to the sky and the other shaded from just the direct solar component using either a mobile shade or a curved strip of metal that follows the path of the sun. Figure 3-12 shows some examples of these types of equipment.



Solar Tracker



Pyranometer



Shaded Pyranometer



Multiple Units

Figure 3-12: Different equipment used for solar radiation measurements.

(Images taken from <http://www.eppleylab.com/PrdShadingDevices.htm>)

3.5.1 Deriving Direct and Diffuse Values

To calculate direct beam radiation, the diffuse horizontal value must first be subtracted from the global horizontal value to obtain the direct horizontal solar radiation. To convert from incidence on a horizontal surface to incidence on a theoretical surface normal to the direct beam, the resulting value must be cosine-corrected to reflect the incidence angle the direct sun makes with the horizontal surface at the exact time of the measurement. Solar position is usually given as an azimuth (relative to North) and an altitude (relative to the ground plane). For a horizontal surface, whose normal points directly up towards the zenith of the sky, the incidence angle of the sun in degrees can be taken as $90^\circ - \text{SolarAltitude}$. Thus, to obtain direct beam radiation, the direct horizontal solar radiation must be divided by the cosine of the instantaneous incidence angle.

Depending on the type of pyranometer used, this can sometimes be problematic as values for the direct component of global horizontal radiation are highly dependant on the incidence angle of the sun as it moves through the sky. Recorded values are typically integrated over time to give period-averaged values or sampled instantaneously at regular intervals, so it is critical that solar altitude is calculated at the precise times at which each recording was made. This is because the results are highly sensitive to even the smallest error, particularly at very low altitudes. This is even more of a problem if the recordings are integrated, as the same hourly value will pertain to both the time just after sunrise and to that up to 59 minutes later – during which time the solar altitude will have changed considerably.

Such problems can be overcome by using a more expensive cosine corrected pyranometer. As shown in Figure 3-13, these can use special lenses to focus radiation onto the sensor regardless of direction, and require built-in correction factors to account for focal variation. However, these sensors essentially measure global radiation, not global horizontal. This makes the derivation of the direct beam component much simpler, becoming a straight-forward subtraction. However, as hourly weather data for many locations is often NOT readily available from recognised sources, it is usually good to confirm the type of recording equipment used before applying corrections and deriving the various components.

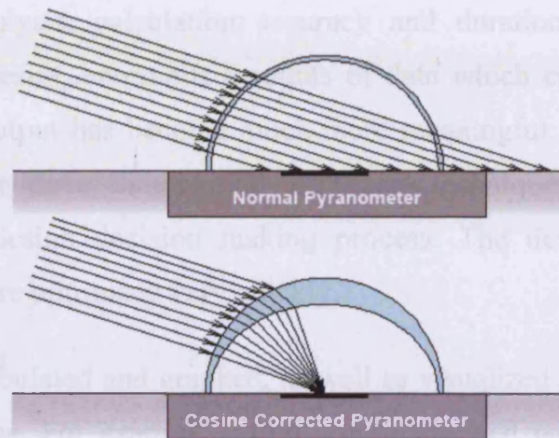


Figure 3-13: The difference between normal and cosine corrected pyranometers.
 (Image source: <http://www.squ1.com/>)

This issue has further implications when calculating radiation incident on surfaces, however these are explained later in the work.

3.5.2 Global Radiation

Global differs from global horizontal in that it is a theoretical maximum amount given as the sum of direct beam and diffuse horizontal. Obviously no single surface can always be simultaneously horizontal (collecting diffuse horizontal) and normal to the direct radiation (collecting direct beam). As a result, this value is not meant to represent the maximum amount of radiation that can *fall* on any specific surface, but simply to indicate the total amount of instantaneous solar radiation *available* at any time.

3.6 Sources of Solar Data

Local solar data is usually available from a local metrological station, United Kingdom Met Office Data sets (UKMO), European Space Agency's data centre (ESA), the National Aeronautics and Space Administration's data centre and solar observatory (NASA), various satellite databases (NASA 2003) and the European Solar Atlas (Met Office 2004). Also the SOHO (Solar & Heliospheric Observatory) project is the Solar and Heliospheric Observatory project is being carried out by the (ESA) and (NASA) space project for exploring the Sun and its geophysical affects over the Earth since 1995 (bernhard 2003)

Hourly weather data itself may not be directly applied for any calculation manually in terms of modern building design methods. As the computer evolves especially in

building design analysis, calculation accuracy and duration have been changed dramatically. As a result, enormous amounts of data which can be used have been improved and the output has become much more meaningful. The outlet results are produced in two or three dimensional simulated techniques by comprising and facilitating of the design decision making process. The design decision making process becomes more optimized very quickly.

These data can be tabulated and graphed, as well as visualized and considered as part of the design process. For example, using a computerized weather tool created by Square One research one can visualize various weather data in colourful two or three dimensional graphs, heliograms, maps, charts, tables, masks etc. as Figure 3-14 shows Cardiff's sun path diagram. This indicates the sun's exact positions over the sky dome on 12th March at 10:00 am o'clock, Horizontal Sun Angle of 139° and Vertical Sun Angle of 146.2° as well as the Sun's position; altitude of 27.0° and azimuth of 139.50°.

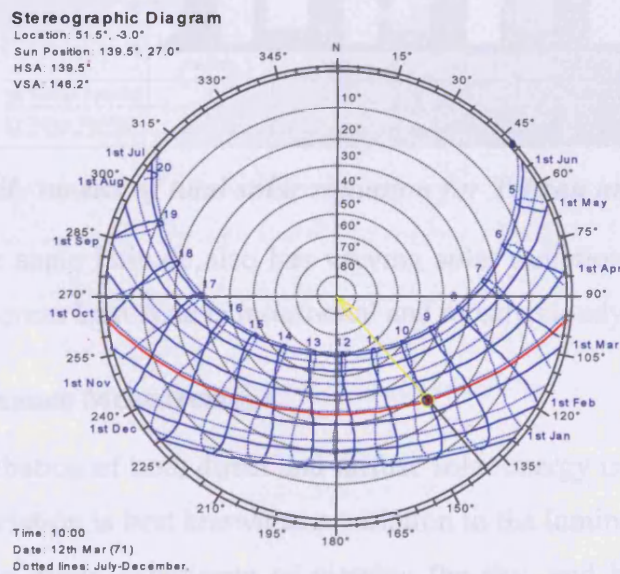


Figure 3-14: Sun path diagram for the cities of Cardiff, South Wales

Solar data measurements around the world vary with the season, latitude and locations. However, areas of equal latitude do not necessarily receive the same amount of solar radiation (direct and diffuse) as illustrated by the graph in Figure 3-15 created using data from Dickinson’s Solar Energy Technology Handbook, 1980 (Dickinson and Cheremisinoff 1980). It clearly shows Tehran and Tokyo, although exactly same latitude of 35.60° N, have very different solar radiation data and whilst having the same amount of solar radiation in January they do not experience similar weather conditions. For instance Tehran has a very low annual precipitation rate compared to Tokyo.

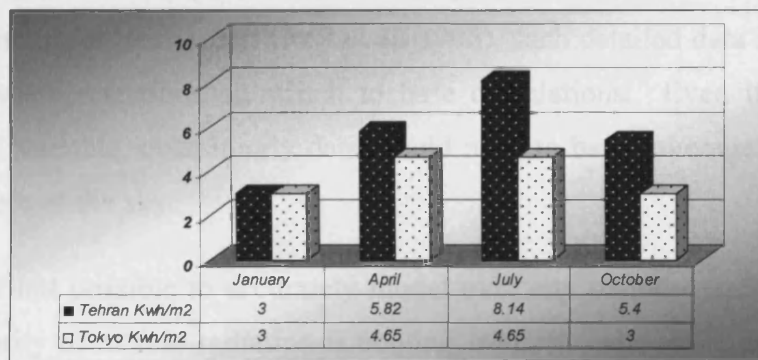


Figure 3-15: Daily means of total solar radiation for Tehran and Tokyo (35.60° N).

Regarding of the same latitude also has varying solar radiation e.g., Middle East is mostly sunny whereas East Asia is monsoonal and mostly cloudy.

3.7 Sky Luminance Measurement

The radiant distribution of both direct and diffuse solar energy is not uniform over the whole sky. Its variation is best known as a variation in the luminance of the sky. This is a matter of the direct experience of viewing the sky, and has also been studied systematically. For a clear sky, the corona around the Sun obviously dominates the overall distribution with the rest of the sky being much less luminous. In this case the corona moves through the sky each hour with the Sun. Similarly, as clouds gather and disperse, pretty much any area of the sky can be at times bright or dark, as shown in Figure 3-16 below. This makes for very dynamic conditions which can change significantly within just a few minutes.



Figure 3-16: Examples of variation in the luminance distribution over the sky dome under different sky conditions.

(Image source: <http://www.squ1.com/>)

Whilst Task 21 (Daylighting in Buildings) of the IEA Solar Heating and Cooling Programme included a number of research projects in which real-time recordings of actual sky conditions were taken (Roy et al. 1995), such detailed data is not available from most weather stations on which to base calculations. Even if it were, with conditions so variable, even hourly data would need to be an average of the minute-by-minute state of the sky.

Thus, as it is not possible to accurately model over any period exactly where in the sky the majority of diffuse radiation is coming from, it make sense that calculations are based on long-term average conditions. For this purpose, CIE have developed standard mathematical models of sky illuminance under different sky conditions (Commission Internationale 1973). Figure 3-17 below illustrates the CIE Standard Clear, Intermediate and Overcast Sky models. A further Uniform Sky model can be used, but is not illustrated below as all areas of the sky are taken to emit the same level of radiation.

The computer simulations that will be referred to later in this thesis require knowledge of the variation in diffuse radiance over the sky dome across the whole solar spectrum. As there is no available data for this, the distribution of radiance will be assumed to be the same as for luminance. It should be emphasised that this refers only to the proportions of the radiance in different regions of the sky, not to the overall amount, for which measurements are, of course, available.

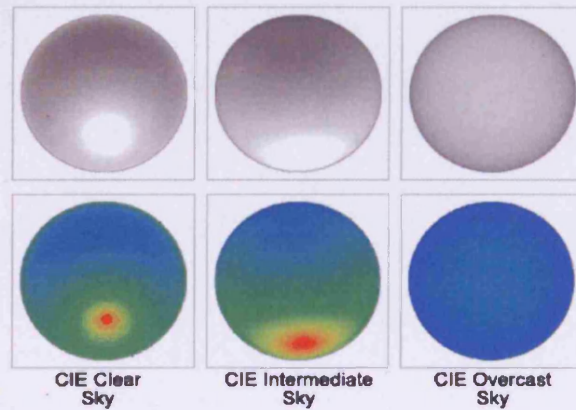


Figure 3-17: The three major CIE sky models.

(Image source: <http://www.squ1.com/>)

CHAPTER FOUR

Predicting Received Solar Radiation on Surface

4 Predicting Received Solar Radiation on Surface

4.1 Calculating surface Irradiance

In many climates, insolation on the external surfaces of buildings is a major source of internal heat gain. This can occur through both exposed glazing and the opaque fabric of the building if it is not adequately insulated.

Traditional glazing and shading strategies tend to treat each façade homogeneously, assuming the entire surface to be similarly exposed to solar radiation. However this is not always the case, especially with curvilinear façade systems and more complex building shapes where small angular differences and self shading can result in significant variation. Similarly, complex site overshadowing by surrounding buildings in dense urban environments can also create large differentials in the distribution of insolation over each façade.

If this information is available to the designer sufficiently early in the project it can be an important influence on both the building form and its exposed fabric. Knowing which parts of a surface are subject to high levels of solar stress, and which aren't, can yield significant economies in the application of appropriate façade systems, allowing the designer to specifically target problem areas and develop localised and optimised solutions. In colder climates the aim is more often to make best use of a limited resource, both for utilising direct gain and for optimising the location of photovoltaics and solar collectors.

4.2 Surface Mapping

Mapping the availability of natural light and/or solar radiation over external building surfaces has been addressed by a number of other researchers. Principle among these is the work of John Mardaljevic using Radiance to map irradiance levels distributed over dense urban cityscapes (Mardaljevic and Rylatt 2003). Figure 4-1 illustrates the kind of analytical images that can be generated using Mardaljevic's methodology.

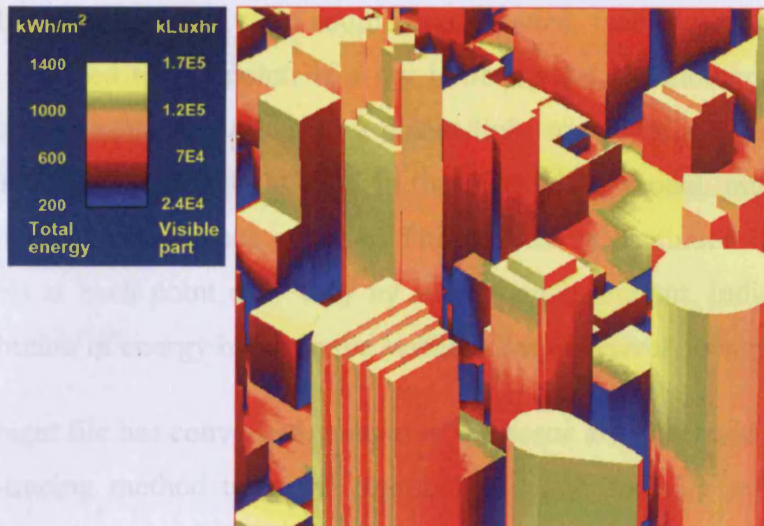


Figure 4-1: An example of the work of John Mardaljevic, using Radiance to map irradiance levels over building surfaces.

These images provide useful guidance for designers, but require human interpretation and, in the case of Mardaljevic's ICUE system, actual intervention in order to determine absolute values on specific surfaces. The next section discusses this in detail and proposes an alternative approach that is more suitable for the reverse computation.

4.3 Details of the Methodology

The Radiance software takes as input a detailed geometric description of building surfaces, their colour and materiality as well as a description of the distribution of light over the sky dome and/or other luminous surfaces in the model. It then generates an ambient file containing ambient light levels at sampled points over each surface in the model. The number and location of points on each surface can be influenced by variables set by the user, but are essentially based on the spatial subdivisions found in the octree file and the ratio between the largest and smallest surfaces in the model. If adjacent points on any surface are found to vary significantly on level, additional super-sampled points will be added between them to better quantify the degree of variation.

The ambient levels at each point are determined iteratively using a radiosity-based technique in which rays are sprayed both directly to each light source in the model and spherically from each point to determine the diffuse and inter-reflected

component. If a ray reaches a sight source unobstructed, then the direct contribution of that light is added to the point. If a ray is obstructed by another surface in the model, the ray is treated as having hit a planar light source with a luminance value equal to the average ambient light level in that part of the model, multiplied by the reflectance of the struck surface material. This process is continued iteratively until the light levels at each point only vary by a very small amount, indicating that the radiant distribution of energy between the surfaces has effectively converged.

Once the ambient file has converged, images of the scene are generated using a hybrid radiosity/ray-tracing method to enable transparency and specular reflections to be accommodated. Rays are sprayed from a user-specified eye position into the scene, one for each pixel in the image. On hitting transparent or specular surfaces, additional sub-rays are generated and traced to extinction. If a ray hits an object in the model, the ambient file is interrogated to determine the average light level at that point and, in exactly the same way as in the ambient file, this is multiplied by the reflective properties of the intersected surface. The final value at the pixel is then the sum of contributions from the original ray as well as any sub-rays generated. Radiance is unique in that it can store high dynamical range values for both radiance and irradiance at each pixel, instead of just an RGB colour triplet.

4.4 Instantaneous or Cumulative Skies

Radiance is usually used to calculate instantaneous light levels either reflected off surfaces (luminance) or falling on surfaces (illuminance) under a given sky condition. This sky condition is typically generated from one of the CIE standard sky models together with a total sky illuminance value. If, instead of total sky illuminance, total sky irradiance were used, then the resulting values on each surface would be reflected or incident radiation instead of luminance or illuminance. In this way it is possible to use the Radiance software to calculate the radiant distribution of solar energy over surfaces.

Now, just as total light levels at any point can be calculated by adding the effects of multiple distinct artificial light sources, one can imagine that if multiple Sun positions were specified, the resulting radiation levels would be additive sum of all Suns. When dealing with solar radiation, exposure over time is a useful value. This can be simulated by adding, for example, a Sun source for each hour of the day. This would

mean a series of solar sources travelling through the sky from east to west. If this were done for all daylight hours over the year, then a sky distribution representing the total annual cumulative solar radiation could be generated. This is exactly Mardaljevic's approach.

4.5 An Image-Based Approach

The results of either the lighting or cumulative solar radiation analysis is a 2D image, formed by an array of pixel values in column and row format. Any association of individual pixels with the specific surfaces they represent is lost. In order to determine the value on a specific window in the model, a human viewer must first visibly identify the window within the image and then locate a mouse pointer on one of the pixels that form its images. The value at the selected pixel can then be displayed.

This is very useful in the hands of a designer as they can interpret the displayed value and the variation in colour around the displayed pixel in order to get a 'feel' for the likely average value over the whole surface. It also allows them to do this quickly for the many different areas of the image. However, this system is not useful if the aim is to computationally determine either average or total values over specific objects.

4.6 An Object-Based Approach

In many cases, the reason for doing this kind of analysis is to calculate solar gains over a specific set of surfaces – a series of windows over a façade for example. An image-based approach makes this very difficult to do automatically as it requires manual interpretation of the image in order to identify the exact pixels to sum for each surface.

An alternate approach is to maintain the link between calculated values and specific surfaces. This can be achieved in Radiance by interrogating the ambient file directly to determine values at particular points within the model. In this way, a program such as Ecotect can be used to generate a series of points distributed over the surfaces of interest in the model, and then each point together with the object's surface normal exported to a file for Radiance to process. Once complete, the resulting irradiance values for each point could be read back in and assigned to the original objects.

Using Radiance has the obvious benefit that it is a highly regarded existing system which deals well with diffuse and inter-reflected light. However, if values for only one window were required, it would still be necessary for Radiance to generate values over the entire defined model, which could include many surrounding buildings and a vast amount of redundant calculation time. Also, as it has been implemented as a series of individual executable programs, real-time management of the creation, analysis and data collection process can be difficult, especially if used within an iterative calculation process that requires performing many hundreds of analysis on subtle changes in geometric and/or surface properties. In these cases the redundant calculation times and the potential for mismanagement of the data is magnified many hundreds of times.

4.7 An Alternate Approach

In order to respond to these issues, an alternate method for the calculation and display of surface insolation has been developed and implemented by the author's supervisor within the Ecotect software (Marsh 1997). This new approach is necessary as it forms the basis by which the effects of shading and obstruction on surfaces can be quantified. This underpins all the subsequent work in this thesis.

The following sections therefore discuss the concept on which this methodology is based as well as showing how it has been extended by the author - and in some ways reversed - to provide a means for the interactive and numerical design of shading devices.

4.8 Incident Radiation

In this research, Ecotect software was used to calculate the amount of insolation falling on model surfaces. The author has worked closely with Dr. Andrew Marsh, the developer of this software, in the testing and application of different solar algorithms so the aim of this section is to explain in detail how Ecotect performs these calculations and the many different factors involved.

4.9 Solar Radiation Values

In Ecotect, incident solar radiation is calculated directly from the geometry of the model using hourly recordings of *direct beam* and *diffuse horizontal* solar radiation

values taken from the currently loaded weather data file. In the weather data file format, the direct beam component of solar radiation (G_{direct}) is given as a value in W/m^2 and is measured on an imaginary surface directly facing the Sun. As the Sun moves through the sky, this measurement surface tracks it so that the direction of incident radiation is always normal (straight on) to it. The diffuse horizontal component (G_{diffuse}) is also given in W/m^2 and is taken as the energy from the entire sky dome that falls on a horizontal surface, minus the effects of direct beam radiation as it hits the horizontal. In fact, all of these values are for the whole of the sky without any obstruction.

It is important to note that insolation refers only to the amount of energy actually falling on a surface, which is not affected in any way by the surface properties of materials or by any internal refractive effects. Material properties only affect the amount of solar radiation absorbed and/or transmitted by a surface.

The total insolation (G_{incident}) on a given surface at any instant is therefore affected only by:

- the angle of incidence of the solar radiation (γ),
- the fraction of the surface currently in shade from surrounding geometry (F_{shad}),
- the fraction of the sky visible from the surface (F_{sky}) and,
- the area of surface exposed to the solar radiation (A_{exposed}).

These factors affect the direct (G_{direct}) and diffuse sky (G_{diffuse}) radiation differently, such that: $G_{\text{incident}} = [(G_{\text{beam}}) \times \cos(\gamma) \times (1 - F_{\text{shad}}) + (G_{\text{diffuse}} \times F_{\text{sky}})] \times A_{\text{exposed}}$

4.9.1 Sky Subdivision

There are many ways to divide up the sky into small segments or illuminance/irradiance zones. Early work by Tregenza suggested that the optimum diameter of a sky zone was approximately 0.2 radians (11.5°) (Tregenza and Sharples 1995). From this work, the Commission Internationale de l'Eclairage (CIE) recommended the use of a 145 segment equal-area subdivision based on 8 equal

altitude bands which, without noticeable error, allows each zone to be considered as approximating a point source (Commission Internationale 1989).

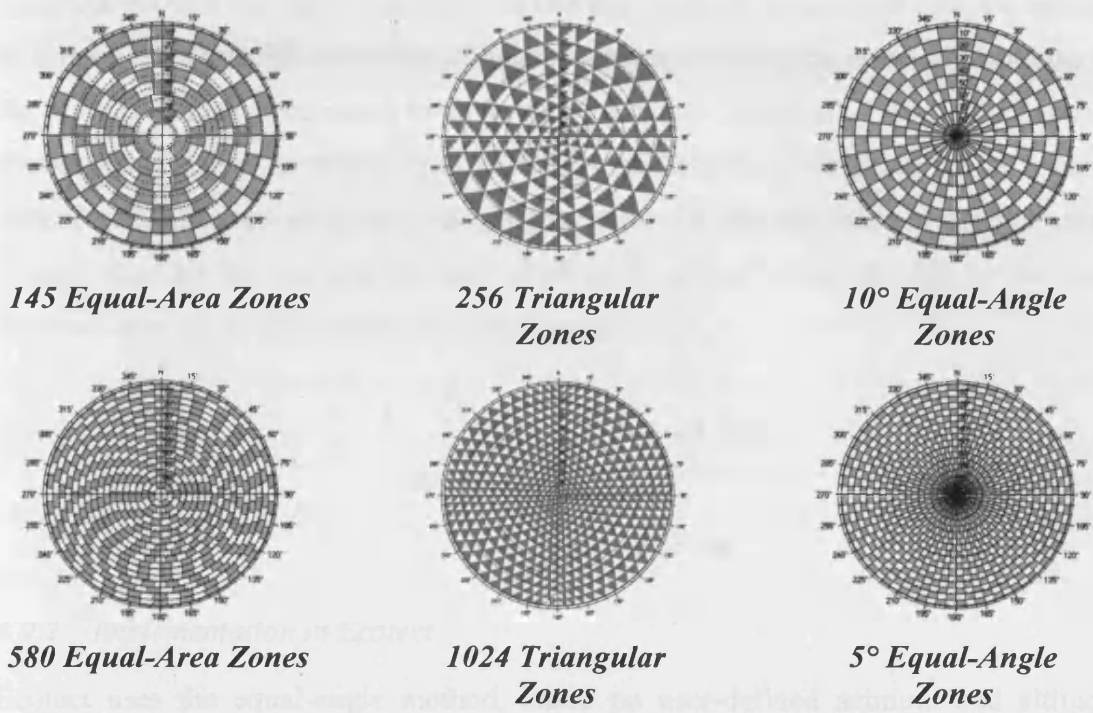


Figure 4-2: Some examples of different approaches to sky subdivision.
 (Image source: <http://www.squ1.com/>)

To define segments, each altitude band has a different number of azimuth segments apportioned such that they each have a roughly equal solid angle. As this technique requires that there be an integer number of segments in each band, it is not possible for each to have exactly the same area – however the variation across all segments is relatively small. This subdivision method is shown on the far-left in Figure 4-2.

As can also be seen in Figure 4-2, it is possible to vary the resolution of this method to accommodate any number of segments. Obviously the variations in area will be greater for some numbers of zones as it is more difficult to evenly apportion them between bands. However the algorithm is very simple so it is possible to test many different numbers in order to minimise this variation if required.

The triangulated subdivision in the centre of the figure is based on methods developed by Song and Kimerling (Song et al. 2002) for the projection of an equal area global grid onto the surface of a sphere by small circle subdivision. In this method the triangular divisions are close to but not exactly equal area, however the greater the number of sub-divisions the lesser the variation.

Figure 4-2 also shows two equal-angle methods on the right. These simply divide the sky hemisphere into azimuth and altitude bands, much like lines of latitude and longitude around the Earth's surface. In this approach, these azimuth bands converge to a point at the zenith, resulting in huge variation between the areas of segments at the horizon (largest) compared to those near the zenith (smallest). When using such a system, the relative contribution of each segment is simply weighted by its relative area. To do this, area-weighted averaging is used such that any value in each segment is multiplied by its area and the sum of all such values is then divided by the total summed area, as shown in the following equation:

$$\text{Sky} = \frac{\sum (Z_{\text{area}} \times Z_{\text{value}})}{\sum Z_{\text{area}}}$$

4.9.2 Implementation in Ecotect

Ecotect uses the equal-angle method, based on user-defined azimuth and altitude angles. This obviously biases accuracy towards the zenith of the sky dome when compared to the horizon as each segment is much smaller in that area. However this is exactly the reason this method was used rather than an equal-area method. First it is much quicker to calculate the exact array index given any solar position (as this is done many tens of thousands of times during an annual calculation, such a consideration is quite important), and second it is more accurate when considering the effects of shading devices immediately above a vertical window - which form by far the majority of shading design conditions.

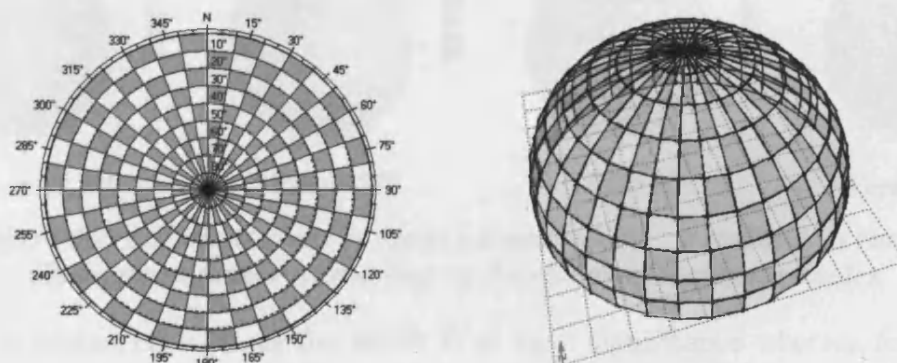


Figure 4-3: 10° equal-angle subdivision showing bias in accuracy towards the zenith.
 (Image source: <http://www.squ1.com/>)

By default, detailed sky calculations in Ecotect are done using 2° angular segments, however even with 10° angular segments this method is still more accurate at the horizon than the standard 145 zone equal-area method based on 12° bands.

4.9.3 Diffuse Incidence Effects

Once the sky has been subdivided, the orientation and tilt angle of any surface can be used to determine which parts of the sky it is actually exposed to. For example a vertical surface, no matter which way it faces, will only ever ‘see’ at best one half of the sky dome - meaning that it will only ever receive a maximum of one half of the available diffuse component. A horizontal surface that faces upwards, however, could see it all.

However for a horizontal surface, any light from the zenith of the sky arrives normal to that surface whilst light from the horizon arrives at grazing incidence. For a vertical surface the reverse is true – light from the zenith arrives at grazing incidence whilst light from the horizon arrives along its normal. This means that the area of the sky that contributes most to any surface depends greatly on its tilt angle. Figure 4-4 below shows a surface at different inclinations and its corresponding incidence angle effect mapped over a mask. This is simply the cosine of the incidence angle the geometric centre of each sky segment makes with the surface normal.

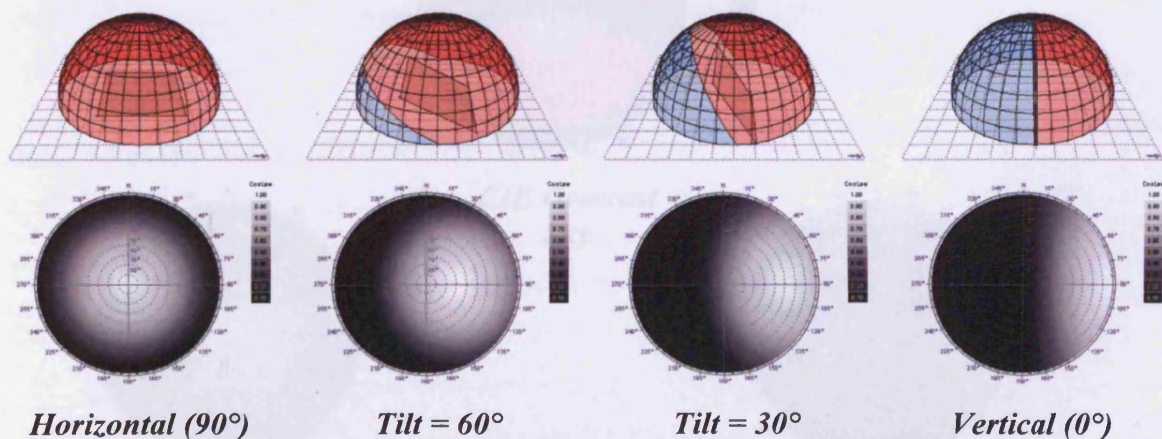


Figure 4-4: Different areas of the sky dome ‘visible’ to surfaces at various tilt angles together with a map of the effects of incidence angles.

Thus, for horizontal surfaces the zenith is of most significance whereas for vertical surfaces it is those sky zones closer to the horizon and directly in front.

4.9.4 Sky Radiant Distribution

The CIE Standard Overcast Sky distribution, taken as representative of long-term average cloudy sky conditions, assigns sky luminance values at the zenith three times greater than those at the horizon. Assuming a close to linear relationship between luminance and radiance, this means that under overcast conditions the zenith has a much greater overall contribution to diffuse solar gains than the horizon. Thus, for a vertical surface that is exposed to half the sky, incidence angles mean that the zenith contribution is lost – making the maximum possible diffuse radiation available on an overcast day only 40% of that available to a horizontal surface (this is explained further in the Vertical Sky Component section).

To illustrate this, Figure 4-5 below shows an example CIE Overcast Sky distribution together with incidence angle effects for a horizontal and vertical surfaces. To obtain the unobstructed diffuse radiation incident on either surface, each zone in distribution map is multiplied by the incidence angle factor in the corresponding zone of the incidence mask. This clearly shows why vertical surfaces receive significantly less than half the radiation available to the horizontal.

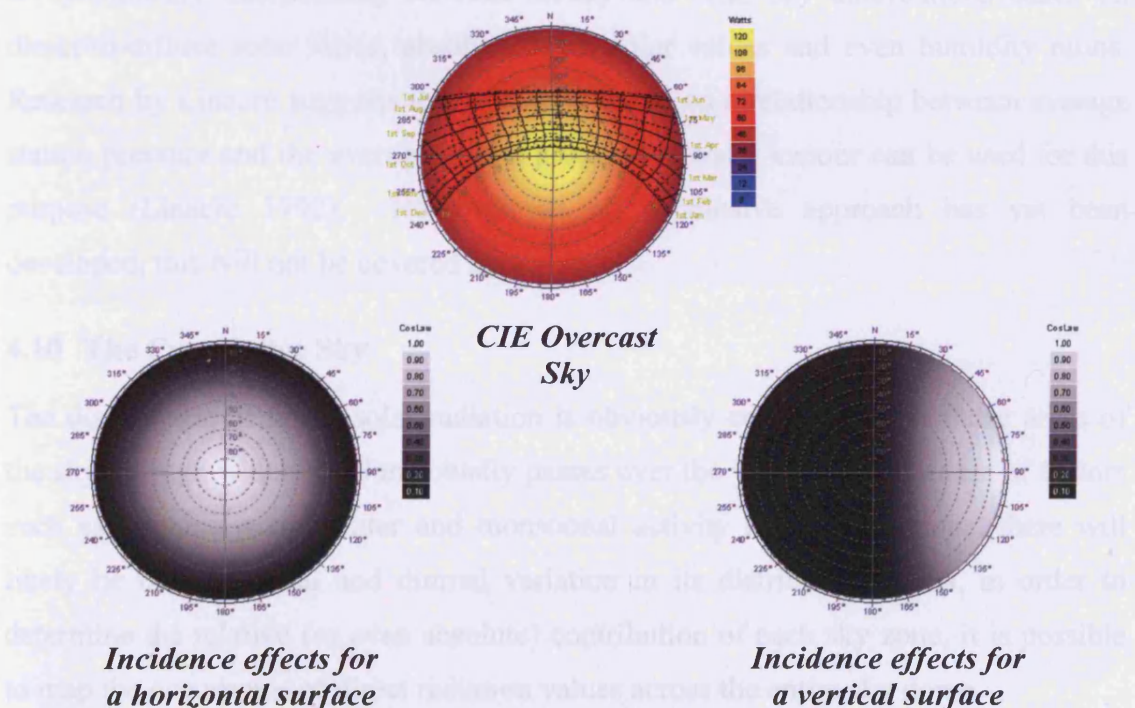


Figure 4-5: An example overcast sky distribution along with different incidence masks.

(Image source: <http://www.squ1.com>)

4.9.5 Relating Skylight and Radiation

Ecotect assumes a linear relationship between the luminous distribution of the sky and its radiant distribution. This is required as there is only limited information on the radiant distribution of energy from a sky dome under different conditions, whilst luminous distribution is relatively well known and data is readily available. Whilst light represents just one part of the full spectrum of radiation from the sun, it is a reasonable assumption that variations in light level over the sky results from obstruction and absorption of the full radiant spectrum and that the overall spectral response of the obstructions and absorption is linearly related to their effect on that part of the spectrum containing light.

This way Ecotect allows the user to choose between either the CIE Overcast or CIE Uniform Sky to govern the distribution of diffuse radiation. The resulting map can be generated for any hour of the year based on the corresponding measured diffuse solar radiation component in the weather file.

To represent conditions more accurately in Ecotect, there is ongoing research looking at dynamically interpolating between cloudy and clear sky distributions based on direct-to-diffuse solar ratios, absolute direct solar values and even humidity ratios. Research by Linacre suggests that a method based on a relationship between average station pressure and the average partial pressure of water vapour can be used for this purpose (Linacre 1992). However, as no conclusive approach has yet been developed, this will not be covered here.

4.10 The Cumulative Sky

The distribution of direct solar radiation is obviously concentrated in those areas of the sky through which the Sun actually passes over the year. Also, because of factors such as cloudiness in Winter and monsoonal activity in the afternoons, there will likely be both seasonal and diurnal variation in its distribution. Thus, in order to determine the relative (or even absolute) contribution of each sky zone, it is possible to map the occurrence of direct radiation values across the entire sky dome.

This requires that the position of the Sun as it crosses the sky each day of the year be calculated and measured direct beam solar radiation values in the weather file at each time apportioned to the sky zone through which it passes. To avoid concentration of

solar radiation in specific zones that correspond to the exact hourly values, Ecotect uses 5 minute time steps (hour/12) and linearly interpolates between hourly recorded radiation values. Where consecutive time steps result in the same sky zone, a zone-averaged value is apportioned.

A radiation map is then formed by summing data for each zone, to give a cumulative sky showing the annual radiant distribution. If this is divided by the number of times the sun was in each zone, an annual average hourly radiant distribution can be displayed - an example of which is shown in Figure4-6 below.

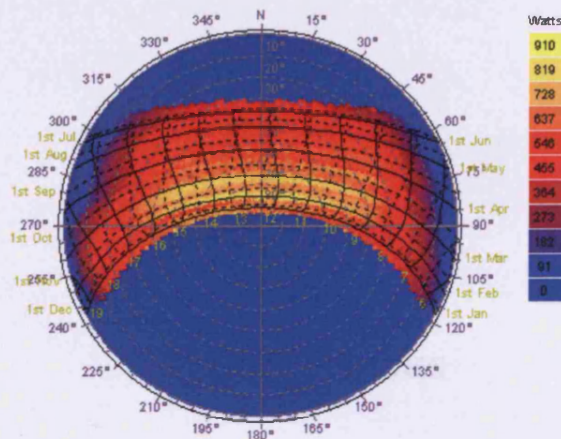


Figure4-6: An example annual averaged hourly direct solar gain cumulative sky distribution.

CHAPTER FIVE

Shading Masks

5 Shading Masks

5.1 Introduction

The aim in most overshadowing analysis is to determine when a particular point in a model is exposed to direct sunlight and when it isn't. This can be done manually by projecting shadows over the model at various times of the day/year and recording whether the point is in shade or not, as shown in Figure 5-1 below. However this can be quite laborious and even then gives information only for the shading from direct solar radiation.

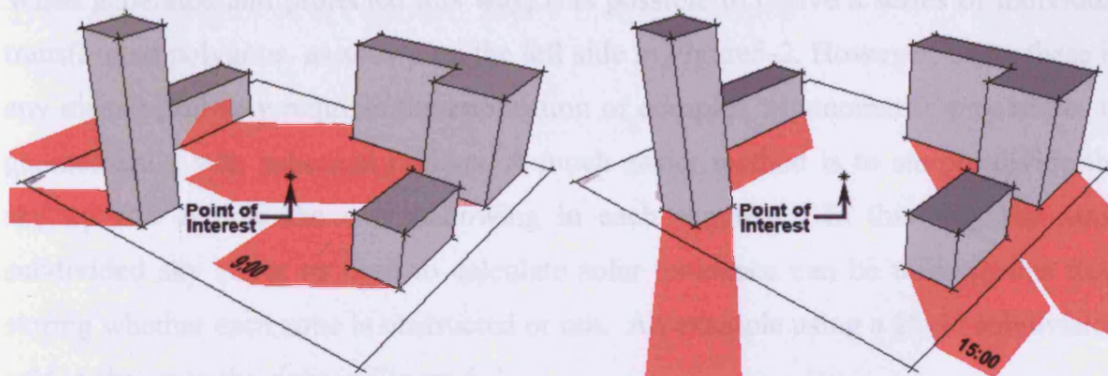


Figure 5-1: Diagram showing shadow projects at different times of the day.
(Image source: <http://www.squ1.com/>)

Visually in the one image, the above method displays shadows over the whole site for a single instance in time. An alternate method is to project the surfaces of all potential obstructions back towards the point of interest and onto a theoretical hemisphere centred at the point of interest. If the resulting spherical shapes are rendered on a sun-path diagram, the individual regions obstructed by each object can be quickly determined. As shown in Figure5-2 below.

If the annual path of the sun is overlaid on the diagram, it is possible in the one image to display the overshadowing for the whole year for a single point in space. Moreover, the diagram also shows the relative area of the sky that is obstructed at that point, thus providing information on the availability of diffuse radiation as well.

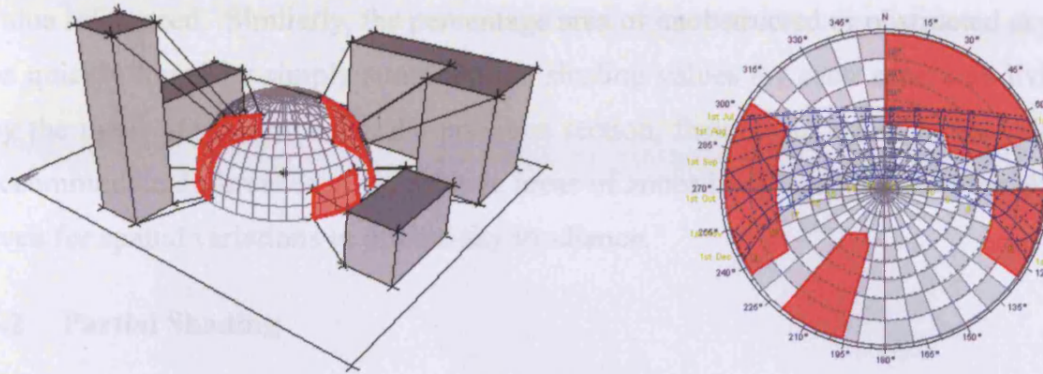


Figure 5-2: Diagram showing site obstructions projected onto an imaginary hemisphere centred on the point of interest.
 (Image source: <http://www.squ1.com/>)

When generated and projected this way, it is possible to derive a series of individual transformed polygons, as shown on the left side in Figure 5-2. However, using these in any meaningful way requires the application of complex trigonometric procedures to geometrically sum spherical regions. A much easier method is to simply divide the sky up and sample the overshadowing in each segment. In this way the same subdivided sky zones as used to calculate solar incidence can be utilised, this time storing whether each zone is obstructed or not. An example using a $2^{\circ} \times 2^{\circ}$ subdivision grid is shown to the right in Figure 5-3.

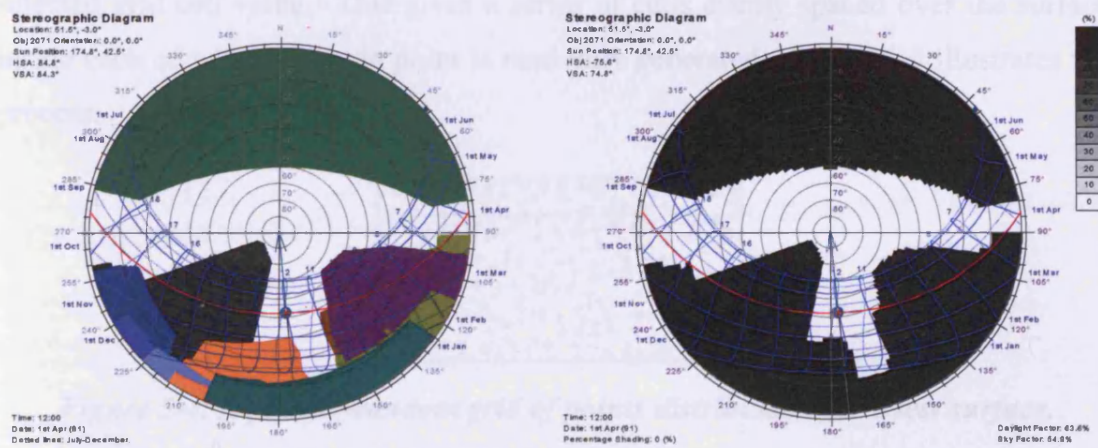


Figure 5-3: Two example shading masks for a shadowed point – on the left shading polygons for each obstructing surface are projected and drawn in the sun-path diagram whilst on the right the sky dome is divided into sky zones, each either shading or not shading.

The benefit of using the sky zone approach is that the resulting data is easy to access and immediately useful in a whole range of numerical analysis. Determining if the point is in shadow at any time simply requires the altitude and azimuth of the sun, from which the specific sky segment can be determined and the appropriate shading

value referenced. Similarly, the percentage area of unobstructed or obstructed sky can be quickly found by simply summing the shading values for each zone and dividing by the total. As described in the previous section, factors can easily be included to accommodate differences in the relative areas of zones in different parts of the sky, or even for spatial variations in diffuse sky irradiance.

5.2 Partial Shading

As shown in the subdivided sky in Figure 5-3 above, the shading mask for a single point is hard edged - it is either in shade at a particular time or it isn't. The shading mask for a planar surface however is more often soft-edged as only a portion of the surface may be in shade at certain times. One of the simplest ways of determining partial shading for a surface is to sample it as a series of distributed points over the surface and average the results into a single mask. This way each sky segment can be used to store fractional obstruction values or shading percentages.

The first step is to generating a grid of pseudo-random points positioned over the window surface. This is done by determining the extents of the object in each of the three major axis and then evenly dividing the two with the largest distance by a user-selected grid cell value. This gives a series of cells evenly spaced over the surface, inside each of which a single point is randomly generated. Figure 5-4 illustrates this process.

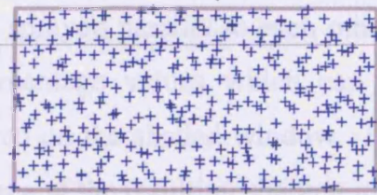


Figure 5-4: A pseudo-random grid of points distributed over a test surface.

The points are randomly positioned in each cell in order to avoid large numbers of rays either exactly lining up with or just missing long linear edges within the model. By introducing a slight randomness, some of rays will travel one side of the line and some will travel the other.

The next step is to generate test rays from each surface point out into the model. If a ray is obstructed by an opaque object, then that point is in shade and assigned a zero value. If a ray is not obstructed, then the point is exposed and assigned a value of 1.0.

If the ray passes through one or more transparent objects, then the point is assigned the product of all the transparency values of the objects through which it passes. The percentage in shade for any set of rays is then simply the sum of all the assigned values for each surface point, divided by the total number of surface points and multiplied by 100, as shown in Figure5-5 below.

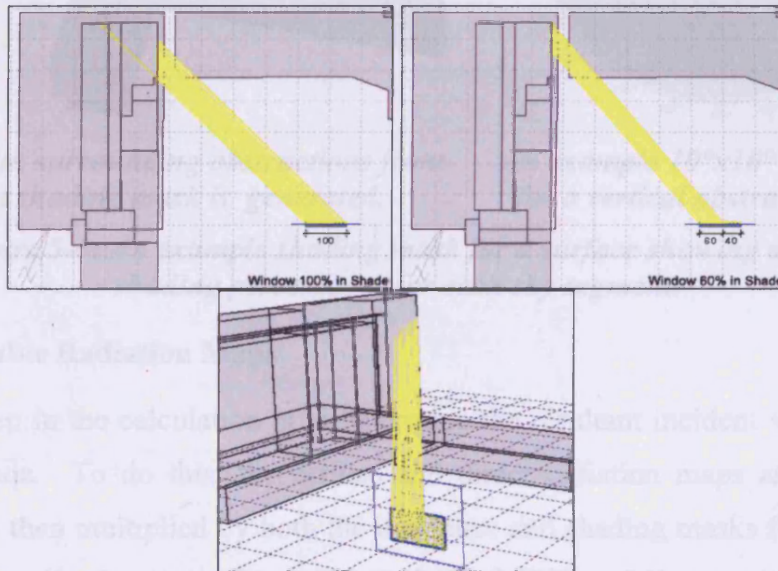
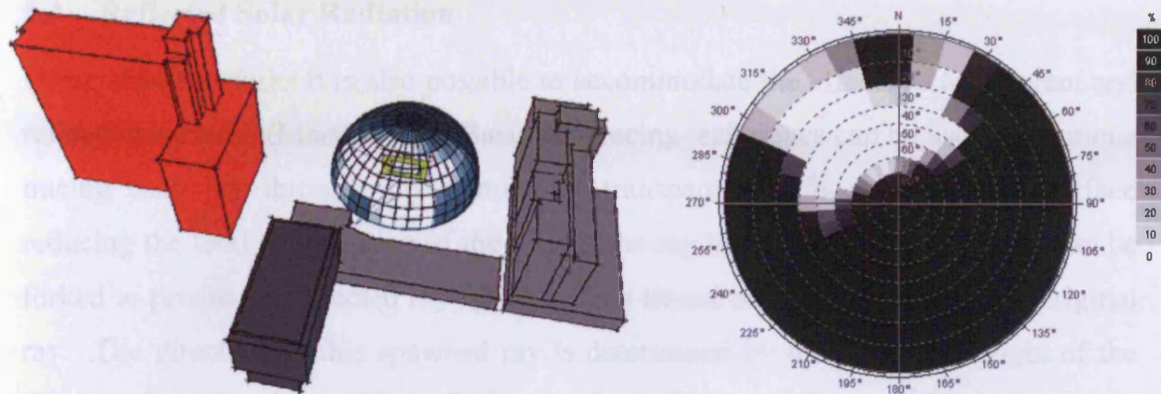


Figure5-5: Examples images showing ray-tracing approach to the calculation of partial overshadowing using rays distributed randomly over each surface.

This process is carried out for each segment in the current sky subdivision. As the sky dome is assumed to be a very large distance away, each sky segment is taken to represent a particular azimuth and altitude angle relative to the surface. This way rays from each surface point are sprayed parallel to each other. The result of this process is an array of shading percentage values which can be shown mapped over an imaginary hemisphere centred on the shaded window. Figure 5-6 shows an example of a simple site configuration and the resulting shading mask for the central window.

To calculate the total incident solar radiation on the surface, the contribution of each sky segment in the solar availability map is assumed to give an overall value. If the cumulative direct and diffuse sky maps contain the summation of total annual values, the result is the total annual incident solar radiation in Watt Hours (Wh). If the sky maps contain time-averaged hourly values, then the result is the average incident solar radiation in Watts (W).



A window with surrounding obstructions from which its shading mask is generated.

An example 10°x10° shading mask for a vertical obstructed window.

Figure 5-6: An example shading mask for a surface showing actual shading percentages for each sky segment.

5.3 Available Radiation Maps

The final step in the calculation is to determine the resultant incident solar radiation on the surface. To do this, the diffuse and direct radiation maps are first added together and then multiplied by both the incidence and shading masks for the surface to give an overall solar availability map, as shown in Figure 5-7.

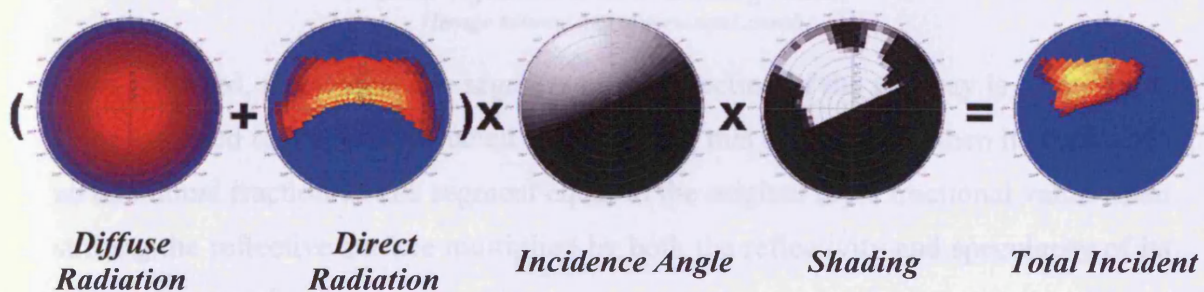


Figure 5-7: The sequence required to generate a solar availability map for any surface and, from it, the total incident solar radiation.

To calculate the total incident solar radiation on the surface, the contribution of each sky segment in the solar availability map is summed to give an overall value. If the cumulative direct and diffuse sky maps contain the summation of total annual values, then the result is the total annual incident solar radiation in Watt Hours (Wh). If the sky maps contain time-averaged hourly values, then the result is the average instantaneous incident radiation in Watts (W).

5.4 Reflected Solar Radiation

Using shading masks it is also possible to accommodate the effects of transparent and reflective surfaces (Marsh 2005). Basic ray-tracing techniques can be used to continue tracing each ray through any number of transparent surfaces, with each surface reducing the total contribution of the ray. If the ray hits a reflective surface, it can be forked to produce a reflected ray which is then traced in the same way as the original ray. The direction of this spawned ray is determined by mirroring the origin of the first ray about the plane of the reflective surface, as show in Figure 5-8 below.

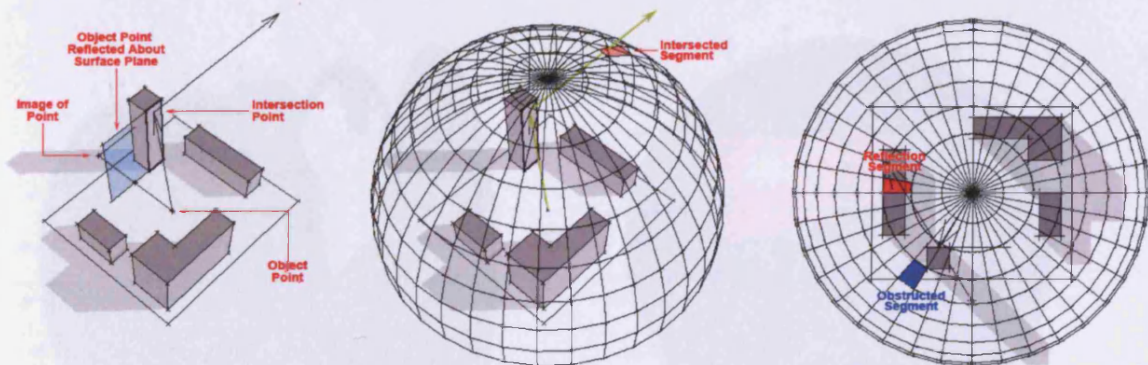


Figure 5-8: The process of tracking the contribution of solar reflections in a shading mask.

(Image source: <http://www.squ1.com/>)

Once reflected, the closest sky segment in the direction of the new ray is determined. If the reflected ray is not obstructed before hitting this sky segment, then it contributes an additional fraction to this segment equal to the original ray's fractional value when striking the reflective surface multiplied by both the reflectivity and specularity of its assigned material.

The sky segment that the reflected fraction is added to is usually in a completely different part of the sky than the original segment being tested. Additionally, it is possible for several reflective surfaces to contribute reflections the same sky segment. In such cases, it is even possible with focusing effects to have a sky segment with a fractional contribution greater than 1.0. To accommodate this, an additional layer of reflected radiation data is added within the shading mask.

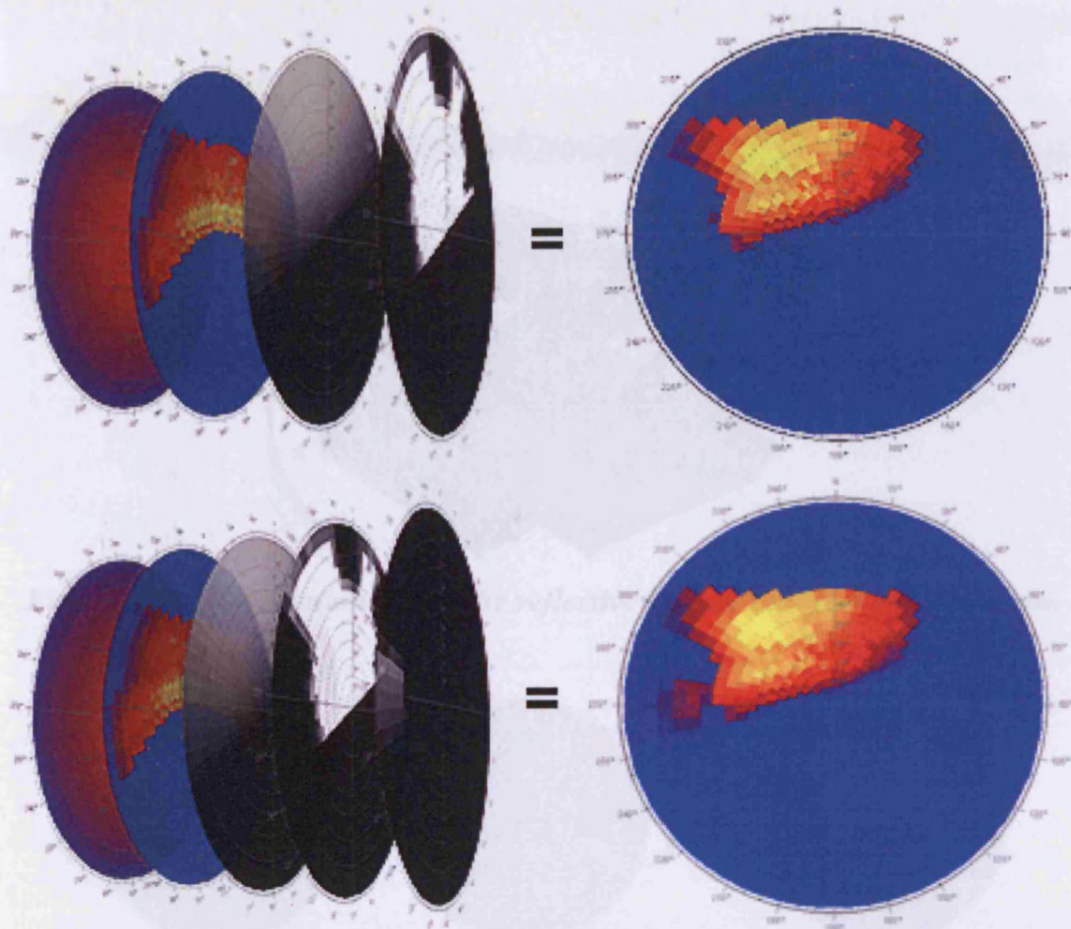


Figure 5-9: Shading masks can accommodate any number of separate layers of information. The above examples show the effect of an additional reflected radiation layer on the solar availability map.

It is also important to note that reflected radiation is in addition to unobstructed radiation. This can be done simply by adding the shading fraction and reflected fraction layers together, before calculating total solar incidence. An example of this process is shown in Figure 5-10 below.

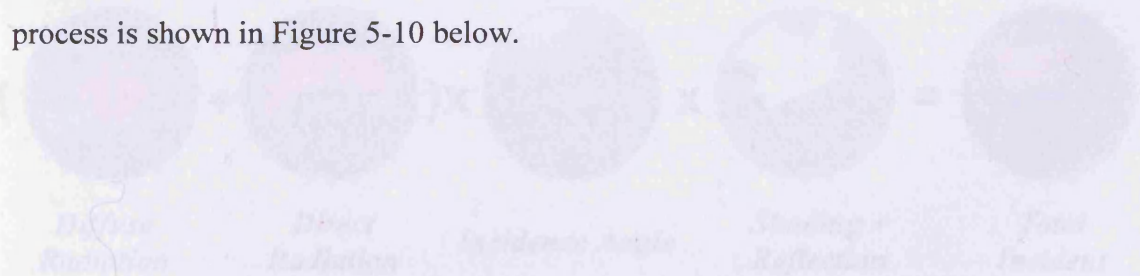


Figure 5-10: The sequence required to generate a solar availability map for any surface.

This figure explains that diffuse radiation is over the entire area but direct radiation is only over the shaded area. However, it has been taken into the account of total however can not be shown as a clear differential value on total incident.

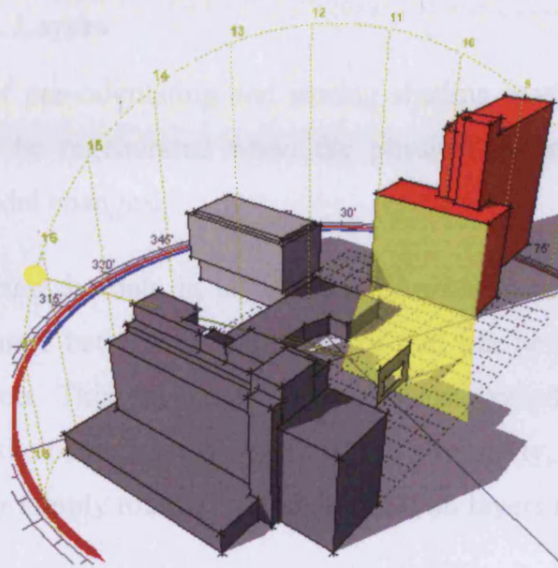


Figure 5-10: The relationship of the reflective surface to the analysis window.

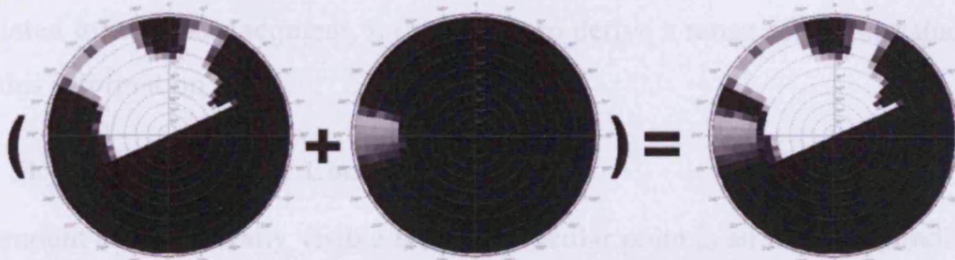


Figure 5-11: The effect of a reflective surface is to add an extra fraction of solar radiation. This can be accommodated by simply adding the shading and reflection layers of the shading mask together.

This means that the same overall mask summation process can be used to generate the new solar availability map, as shown in Figure 5-12.

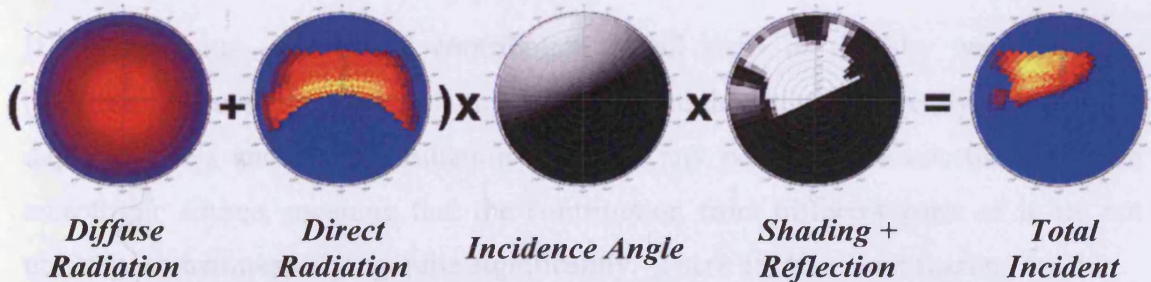


Figure 5-12: The sequence required to generate a solar availability map for any surface

This must be explained that diffuse radiation's layer has different scale than direct radiation's layer but it has been taken into the account in total however can not be shown as a clear differential value on total incident.

5.5 Shading Mask Layers

One major benefit of pre-calculating and storing shading masks for each surface is that they need only be regenerated when the physical geometry, transparency or reflectivity of the model changes.

Additionally, by storing the data in layers, it is possible to re-use elements in each array that do not change between calculations, or that can be simply transformed to match different objects. This way many different time periods can be analysed by simply recalculating the cumulative radiation layers. Similarly, changes in orientation can be tested again by simply rotating the solar radiation layers relative to the others.

5.6 The Application of Shading Masks

Once the sky dome has been subdivided, with incidence and percentage shading calculated for each sky segment, it is possible to derive a range of useful values using only this information.

5.7 Sky Factors and Sky Components

The amount of sky actually visible from a particular point is an important indicator of its exposure to both daylight and solar radiation. A point at the centre of a cricket pitch is likely to 'see' around 90-95% of the sky as there are very few surrounding obstructions. However, a point on a street in a built up urban area will 'see' far less, maybe as little as 20-40%, whilst deep inside a room there may be no view of the sky at all.

If the luminous and radiant contribution of all parts of the sky were isotropic (uniform), then the visible percentage of sky could be used directly to calculate daylight levels and diffuse radiation values at any point. However, the sky is an anisotropic source, meaning that the contribution from different parts of it are not uniform, sometimes varying quite significantly. There are two main reasons for this:

- The passage of the sun across the sky as well as reflection/obstruction by changing cloud formations mean that patterns of relative brightness and dullness are highly dynamic, changing almost minute by minute. As discussed earlier, statistical averages can be used to generate mathematical models of idealised sky types, all but one of which show significant variation near the

current sun position and between the zenith and the horizon – this being of course the CIE Uniform Sky.

- Typically light is used and measured on flat surfaces. Both light and radiation from different parts of the sky arrive at different incidence angles on flat surfaces. Thus - as a result of the cosine law - the contribution of different areas will depend on the orientation of the receiving surface.

The terms *sky factor* and *sky component* refer to the actual contribution of the sky to daylight, after considering both luminous distribution and incidence angle effects. The use of the words *factor* and *component* really depend on the type of value being calculated and its use. A factor is typically used as a modifier to other values, such as lighting or shading level, whilst a component refers to one part of a more complex assembly of values, such as a direct or diffuse lighting component. There appear to be no hard and fast rules as to the type of sky distribution to be used with either term; however they are typically calculated using averaged conditions such as the CIE Uniform Sky or CIE Overcast Sky in order to remove the dynamic effects of any direct beam solar component.

Both values can be calculated directly from the shading mask. Only the shading and incidence angle layers are required, along with the diffuse radiation layer - but with no contribution from the beam radiation layer. As they are given as a percentage value, the diffuse layer is generated such that the sum of all sky segments totals exactly 100, using the user-selected CIE sky model to calculate the relative contribution of each individual segment. The resulting percentage is calculated by multiplying the layers in each segment together and then summing the product of all segments.

5.7.1 *Vertical Sky Component*

The daylight reaching a surface is often expressed as a daylight factor. This is the amount of light that reaches the surface expressed as a percentage of the daylight that would reach a horizontal surface in the same position under an unobstructed sky. The sky is usually taken to be a standard CIE overcast sky, so that only diffuse light is considered. Usually the daylight factor is assessed for horizontal surfaces inside windows. In most calculation techniques, the daylight factor has three components,

the sky component, which is the percentage reaching the surface directly from the sky, the externally reflected component, which is the percentage reaching the surface from the sky but reflected from external surfaces, and the internally reflected component, which is the percentage reaching the surface reflected from surfaces inside the room. However for some purposes it is not the light reaching a horizontal internal surface that is of interest, but the light reaching the window externally. One of these purposes is in assessing the window's "right-to-light". Taking the window to be a vertical surface, the value that is defined is the vertical sky component. In this sense, the Vertical Sky Component (VSC) refers specifically to the value defined by the UK Building Research Establishment (BRE) for use in right-to-light and daylighting calculations.

The VSC is described by the BRE as "*the ratio of the direct sky illuminance falling on the vertical wall at a reference point, to the simultaneous horizontal illuminance under an unobstructed sky*" (Littlefair 1991). It also states that the CIE Standard Overcast Sky model is to be used for the sky illuminance distribution. This means that the reference value for the VSC percentage is effectively the unobstructed horizontal sky component.

If we look at both the incidence angle effect and the distribution of diffuse radiation over the CIE Overcast Sky, as shown in Figure 5-13 below, we see a concentration of radiation at the zenith which arrives at the vertical surface at close to grazing incidence - hence having little effect. The result of this is that the maximum possible overcast sky radiation visible to a vertical surface is not 50% of that on the horizontal plane, but only 40%.

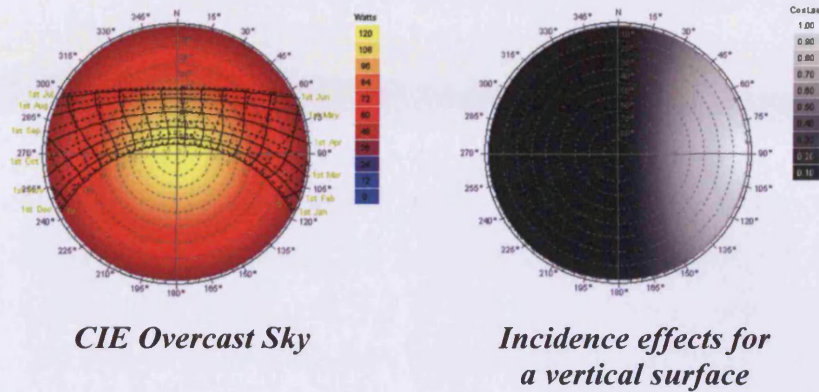


Figure 5-13: The two component shading mask layers for an unobstructed Vertical Sky Component.
(Image source: <http://www.squ1.com/>)

The VSC is used in the UK as an indicator of daylight potential. Planning guidelines from the BRE give minimum VSC values for windows in a range of different situations and use it for comparative testing in more complex highly-overshadowed contexts.

The VSC is calculated from the shading mask in exactly the same way as for a horizontal sky factor using a CIE Overcast Sky. The diffuse layer is generated such that the sum of all segments totals exactly 100 and, once surface shading has been calculated from the geometry of the site, the VSC calculated by summing the product of the diffuse, shading and incidence angle effects layers in each segment. It is important to note that the reflected layer is NOT used as the VSC does not include external reflections of any sort.

CHAPTER SIX

Optimizing Solar collector angle

6 Optimizing Solar Collector Angle

6.1 Introduction

There has been much previous research on the optimization of collector angles for maximum solar exposure. However, the full impact of obstructions and complex site overshadowing is rarely considered. In an increasingly dense urban environment, these issues are critical to the effective utilization of photovoltaics and water/space heating systems at the actual point of use - on the roofs and walls of the buildings in which the power or hot water is to be used.

This chapter demonstrates a technique for solar collector optimization that fully accounts for complex overshadowing situations, as well as both dynamic shading systems (such as that due to deciduous vegetation) and complex load-matching requirements in which the optimization is biased towards a specific range of dates and times. The basis for this technique is presented along with a quantified example of the increased efficiencies possible.

6.2 Collector Efficiency

As demonstrated by Morcos (Morcos 1994) the efficiency of a flat-plate solar collector is based on the amount of both direct and diffuse solar radiation incident upon its surface. Whilst diffuse radiation arrives from all parts of the sky and off reflective surfaces in the environment, direct solar radiation is a much more directional source with significantly higher energy potential. Thus, collectors that dynamically track the current Sun position - thereby keeping the direct incidence angle close to the surface normal of the panel - are significantly more efficient, shown by Neville to be as much as 50% more than a fixed system (Neville 1978). However, it is not always viable or even possible to install tracking systems in all situations.

For a fixed system, the orientation and tilt angle of any flat plate solar collector is a major determinant of its performance. Both of these angles are traditionally based on the latitude (β) of the installation site, oriented towards the equator with a tilt angle equal to β itself for locations less than 40° and $\beta+10^\circ$ for higher latitudes (Bari 2001).

Given the Earth's revolution around the Sun, changing sky conditions throughout the year and the effect of external obstructions, direct solar radiation can be a highly variable source. In many parts of the world local diurnal weather patterns can be measurably periodic, resulting in an uneven distribution of available cumulative solar radiation over different areas of the sky. For example, monsoonal conditions near the equator can bias solar availability more towards the mornings as cloud build-up and rains restrict the available radiation in the afternoons.

With the increasing availability of detailed hourly solar radiation measurements in many countries, it is possible to calculate the cumulative distribution of solar radiation for a site and consider its effect when optimizing solar collector angles.

6.3 Overshadowing Effects

In a dense urban environment, adjacent buildings, trees and other obstructions are likely to impact on the amount of solar radiation falling on any collector surface. In many situations, this loss in efficiency may be small compared to the benefits of locating the collector at or near the point of use - such as on a wall immediately beneath the space being heated or on the roof near the hot water tank. Thus, a detailed consideration of overshadowing is important if photovoltaics, solar hot water and air heating systems are to be used effectively in cities.

The effects of overshadowing can be quite complex. In addition to reducing the overall annual radiation falling on any surface, it is likely that particular obstructions will block the Sun for very specific periods of the day at different times of the year. To maximize collection in these circumstances, it may be necessary to significantly re-orient the collector in order to better face those areas of solar exposure it does have.

Thus, just as local climatic conditions affect those areas of the sky from which solar radiation is available, so too will local site conditions. Just as cumulative solar radiation can be mapped over the sky dome, so too can overshadowing effects for any point on a site.

6.4 Solar Collector Optimization Techniques

Much work is being done on design optimisation algorithms and their application to building systems. Tools such as GenOpt from Lawrence Berkeley Laboratories

(Wetter 2004), and others such as DOT (Vanderplaats 2001) and SimuSolv (Struub 2005), allow for low level optimisation of multiple numeric parameters by linking and invoking different analysis tools as part of an iterative solution.

As this work's initial concern is the translation of analysis results into geometric decision-making and the computational generation of building form to meet performance criteria. The integration of more efficient optimisation techniques will follow as the work progresses; however at this stage a much simpler brute-force approach has been taken.

6.4.1 Hemispheric Sampling

The most obvious way to determine the best angle and orientation for a solar collector is to exhaustively test a wide range of them. This can be done by an iterative process involving analysing and adjusting the angle and orientation in set increments. If this were done in 10 degree increments, a total of 289 ($8 \times 36 + 1$) calculations would be required. These could all be done at once if a small sphere were analysed, with facets corresponding to the angular increments. An example of such a sphere is shown in Figure 6-1.

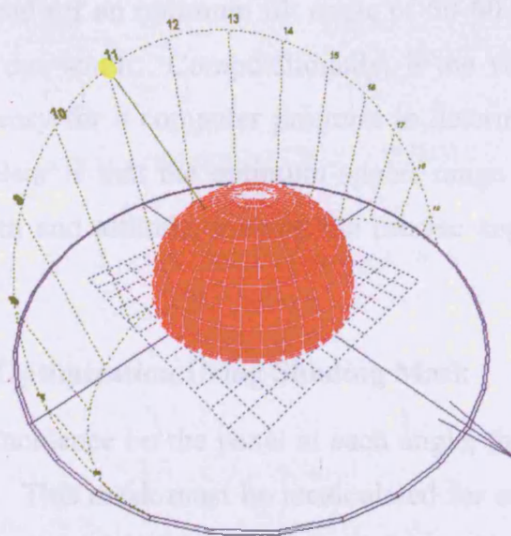


Figure 6-1: Half hemisphere with 351 facets.

When cumulative incident solar radiation values are calculated and displayed for each facet, a distribution similar to that shown in Figure 6-2 is evident. The exact nature of shading varies, not one generated on a particular surface, but one generated for a single point at the centre of the collector.

the distribution depends on the hourly data for direct and diffuse radiation as well as the latitude and longitude of the site.

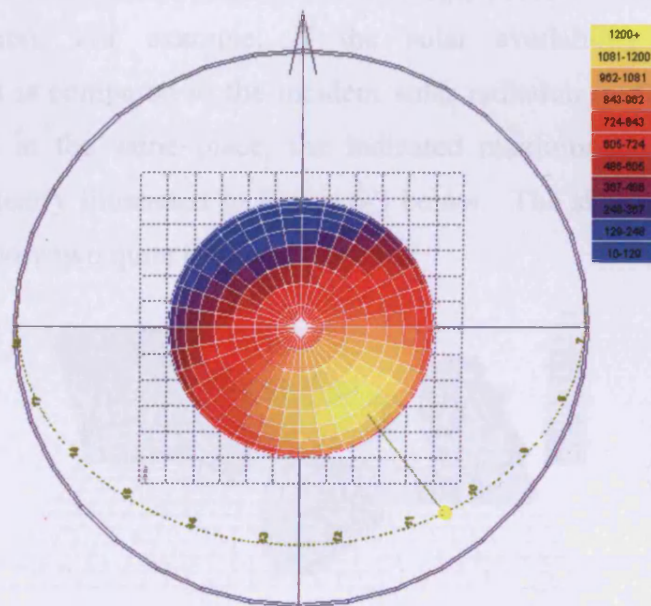


Figure 6-2: Average daily direct solar incidence on a faceted dome – in this case calculated using Moscow weather data and location.

Simply looking at this sphere it is clear which facets receive the most radiation. In this case it is possible to read off an optimum tilt angle of 50-60 degrees and azimuth of 25-30 degrees east of due south. Computationally, if the values for each facet are stored, it is also very easy for a computer program to determine the optimum angle range. What is also clear is that the optimum angles range over approximately 20 degrees in both azimuth and altitude, making the precise angle not too sensitive to small variation.

6.5 Solar Collector Optimization Using Shading Mask

To calculate the solar incidence on the panel at each angle, the process of generating shading masks is used. This mask must be recalculated for each surface orientation. When generating the image of incidence on a sphere, as shown in Figure 6-2, the calculation must be done 289 times – once for each facet. To expedite this process, the aim is to develop a means of reducing this calculation load whilst still accurately determining the optimum angles. One option for this is to examine in more detail the shading mask, not one generated on a particular surface, but one generated for a single point at the centre of the collector.

The resulting solar availability mask by itself is not a useful indicator of the optimum collection angle. Angling a surface towards the segment or cluster of segments with the maximum solar radiation values will not necessarily result in the highest overall cumulative collection. For example, if the solar availability mask for an overshadowed point is compared to the incident solar radiation on the surfaces of a hemisphere centred at the same place, the indicated maximums are substantially different. This is clearly illustrated in Figure 6-3 below. The shading mask and the distributed sphere show two quite different patterns.

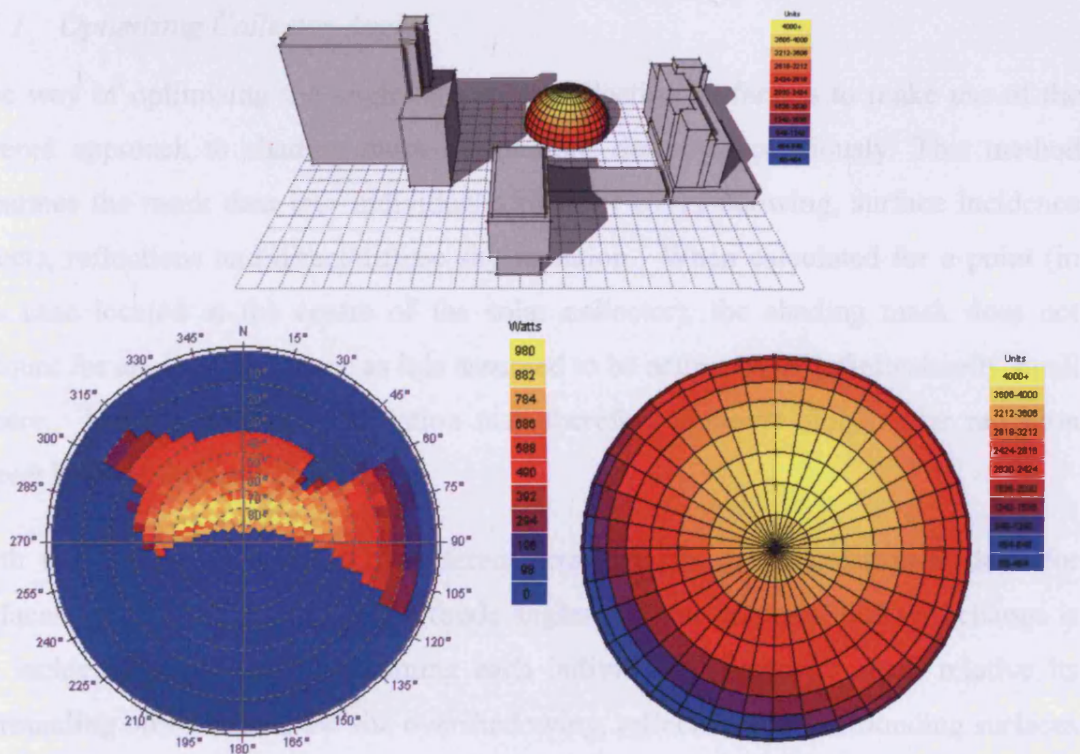


Figure 6-3: Comparison of solar availability mask with the insolation falling facets of a sphere.

This is because each facet of the hemisphere's surface is actually exposed to a wide area of the sky. At relatively high tilt angles and at orientations away from directly equator-facing, a significant portion of the radiant sky dome may actually be behind the surface. Whilst the *cos law* will significantly moderate direct radiation at high incidence angles, any calculation of incident gains must therefore consider the sum of all visible segments.

To test any surface, the data in the mask must be processed by calculating the cosine of the incidence angle of each sky segment on the surface before summing its value.

The result is the total cumulative solar collection on that surface for the period over which the sky distribution was calculated.

The benefit of the solar availability mask is that it is pre-calculated for a point and can be very quickly processed in this way. The speed of the resulting calculation is such that an exhaustive test of many different orientation and tilt angles can be carried out very quickly as the trigonometric component has been removed, becoming a simple matter of multiplying arrays or numbers.

6.5.1 Optimizing Collector Angle

One way of optimising the angle of a solar collection surface is to make use of the layered approach to shading mask calculations described previously. This method separates the mask data into individual arrays for overshadowing, surface incidence effects, reflections and direct/diffuse sky radiation. When calculated for a point (in this case located at the centre of the solar collector), the shading mask does not account for angle of incidence as it is assumed to be acting on an infinitesimally small sphere. The resulting solar radiation map therefore contains global solar radiation (direct beam + diffuse horizontal).

With this information stored in different arrays, when the calculation is done for surfaces at different azimuth and altitude angles, the only element that will change is the incidence angle data. Assuming each individual collector is small relative its surrounding obstructions, the site overshadowing, reflections off surrounding surfaces and the radiant distribution of the sky will all remain exactly the same.

The effects of incidence angle really need only to be calculated once for each altitude increment. As the equal-angle sky subdivision is symmetrical when rotated about the Z axis, each orientation/azimuth can be tested by simply rotating the calculated data by the required number of azimuth segments. This significantly reduces the number of trigonometric calculations required and greatly speeds the process with no loss in accuracy. Figure6-4 shows some examples of the resulting incidence angle effects for surfaces at different angles mapped over a segmented sky dome.

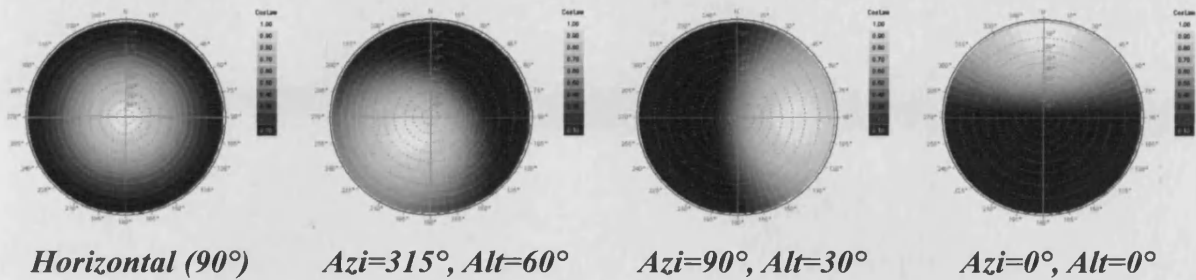


Figure 6-4: A range of incidence angle effects for surfaces at various azimuth and altitude angles.

The calculation of total insolation is then a relatively simple matter of multiplying the layers for each segment in the array and summing the result. Thus, to calculate the optimum angle for the collector surface, a shading mask with incident radiation is calculated at its geometric centre or, if given, a specific pivot point. Then, the total radiation falling on a surface at each combination of azimuth and altitude angles can be evaluated. When doing this, the effects of any geometry within the collector itself, and all its fixtures and fittings, must be completely ignored.

6.5.2 Benefits

Using this method, all 8100 segments in a hemisphere divided in $2^\circ \times 2^\circ$ angles can be evaluated on a standard desktop computer in just over 1 second. The 324 segments in a hemisphere divided in $10^\circ \times 10^\circ$ angles still gives reasonable accuracy (the previous section showed that maximum collection angles are not sensitive to slight variations in orientation/altitude), and is much quicker to calculate.

Obviously the initial calculation time for the shading mask will depend on the geometric complexity of the model itself, however the time required for the optimum angle analysis process is completely independent of model complexity. Thus, by effectively caching the computationally intensive overshadowing and reflection data in separate layers of a shading mask, it is possible to evaluate any range of sky distribution and any surface orientations very quickly for many points in a model.

This also means that it is possible to investigate differences in optimum collector angles for different times of the year. For example, some situations may be more dependant on collection during the winter months, so it is possible to base the cumulative sky on only the three months of winter or to weight the 12 months of the year differently depending on the application.

6.6 An Urban Example

As an example to demonstrate the need to consider external obstructions, take a dense inner city development site such as that shown in Figure 6-5. The comparative analysis is performed in two stages, the first to show the extent of variation caused by overshadowing and the second to show the potential increase in efficiencies possible. (This model is located inside the city of Philadelphia in the US).

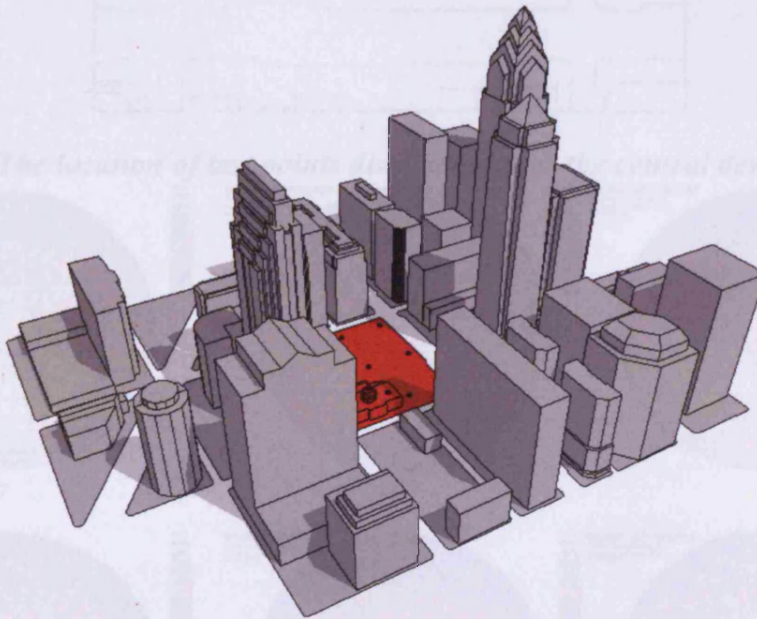


Figure 6-5: An example of a highly overshadowed urban development site.

6.6.1 The Extent of Variation

To demonstrate the effect of overshadowing on optimum solar collector angles, a series of spheres were generated at different positions within the central open area in the model. If overshadowing is significant, then noticeable differences should be evident in the distribution of solar radiation over the surfaces of spheres located at different points within the site. Figure 6-6 shows the exact positions of each sphere, most at ground level and one on top of an existing building.

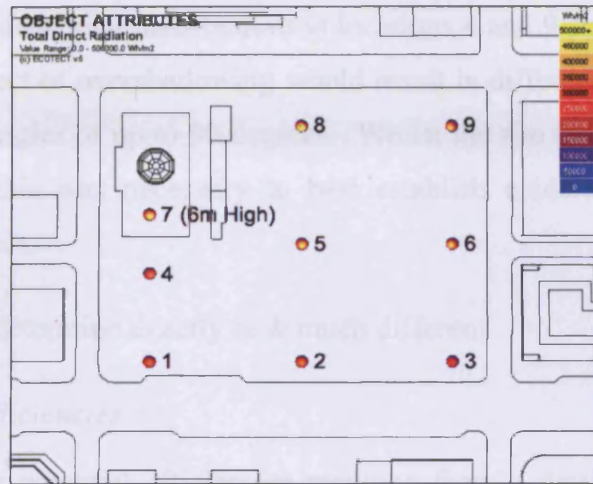


Figure 6-6: The location of test points distributed over the central development site.

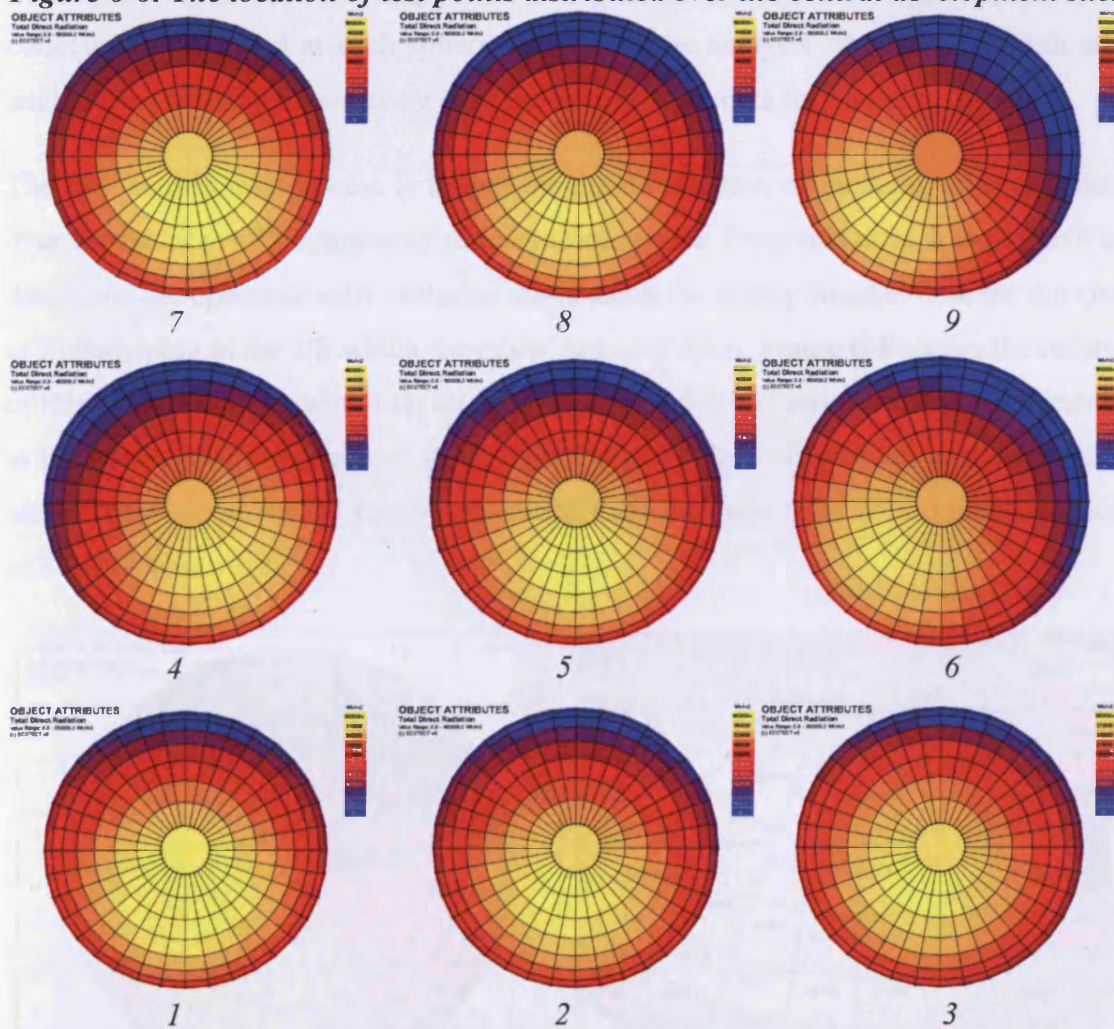


Figure 6-7: The distribution of solar radiation over the surfaces of each test sphere, relating to the location indicated by the number immediately beneath.

Comparing the incident solar distributions at locations 4 and 9 shown in Figure 6-7, it is clear that the effect of overshadowing would result in differences in optimum solar collector azimuth angles of up to 90 degrees. Whilst the site represents something of an extreme case, this was necessary to best establish evidence for the extent of overshadowing effect.

The next step is to determine exactly how much different

6.6.2 Potential Efficiencies

To demonstrate the potential efficiencies resulting from a detailed consideration of overshadowing when optimising collector angles, a representative 1m² flat plate solar collector is generated at each sphere location in the analysis site. The azimuth and angle of the collector is set using only the base climate data for that site.

The first step in this process is to analyse the distribution of incident solar radiation over the surfaces of a completely unobstructed sphere. From this data, it is possible to determine the optimum solar collector angle using the hourly weather data for the city of Philadelphia in the US which the model is based upon. Figure 6-8 shows the results of this calculation, showing that an azimuth angle of -175° and an altitude 55° results in the greatest solar collection value. A flat panel solar collector set to those angles would therefore expect to receive an annual total incident direct solar radiation value of 870868 Watts/m².

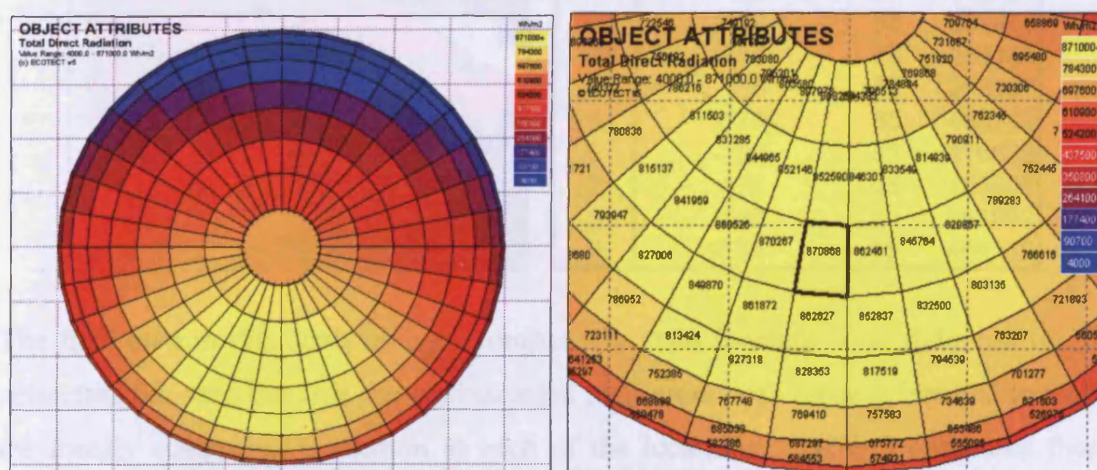
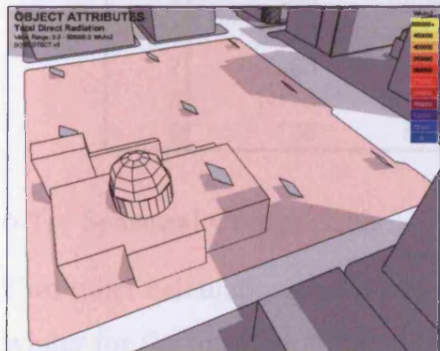


Figure 6-8: The distribution of incident solar radiation over a completely unobstructed sphere.

The next step is to determine the difference overshadowing makes. Table 1 shows the collected radiation within the actual site by flat plate solar collectors at each of the 9 site locations and oriented towards the unobstructed maximum. This shows that at these locations, incident solar gains can be reduced by as much as 70%, with the average being just under 50%.

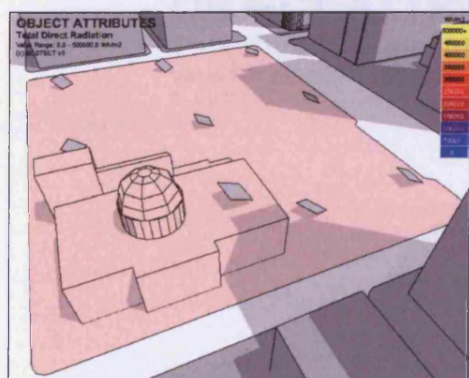
Table 1: The relative effect of overshadowing at the 9 locations within the site.



Loc.	Ref.	Unobst.	Percent	Increase
1	345990	870868	39.73%	-60.27%
2	372715	870868	42.80%	-57.20%
3	266837	870868	30.64%	-69.36%
4	359670	870868	41.30%	-58.70%
5	479443	870868	55.05%	-44.95%
6	424071	870868	48.70%	-51.30%
7	470696	870868	54.05%	-45.95%
8	551166	870868	63.29%	-36.71%
9	429864	870868	49.36%	-50.64%

Based on the analysis of test spheres at each location described previously, it is possible to determine the optimum collector angles for each sphere. The figure beside Table 2 shows the flat plate solar collectors oriented towards the locally obstructed maximum, with the exact angles and collected totals shown in the adjacent table.

Table 2: Optimum collector angles and totals for each obstructed test location.



Loc.	Optimum Collector Data		
	Azi	Alt	Total
1	-175	65	355663
2	-165	65	382465
3	-155	75	285105
4	155	65	373137
5	-175	65	486342
6	-135	55	470822
7	175	65	495601
8	-155	65	561092
9	-135	55	464110

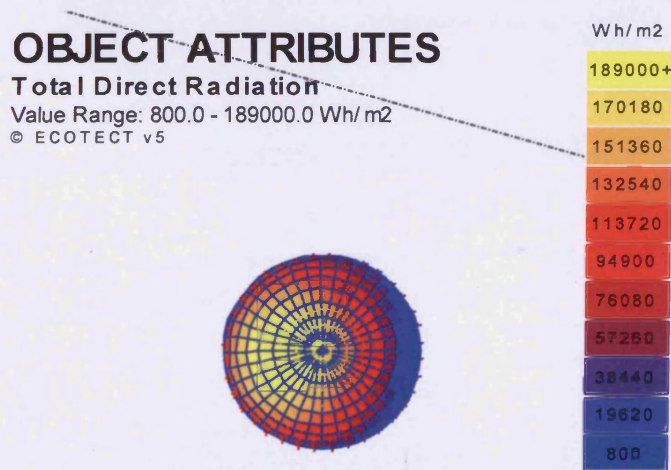
The final step in this analysis is to compare the total incident solar radiation on the collectors oriented towards the unobstructed maximum with those orientated towards the locally obstructed maximum at each of the locations. Table 3 compares these values.

Table 3: The comparison of total annual solar radiation given in W/m² on optimally oriented solar collectors (Total) compared to the same collector at the same location but oriented towards the unobstructed maximum.

Optimum Collector Data				Ref.	Percent	Increase
Loc.	Azi	Alt	Total			
1	-95	64.92	355663	345990	102.80%	2.80%
2	-105	64.92	382465	372715	102.62%	2.62%
3	-115	74.95	285105	266837	106.85%	6.85%
4	-65	64.92	373137	359670	103.74%	3.74%
5	-95	64.92	486342	479443	101.44%	1.44%
6	-135	54.9	470822	424071	111.02%	11.02%
7	-85	64.92	495601	470696	105.29%	5.29%
8	-115	64.92	561092	551166	101.80%	1.80%
9	-135	54.9	464110	429864	107.97%	7.97%

6.7 Seasonal Comparison

Two other calculations have been run to simulate the difference between summer and winter for the location at the centre in the central site. The results shown in Figure 6-9 and Figure 6-10 below clearly illustrate that winter total direct radiation is significantly less than summer total direct radiation. The direction of effective radiation in winter is slightly different from summer total radiation direction which may be considered in design process and collector locating. (In this case Cardiff-UK weather data applied for these calculations.)



**Figure 6-9: Analysis Dome Number (7) for Summer
[Height from the ground ± 0.00]**

OBJECT ATTRIBUTES

Total Direct Radiation

Value Range: 0.0–4000.0 Wh/m²

© ECOTECH v5

Wh/m²

4000+

3600

3200

2800

2400

2000

1600

1200

800

400

0

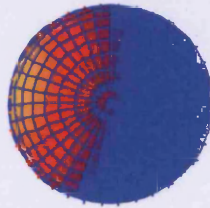


*Figure 6-10: Analysis Dome Number (7) for Winter
[Height from the ground ± 0.00]*

CHAPTER SEVEN

Irradiance Surface Mapping

and

Performance-Based Design

CHAPTER SEVEN

**Irradiance Surface Mapping
and
Performance-Based Design**

7 Irradiance Surface Mapping and Performance-Based Design

7.1 Introduction

Visualising variations in insolation levels over the facades of buildings can be of great benefit to designers. It allows them to quickly assess the relative risks of solar overheating or glare potential as well as developing in their own minds the keys to strategies they might employ to minimise these risks.

In order to show any variation over large surfaces, many shading masks can be generated and cached at distributed points across each surface of the building envelope. Any number of sample points can be used, depending on system memory and available calculation time. Once the shading masks have been calculated, it is possible to calculate incident solar radiation levels at any date and time in the year, or to sum them over any period. This could be the three months of winter, a typical summer day or the entire year. Values shown on each surface can be instantaneous gains, peak gains, hourly/daily/monthly averages or total cumulative gains.

These results can then be visualised over each surface of interest within a 3D model. Figure 7-1 shows a series of examples of this, with cumulative insolation levels shown over the entire façades or just on glazed areas.

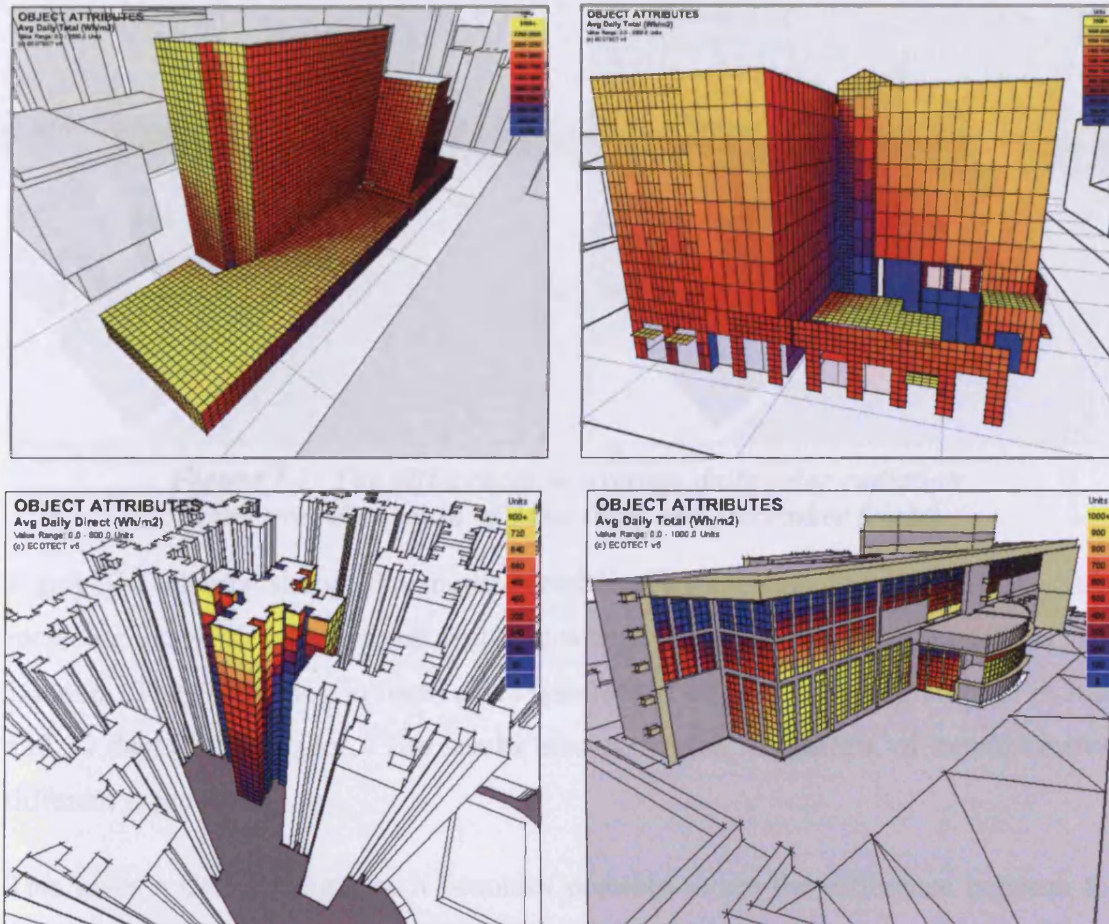


Figure 7-1: Examples of incident solar radiation (insolation) mapped over a range of different buildings and surface elements.

The examples in Figure 7-1 above also show that the methodology fully accounts for self shading in more complex building forms. The manual subdivision of larger surfaces into smaller segments also allows the designer to concentrate greater levels of detail in specific areas of interest such as in corners or nearer the top of the facade.

7.1.1 Dynamic Effects

An additional use of this technique is to examine the dynamic effects of incident gains. As the period over which values are summed or averaged can be changed with only minimal recalculation (the shading masks themselves do not change), it is possible to visualise relative levels as they change over each month of the year, as in Figure 7-2 below, or between seasons, as in Figure 7-3.

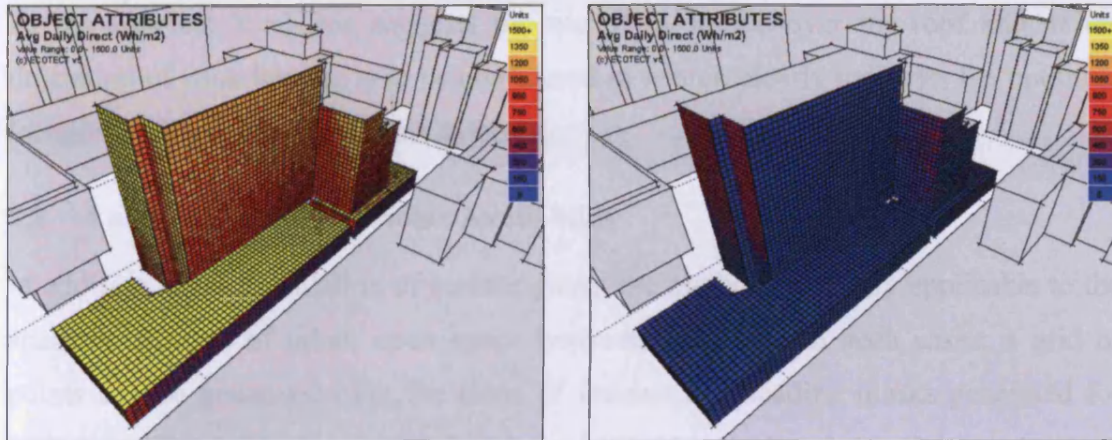


Figure 7-2: The differences in average daily solar radiation taken over the month of June (left) and December (right).

Figure 7-2 clearly shows the marked variation in average daily cumulative solar incidence between mid-summer and mid-winter over a 9 storey building located in London. The calculation in these cases were based on the average of 30 days in June and 30 days in December. The results also show that the pattern of incidence over different façades can vary.

This gives a useful insight as it becomes possible to see the difference between the requirements for solar protection during summer and the availability of solar radiation as a heating source in winter. This is shown to good effect in Figure 7-3 below.

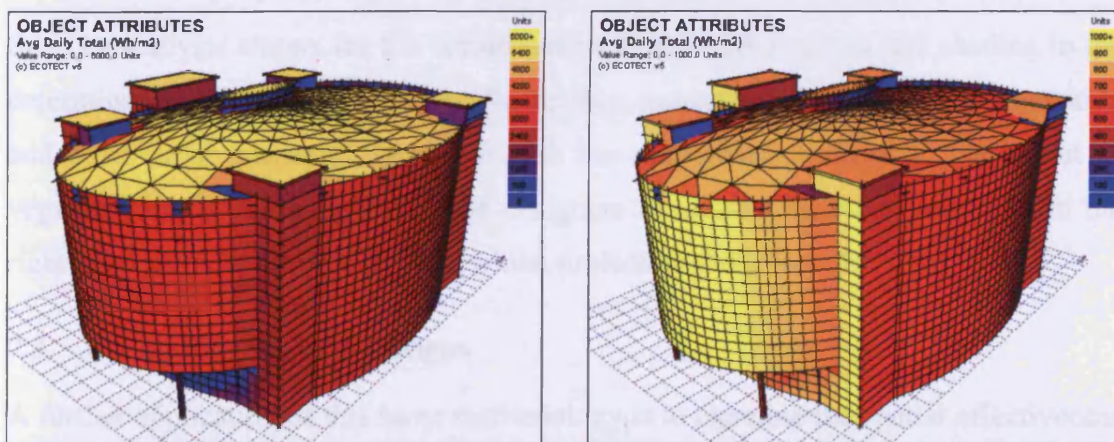


Figure 7-3: Average daily solar radiation levels over the three months of summer (left) or the three months of winter (right) – note the different value scales.

In these two cases average daily total solar insolation has been calculated over the three warmest months and the three coldest. This clearly shows that the roof surface bears the greatest incidence over the day when the sun is highest in the sky in summer. In winter however, the south-facing surfaces receive the greatest incidence.

At the simplest level this suggests the use of insulation over the roof and, if the utilisation of solar heating is to be considered in winter, clearly indicates the optimum location of direct or indirect gain systems.

7.2 Variations in Spatial Solar Availability

In addition to the calculation of surface gains, the method is equally applicable to the analysis of areas of urban open space between buildings. In such cases, a grid of points can be generated over the areas of interest and shading masks generated for each point. Insolation levels can then be calculated at each point in the same way as for a surface (Chung and Mardaljevic 2004), as shown in Figure 7-4.

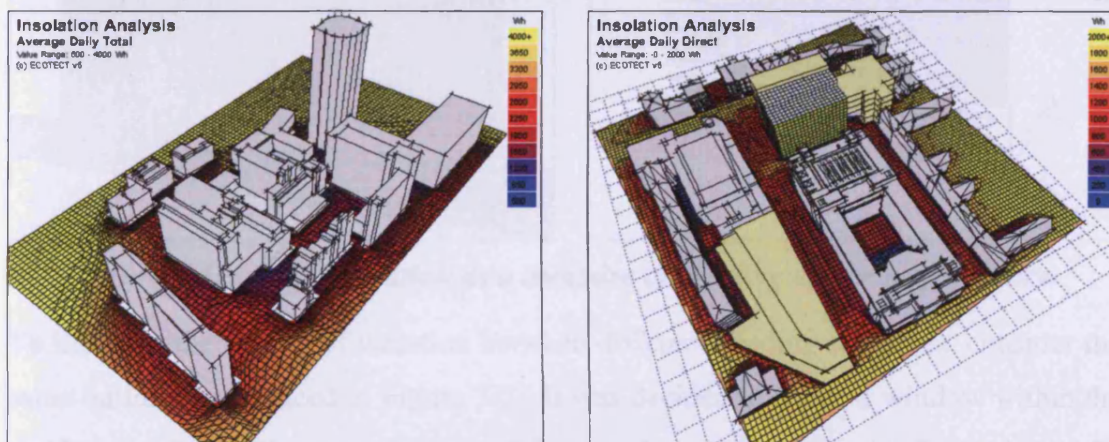


Figure 7-4: Examples of distributed insolation over areas of open urban space.

Such an analysis allows for the consideration of both solar access and shading in the determination of optimum locations for seating, movement routes, areas of vegetation and other urban planning issues. It also has particular relevance to the layout of vegetation plots, allowing landscape designers to locate plants that need sun in the right areas at the right time of year, whilst protecting those that don't.

7.3 Evaluating Shading Designs

A further application of this same methodology is to examine the spatial effectiveness of detailed shading devices on the window surfaces they are intended to shade. Whilst it is possible to perform this calculation for the window as a whole, the result would be a single value. In some cases this would be sufficient for a general overall comparison, however the spatial subdivision of the window area yields additional information which can be used to objectively assess and optimise the design of the shading device or, alternatively, to optimise the design of the window itself.

As an example, consider the solar distribution shown on the left of Figure 7-5. This shows that the shade is quite effective towards the top of the window but less so towards the bottom. This information could be used to apply different types of glass at different heights within the window: allowing clear glazing at the top to increase localised daylight availability and solar control glass at the bottom where it is needed most.

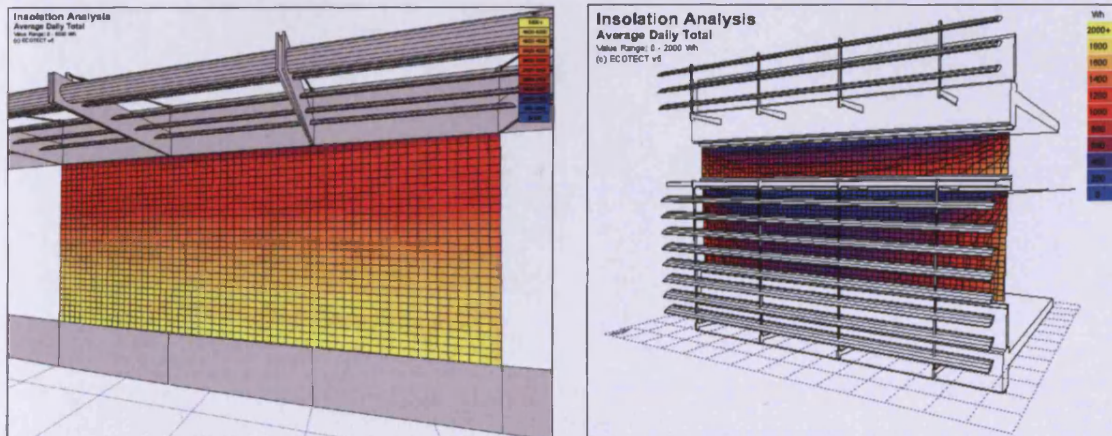


Figure 7-5: Using insolation as a measure of shading device performance.

To illustrate the degree of variation between different shading strategies, consider the same building introduced in Figure 7-3. It was decided to locate a window within the southern wall in order to make use of direct solar gains in winter. To compare the effectiveness of different shading strategies, the window was divided into many small facets and the average daily incident solar radiation calculated for each over the three months of winter.

As a base for comparison, the calculation was first done with no shading applied. The total incident radiation for the window is simply the sum of all values for each facet making up the window. Figure 7-6 shows the results of these calculations for a range of standard louvred shading devices in different configurations.

In usual practice, decisions between these configurations would be based primarily on considerations such as installation cost, view and ongoing maintenance. However, Figure 7-6 clearly shows significant differences in their effect on the solar resource available to the window.

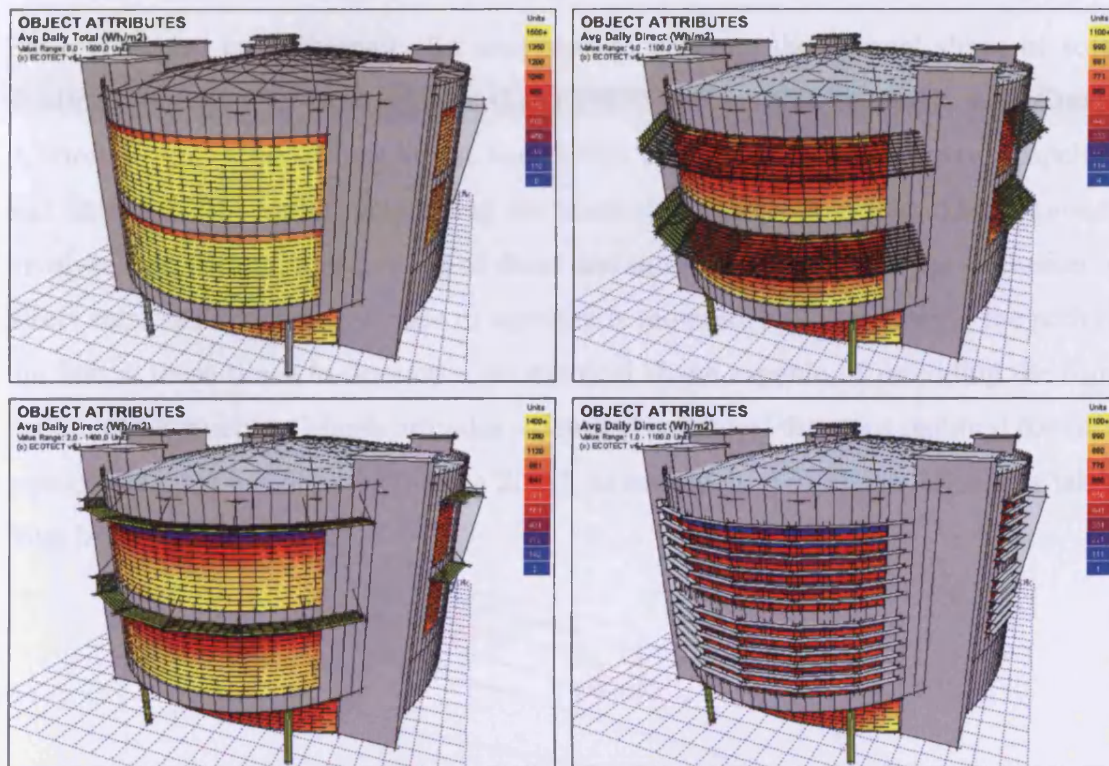


Figure 7-6: The relative performance of different shading strategies..

Thus, the right choice of shading system is critical to the optimum use of solar gains. This methodology allows for the direct quantification and visualisation of shading performance, providing an effective basis on which these choices can be made.

7.4 Section Conclusion

Whilst work on the calculation and visualization of insolation is not new, the process of being able to quantify values for specific surfaces within the model is critical to the ability of an analysis tool to feed back into a system of iterative adjustment. If a target value or range is given, the system must be able to obtain a specific number in order to compare it with the target. This leads on to the next section of this work dealing with the performance-based design of shading devices.

7.5 Performance-Based Shading Design

Solar geometry is traditionally the tool used to generate the optimal shape of solar shading devices. The work of Lam (Lam 1987) outlines this approach, with Cotton (Cotton 1996), Arumi-Noe (Arumi-Noe 1996) and Capeluto and Shaviv (Capeluto and Shaviv 2001) further developing the ideas that shaped this field. This approach involves first determining a series of dates and times between which the exclusion of direct solar radiation on a surface or aperture is required, and then tracing the path of the Sun at these times to develop a geometrical shape capable of providing the right pattern of obstruction. Marsh provides a detailed outline of the steps required for such a process of shape generation (Marsh 2003), as summarised in Figure 7-7 below taken from his work.

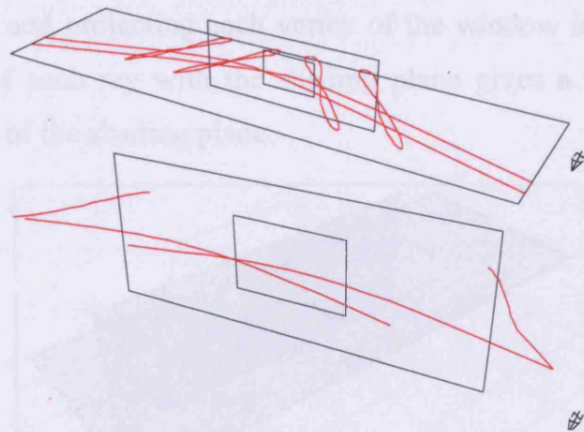


Figure 7-7: The six basic sun tracks reduced to generate a simple shading device based on time and date constraints.

This approach assumes that the dates and times selected for cut-off are meaningful in terms of either the activities they provide protection for or the climate in which they are being used. For example, a computer laboratory in a school will have very specific operating times so; in this case, the shading requirement is very much time-of-day based. Similarly, a direct-gain passive system will only require solar gains when temperatures begin to fall, which in many climates occurs at reasonably predictable times of the year.

However in many situations these dates and times are not as clear cut. With increasingly stringent government legislation controlling energy use in buildings and, in the case of the new 2006 amendments to Part-L of the UK building regulations, actually specifying maximum allowable solar gains in naturally ventilated zones, an approach based on the actual strength and distribution of solar radiation is more

appropriate, protecting from solar radiation exactly when and where protection is required.

7.6 Reversing the Calculation Process

An alternate method to tracking solar position through the sky is to track the path of direct solar radiation. The technique proposed in this work builds on ray-tracing methods developed by Marsh (Marsh 1997; Marsh 2003) as well as work by Kaftan in the development of his Cellular Method (Kaftan 2001).

To illustrate the basic process, consider the simple example shown in Figure 7-8. The selected window is projected onto, in this case, a horizontal plane located slightly above the window head at a certain time. This is done by calculating the position of the sun at this time and projecting each vertex of the window in that direction. The intersection point of each ray with the shading plane gives a transformed polygon lying on the surface of the shading plane.

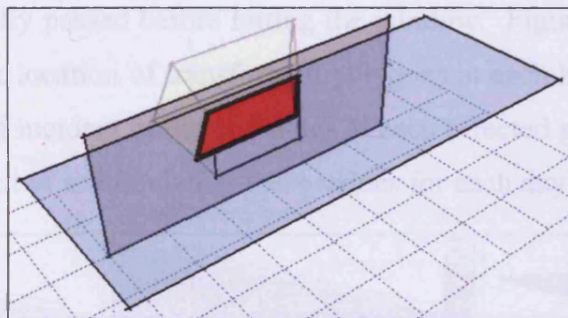


Figure 7-8: The process of projecting a simple window towards the sun at a particular time and onto a shading plane.

The exact location of this polygon within the shading plane will change at each time increment as the Sun moves across the sky, as shown in Figure 7-9.

Figure 7-9: The image on the left shows a rectangular window projected onto a horizontal shading grid at set time intervals. The direct solar radiation at each time is then added to each shading cell. The entire image shows a single-day result. The image on the right shows the daily average value over a single year.

If these instantaneous direct solar radiation are extrapolated at grid cell through which they pass to strike the window, then the total value of each cell can be used as an indicator of the relative importance of the space within that cell to the shading of the window. Four important values can be derived from such an analysis for each grid point:

- the total cumulative result over the whole analysis period.

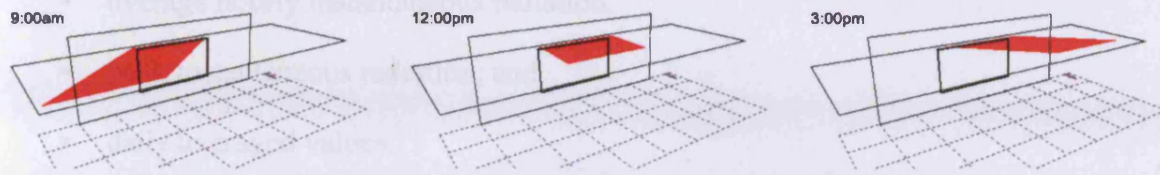


Figure 7-9: The changing location of the intersected polygon at different times of an example day.

If hourly weather data is available, it is possible to determine the value for direct beam solar radiation at each time step, from which solar incidence values can be calculated for the window giving the relative ‘strength’ of the direct gain component. This is useful information as it can be used to determine if shading at that particular date/time is actually required based on regulations or the behaviour of the room.

In order to store and map this information, a grid of cells can be mapped over the shading surface. Using this method it is possible to add the calculated incident radiation values for each time increment to the specific grid cells through which the solar radiation actually passed before hitting the window. Figure 7-10 illustrates this process, showing the location of transformed polygons at each hour over a single day (left), the addition of incident radiation values at each affected grid cell for each hour (centre) and the effect of accumulating these values for each day of the year.

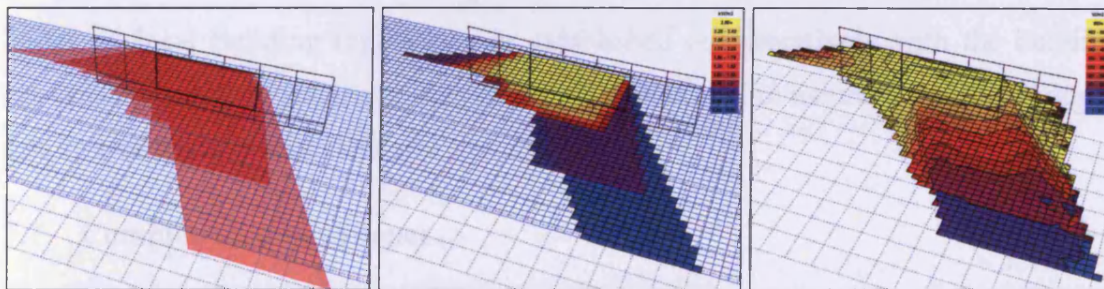


Figure 7-10: The image on the left shows a rectangular window projected onto a horizontal shading grid at set time intervals. The direct solar radiation at each time is then added to each shading cell. The centre image shows a single-day result whilst the image on the right shows the daily average taken over a whole year.

If these instantaneous direct solar radiation are accumulated at grid cell through which they pass to strike the window, then the total value at each cell can be used as an indicator of the relative importance of the space within that cell to the shading of the window. Four important values can be derived from such an analysis for each grid point;

- the total cumulative result over the whole analysis period,

- average hourly instantaneous radiation,
- peak instantaneous radiation, and
- daily averaged values.

Contours of each of these values across the grid can then be used to outline the exact extents of a shade that would allow through no more solar radiation than the value defining the contour. By ‘trimming’ the shade to a particular contour, it is possible to derive detailed shading shapes based on objective performance criteria. Figure 7-11 illustrates this process, showing the extents of the shading required to ensure no more than 75W/m², 150W/m² and 250W/m² incident solar gains on the window.

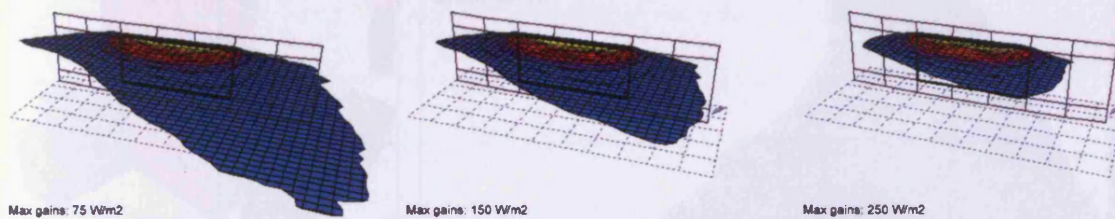


Figure 7-11: An example of shading shapes based in this case on 75, 150 and 250 W/m² instantaneous solar gains on a window.

This way, a designer can determine the exact shape of a shading device based on a maximum allowable incident solar gain value. This maximum allowable value can be based on local building regulations or established collaboratively with the building services engineers to minimise both overheating potential in naturally ventilated zones and system loads in mechanically cooled zones.

7.7 Complex Shading Shapes

This technique can be extended to shading devices of any shape and orientation relative to the window, or even for multiple shaded surfaces. Figure 7-12 shows how it can be applied to a curvilinear shaped shade. The extents of the window polygon on the surface of the shading grid is done by projecting rays towards the Sun from a series of sample points distributed over the window surface and intersecting each grid cell.

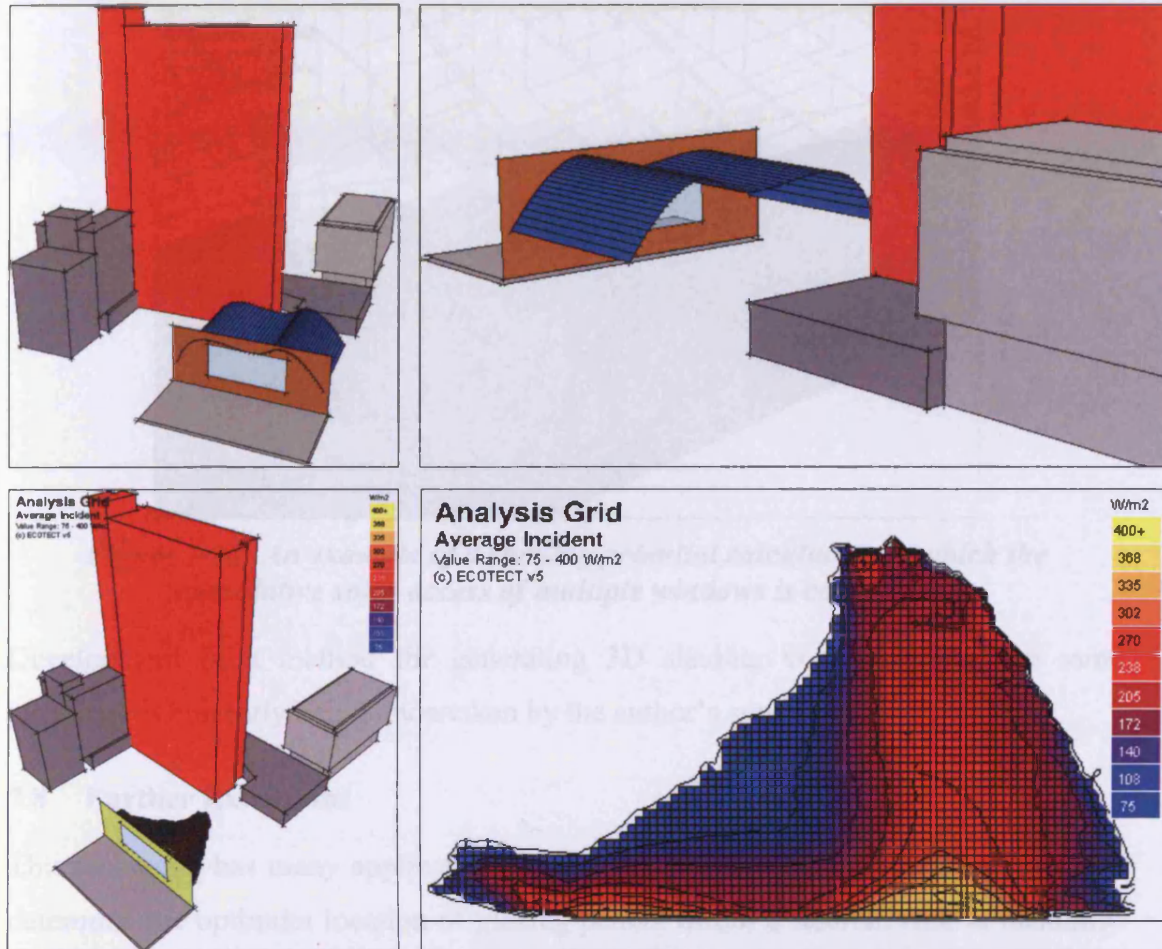


Figure 7-12: An example of a shading potential calculation for a curvilinear shading surface in which the effect of external site obstructions are considered.

As a shading mask is used in the calculation of instantaneous incident solar gains on the window at each time step, the existing shading effects of external obstructions are automatically considered within this process, as also illustrated in Figure 7-12.

Multiple windows can also be handled simultaneously by simply adding the effects of each window to the same analysis grid. Figure 7-13 below shows the resulting contours for average incident solar radiation when considering all the ground floor windows in a multi-unit model. This way the extents of continuous shading devices that must project a number of windows can be similarly determined based on actual solar incidence.

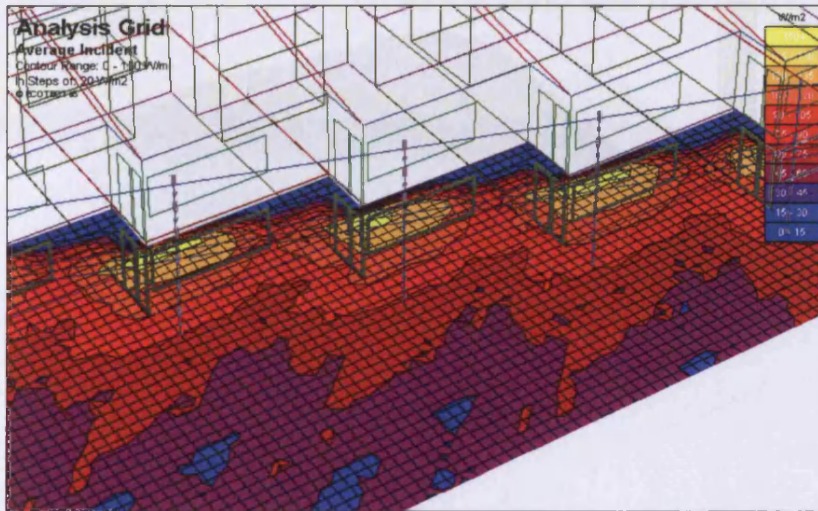


Figure 7-13: An example of a shading potential calculation in which the cumulative solar access of multiple windows is considered.

Development of a method for generating 3D shading volumes using the same technique is currently being undertaken by the author's supervisor.

7.8 Further Extensions

This technique has many applications. One example to illustrate this was a study to determine the optimum location of glazing panels within a stadium roof to maximise solar access to the southern-most section of the playing area in winter in order to promote turf re-growth.

If the solar analysis grid is placed over the entire roof area of the stadium and the entire playing surface is projected back onto it throughout winter, it is possible to map the most significant areas where obstruction should be minimised. This is done by determining which cells in the grid the solar radiation must pass through each hour in order to reach the pitch, and summing the instantaneous solar radiation at each hour over the three months of winter. The cells with the highest overall values therefore represent the area through which the most solar radiation passes, and thus the areas in which to avoid obstruction.

Figure 7-15: The optimum location of roof glazing panels can be quickly determined using projections of the playing surface onto the roof area over Winter.

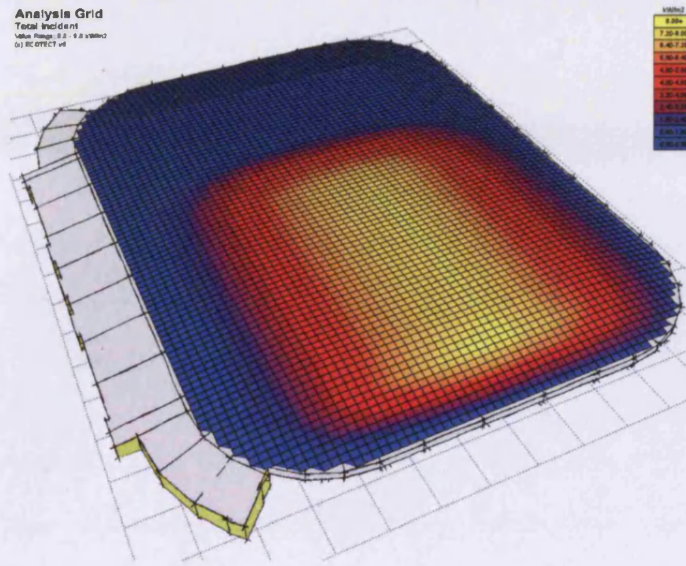


Figure 7-14: The optimum location of roof glazing panels can be quickly determined using projections of the playing surface onto the roof area over the three months of winter.

If the resulting cumulative data is clipped to only the area of the proposed roof, it clearly shows the most effective location for roof glazing panels.

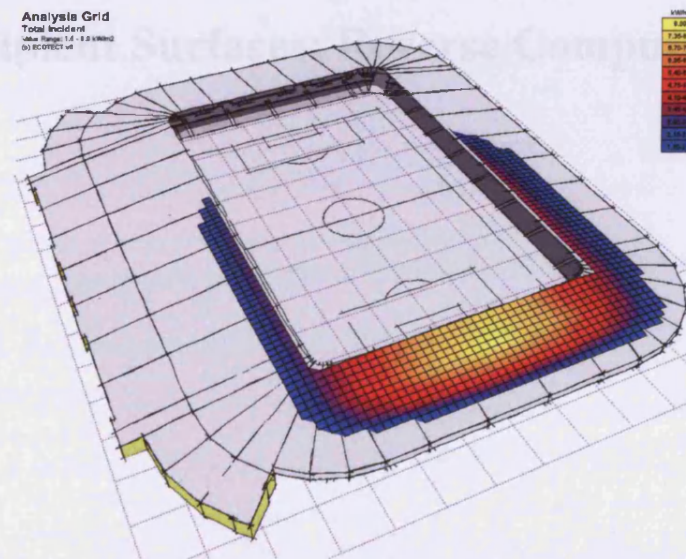


Figure 7-15: The optimum location of roof glazing panels can be quickly determined using projections of the playing surface onto the roof area over Winter.

CHAPTER EIGHT

Envelope Design in Consideration of Existing Recipient Surfaces; Reverse Computation

8 Envelope Design in Consideration of Existing Recipient Surface; Reverse Computation

8.1 Simulation and Generation

Simulation has long been part of the building design process. However its role has typically been as a validation tool, used by consultants towards the end of the design process - testing highly developed proposals to ensure that specific performance criteria within the brief have been met. With the availability of more interactive simulation software, performance analysis is being increasingly used much earlier in the process - and more often by the designers themselves, not just the environmental and services consultants.

One of the primary aims in this thesis was to involve solar performance simulation and optimisation techniques much earlier in the design process, right at the most conceptual stages to guide in the development of the built form. This means devising mechanisms by which useful simulation results can be derived from relatively incomplete models and then used to modify their geometry to improve performance or to generate new geometries.

Progress in developing generative systems has generally been low within the building design industry as the issues involved are very complex and there is often no obvious solution to any particular set of design problems. Also, every building is a compromise between a vast array of competing requirements. Rarely can any single building element be truly optimised for a particular use or application – rather it must be adaptable to many different uses and the compromise is usually the ‘least worst’ solution.

However, this does not preclude the designer from at least knowing what the optimum for a particular application would be. In fact this is how most designers work, they know exactly what they would like to achieve, but then have to work within the constraints of the budget, brief and regulations to achieve the best they can. This is the primary skill of a designer - assimilating a myriad of complex and competing requirements and then making the best set of compromises from a range of available options.

Of most significance here is that designers can work equally well with both objective (quantifiable) and subjective (unquantifiable) constraints. In fact, at the earliest stages of design it is only really possible to work with subjective issues as there is insufficient hard information about the building to calculate many of the objective criteria. Computer systems tend to be of little use in tasks that involve subjective or unquantifiable parameters, but excel at objective tasks with clearly defined and quantifiable parameters, and highly repetitive or iterative problems.

Thus, the purpose of this part of the research is to propose the best compromise. Computational analysis and simulation can make a significant contribution at the very earliest stages of design by generating optimal solutions to very focused and tightly defined problems. The results may not be immediately and directly applicable to the building in its current form, but provide useful information for the designer to assimilate within the broader design context.

These thoughts can be illustrated with reference to the applications discussed in the last two chapters, and one further application

8.2 Simple Preliminary Applications

To begin, consider the techniques for deciding on the optimum tilt for a collecting surface outlined previously in Chapter Six. This is a very tightly defined problem: the optimum angle is that which provides the greatest solar collection, and the constraints are the surrounding buildings. The criterion for success and the constraints on the problem are tightly defined and easily determined. Whilst in a highly overshadowed environment there may be more than one solution, they are all easily calculable and the results are unequivocal. Obviously, of more importance to designers are solutions to much more complex problems. Whilst these techniques represent a relatively trivial application of generative potential, they serve to clearly show that, if the problem can be defined tightly enough, then useful solutions can be generated.

8.3 Insolation as a Loosely Defined Problem

Not all geometric design problems are suitable for this kind of approach, some are considerably loosely defined. For example, consider the stadium design described in Appendix A and shown in Figure 8-1 below. The requirement here was to determine the optimum location and area of roof glazing to maximise the insolation falling on

the playing surface, thus maximising grass growth. The stadium model shows the proposed unglazed roof area together with the total annual distribution of solar radiation over the pitch.

To do this, the roof was divided into segments running from the perimeter inwards. The amount of glazing within each segment was controlled within the analysis script by specifying a depth value at each side of the segment, ensuring a continuous edge running around the stadium.

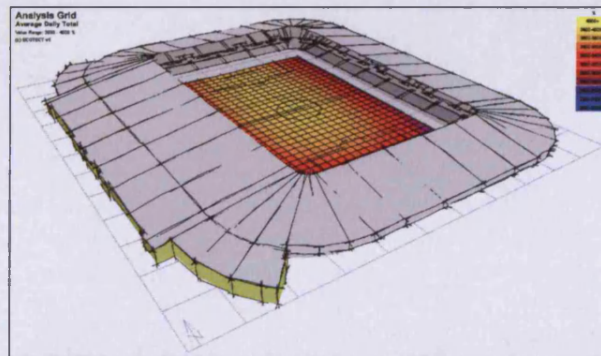


Figure 8-1: Stadium model showing the distribution of solar radiation over the playing surface with an unglazed roof.

The first issue was the determination of a suitable metric for insolation values. Taking the total annual insolation would bias the result towards Summer, when solar radiation is significantly greater than in Winter and when grass growth is not really a problem. Thus the insolation period needed to consider when the playing surface was under most stress – at times of high usage rates and low radiation levels.

Additionally, stress levels are not usually uniform over all areas of a playing surface. Traditionally it is the southern end of a pitch that suffers most in the UK as it is in shade for the longest period in winter. This can be accommodated by summing up only the southern half of the playing surface, or even the southern-most quarter.

The specific insolation period chosen and area of pitch area over which the calculation is done will both directly influence the resulting glazed area of the roof. However, there is no available guidance on whether, for example, to take only the three months of winter, or the coldest three months, or even the coldest seven weeks. Similarly, why not the southern-most third of the pitch instead of the southern-most quarter.

The second issue is the definition of what is optimum. If maximum insolation is the only criteria, then the glazing area simply resolves to the entire roof, as shown in Figure 8-2.

The obvious constraints to offset this are material and maintenance costs. These need only be expressed as ratios between the costs of the opaque and glazed materials. Additionally, maintenance costs require a period over which they are to be calculated. The script then simply calculates the areas of each material and looks for the point where the total cost and insolation curves meet.

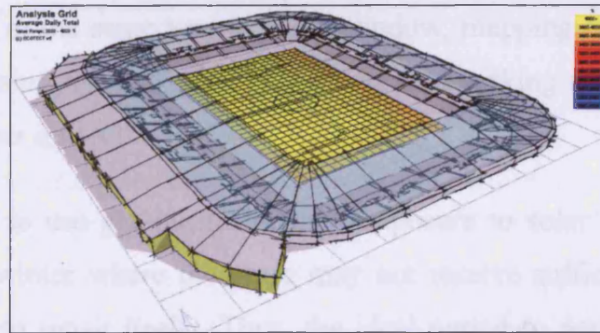


Figure 8-2: *If incident solar radiation is the only criteria, then the entire roof glazed is the 'optimum' solution.*

However, here too the specific values chosen for these parameters significantly affect the result. Figure 8-3 compares two situations in which the capital cost of glazing is twice that of metal decking and its ongoing maintenance is five times higher. The image at the left shows the result if a period of only 10 years is considered whilst the right considers a period of 50 years.

The potential for a single relatively arbitrary parameter to so significantly influence the result may be important in a sensitivity analysis; however it demonstrates the uncertainty underlying the results of loosely defined problems.

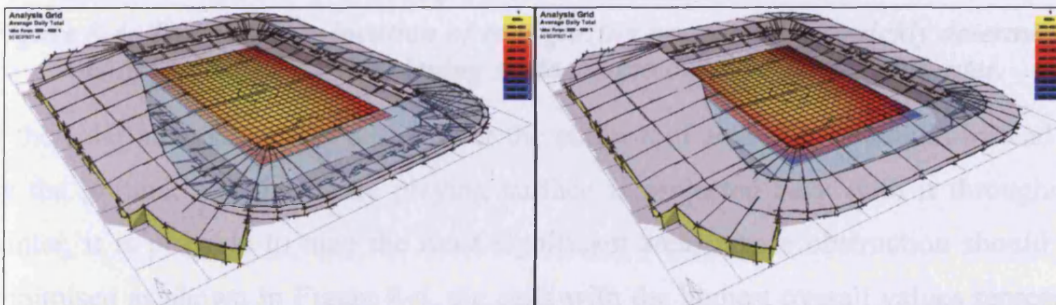


Figure 8-3: *For the same capital and maintenance cost ratios, the left image shows the result when considered over 10 years and the right image over 50 years.*

8.3.1 An Analytical Solution

In this particular instance there was a more direct analytical solution to the problem that did not require the designer to apply cost constraints or specify an arbitrary pitch area in order to generate a solution.

In such a situation, it is possible to apply the same process as described in previous shading device design sections. Instead of using a window as the shaded surface, it is possible to use the actual horizontal pitch area. Then, instead of a flat shading plane, the analysis grid is form-fit to the shape of the intended roof. The solar potential can then be calculated in the same way as for a window, mapping over the roof grid the solar radiation passing through each grid square and striking the pitch at a series of time increments over a specific period.

The intent here is to use glazing to increase exposure to solar radiation during the darkest period in winter where the grass may not receive sufficient light to sustain enough re-growth to repair itself. Thus, the ideal period to perform the calculation over are the three months of winter.

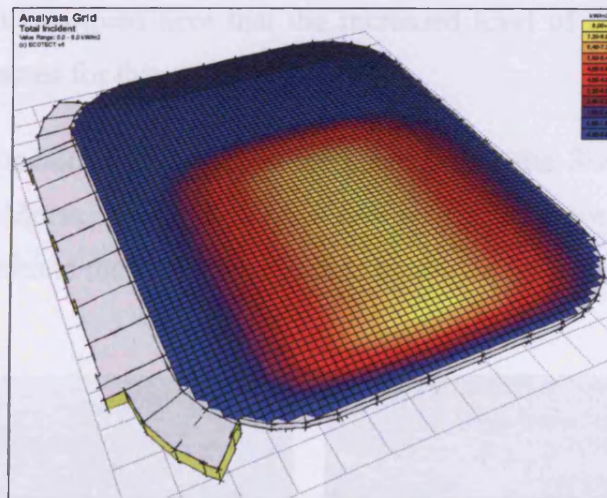


Figure 8-4: The optimum location of roof glazing panels can be quickly determined using projections of the playing surface onto the roof area over Winter.

If the solar analysis grid is placed over the entire roof area of the stadium instead of on the ground, and the entire playing surface is projected back onto it throughout winter, it is possible to map the most significant areas where obstruction should be minimised as shown in Figure 8-4, the cells with the highest overall values represent the area through which the most solar radiation passes, and thus the areas in which to avoid obstruction.

If the resulting cumulative data is clipped to only the area of the proposed roof, it clearly shows the most effective location for roof glazing panels.

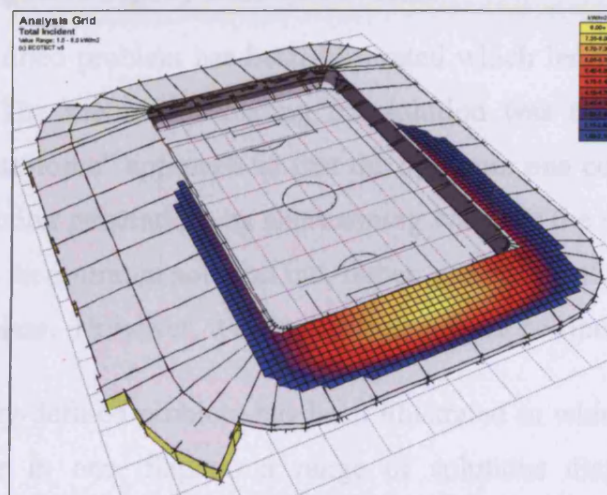


Figure 8-5: The optimum location of roof glazing panels can be quickly determined using projections of the playing surface onto the roof area over Winter.

Whilst the analytical solution is still based on a relatively arbitrary time period, that was the only variable parameter as the entire pitch surface was used. As relative costs were not considered it is possible to argue that the result is less meaningful overall, however it is argued here that the increased level of certainty in the result more than compensates for this.

The actual case considered here was a roof design for the Swansea stadium (also sometimes called Morfa stadium). Figure 8-6 shows bird eye views of the built stadium, which illustrate the final choice made by the designers based on the analysis just described.



Figure 8-6: Swansea (Morfa) stadium built based on the reverse computation technique introduced by the author.

(Image source: www.images.google.com)

8.4 Right-To-Light: A Tightly Defined Problem

So far a tightly-defined problem has been illustrated which led to an equally tightly-defined solution. The method of finding the solution was to try out all possible solutions in a “brute-force” approach so that the optimum one could be selected. As an example of solution generation, its shortcoming was that the method did not steer the design towards an optimum solution but, rather, generated all possible solutions to a fairly trivial problem. However, it does illustrate reverse computation.

Also a more loosely-defined problem has been illustrated in which it was possible to show the designer in one diagram a range of solutions displaying incremental benefits, so that the designer could base a selection from among them on other factors outside the definition of the problem. The simulation again did not generate a solution, but having been shown by the designer the kind of solution that was appropriate, was able to generate comparative evaluations of a range of them. The final choice was up to the designer, but again this illustrated reverse computation.

In this final application, the computation performs a routine that is closer to solution generation than either of these two cases, in that it builds the envelope of a building from a footprint on the site in response to information about the constraints that the final envelope has to obey. It is a more tightly-constrained problem than the stadium, but more significant a design problem than choosing an optimum orientation.

This is the third of the family of problems referred to in the Introduction. The problem, in general terms, is to conserve the illumination falling on a surface, whilst finding the maximum volume for a three-dimensional obstruction that threatens to interrupt this light.

In many urban sites there is a need to determine the maximum available development envelope that conforms to local ‘right-to-light’ regulations. One example of such a regulation in London states that any proposed design shall not reduce the daylight availability on existing windows within the facades of surrounding buildings to less than 80% of the existing value. This is possible for a designer to check manually if

only a small number of windows are involved, however in a complex urban site, such as that shown in Figure 8-7 below, there may be many hundreds of windows to check.

Such a can be solved by a computationally generated optimised solution. If the maximum compliant envelope can be determined at the outset, then there will be no need to continually check each design iteration, resulting in significant time savings during the conceptual phase.

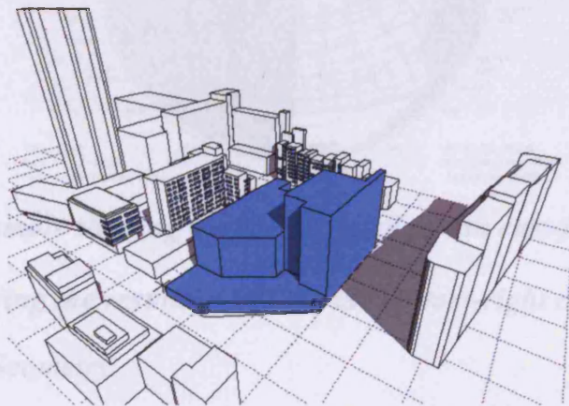


Figure 8-7: Example urban site showing existing site and the windows in surrounding facades whose right-to-light must not be adversely impacted.

Generating the optimum shape requires:

1. A method for computationally determining daylight availability for any window, and
2. A methodology by which the results of each calculation can effectively influence the generation of the next iteration in building form.

8.4.1 Daylight Availability

In this example the UK Building Research Establishment's Vertical Sky Component (VSC) (Littlefair 1991) was used as the metric for daylight availability, calculated directly from the shading mask generated for each adjacent window on the site. Shading masks are calculated in Ecotect using spherical ray-tracing from a grid of points distributed over the surface of each window. Figure 8-8 shows an example mask for an east-facing window, with the BRE VSC shown in the bottom-right corner.

To determine the percentage change, VSC values were first calculated for each adjacent window based on the existing buildings on the site, and stored in a reference

array. The results of subsequent calculations were then compared to these values to test if they were greater than 80% of the original.

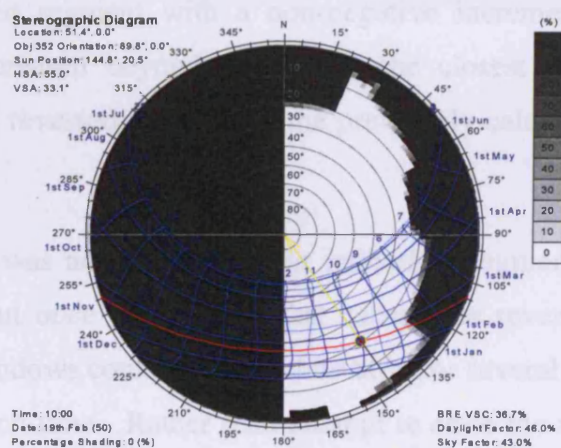


Figure 8-8: An example shading mask calculated for an east-facing window in the site, showing the resulting VSC in the bottom-right corner.

8.4.2 Generative Geometry

In order to generate a development volume, the buildable site boundary was divided into a series of grid segments, as shown in Figure 8-9. The height of each segment could then be independently controlled by the analysis script.

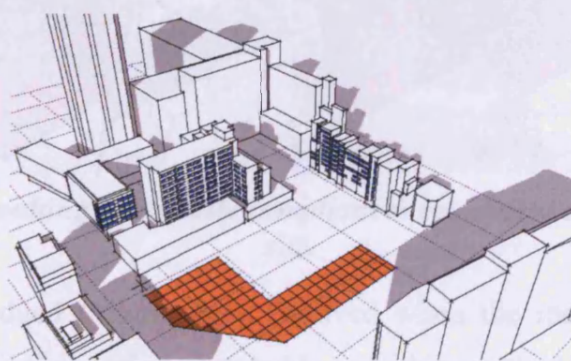


Figure 8-9: The site was divided into grid segments whose height could be independently incremented or decremented.

At the start of the calculation, each grid segment was assigned the same starting height and a positive increment value. On each iteration, the VSC for each adjacent window was calculated and compared with its reference value.

If the calculated value for any window fell below 80%, the closest grid segment was found and its increment divided by negative two. This halved the increment of the segment and reversed its direction. The proximity of each segment was based on the

linear distance from the geometric centre of its base at ground level to the geometric centre of the window. If the increment value of the closest segment was negative, then the next closest segment with a non-negative increment was used. If the calculated value increased beyond 80%, then the closest negative segment was similarly halved and reversed, but only if the previously calculated value was below 80%.

In the initial runs it was not uncommon for individual segments to be reversed and then 'forgotten' about once the window that caused the reversal regained its 80%. This was because windows could remain below 80% for several iterations, reversing a different segment each time. Rather than attempt to store the reversed segments for each window, a limitation of five consecutive negative increments was imposed, after which the segment reverted to a positive increment. Whilst this increased the total number of iterations required for the resolution of the envelope by approximately 9%, it greatly simplified the scripting.

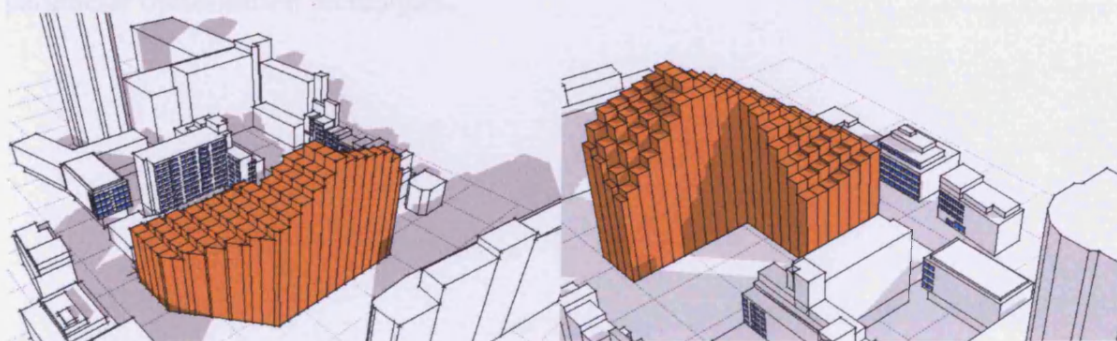


Figure 8-10: The resulting maximally compliant development envelope on the given site.

The process was judged to have been resolved when the increment values of all segments fell below a specified threshold – in this particular case 100mm. The resulting compliant development envelope is shown in Figure 8-10 above.

8.5 Discussion

In all these examples, using solar radiation in the design process has improved the energy efficiency of the solution. The research has shown how the reverse computation approach has been able to offer possible solutions to the designer.

It has also shown via development of a practical method for considering incident solar radiation and site overshadowing effects that performance-based theory can match a

practical approach to forming the design concept in a much more efficient and creative way.

The examples used in this chapter were selected to demonstrate that building geometry can be used as a parameter in optimisation studies, and that the process is of most benefit to the designer when applied to tightly defined problems. Whilst it would seem logical that the more information you can apply to the optimisation of a computational model the more useful the result, in fact, because of the nature of the building design process and of the information available to be applied, the opposite is most often true.

Further work in this research now needs to be done looking in more detail at the comparison of results produced by slightly different approaches to the same problem. This includes using a range of starting points in the model-generation scripts and different decision-making methods, as well as the integration of more complex parameter optimisation techniques.

CHAPTER NINE

CONCLUSION AND SUMMARY

9 Conclusion and Summary

9.1 Introduction

A systematic approach to the research aim was carried out to investigate the process of reverse computation for solving problems in building design concerned with solar radiation falling on building surfaces. Some of processes described make a novel application of environmental software.

9.2 Summary

The introduction to the research in the first chapter explained the aim and objectives, as well as a justification for the research. A background literature review was then carried out to build up a foundation of support for the research.

Chapters Three to Five supplied the necessary background to the work done in the research, reviewing standard approaches to working with solar radiation that are relevant to the research , and describing the tools to be used in the research.

Chapter Three has tried to cover all necessary background regarding the nature of solar radiation and its physical behaviours. This includes types of radiation, solar radiation measurements, weather data source and conversion and visualization of solar data. The accuracy of solar data within the weather files on output results was also discussed.

In Chapter Four, prediction of received solar radiation over surfaces was explained. Irradiance mapping using the ICUE method by Dr John Mardaljevic has been described in detail. The use of cumulative skies and the possibility of representing the total annual cumulative solar radiation is explained as being image-based. Another object-based approach has been explained and its advantages and disadvantages described. An alternative approach for the calculation and display of surface insolation has been developed within the Ecotect software. It has covered how Ecotect calculates incident solar radiation values and how cos law effects the insolation's value. Sky subdivisions were also explained in this chapter and how Ecotect uses those subdivisions.

Chapter Five then dealt mainly with overshadowing and shading masks. It showed how objects cast dynamic shadows as the sun passes through the sky, explaining how this affects direct solar radiation and sunlight. Shading masks and their calculation were then explained as well as reflected radiation and shading mask layers. Sky factors and sky components also were covered here.

These last three chapters presented the tools. Chapter Six to Eight introduced novel applications of the tools for solving recurrent design problems.

Chapter Six investigated the optimization of solar collector angles. In the first place mapping solar radiation and overshadowing effects over a spherical surface was explained. A technique to significantly speed up the calculation using shading masks was then presented. Also the effect of overshadowing on optimum solar collector angles by a series of spheres generated at different positions in a site has been demonstrated.

Chapter Seven described how insolation can vary quite significantly over the surfaces of buildings and that this should be a major design consideration. This has implications for solar control strategies, the location of windows and apertures as well as the layout and use of spaces. Evaluating shading design and the spatial effectiveness of detailed shading design showed that designing a correct external shading system is significant to the optimum use of solar gains. This led to the technique which deals with the performance-based design by reversing the usual computation process for designing complex shading devices.

The technique was taken further in Chapter Eight, looking at envelope and volume generation which has direct application in energy-conscious building design. Conceptual form can be imagined made from some flexible intelligent material responding to weather condition, sun position and its neighbourhood in terms of obstructions. It can then match itself with the complex situation giving the best possible shape and volume based on a specific set of criteria.

In overall, obviously solar radiation represents an important resource for many countries in all part of the world. This is becoming more important as energy prices

and environmental concerns generate pressures on the movement towards more energy-efficient and sustainable building solutions. With the increasing density of development in modern cities, many designers are finding that their sites have less and less access to solar gains due to overshadowing from surrounding buildings. Thus, to make the best use of what is a dwindling resource in our cities, it is likely that the very forms of buildings and the general urban infrastructure will need to carefully consider access to both light and solar radiation at all levels.

9.3 Major Contributions

The major contribution of this research are summarised in the sections below:

9.3.1 Optimizing Angle of a Surface or a Solar Collector

This calculation has been conducted through the spherical optimization method comparing total annual solar radiation on differently oriented examples of the same collector at the same location. This is a novel technique devised by the author of using computation to establish the optimum solution to a tightly-defined problem.

Calculations of this kind can provide a dynamic analytical approach in decision making. The shape of an external surface can be optimised for solar availability by evaluating optimum angles in this manner element by element. This would be a totally new approach for external building's surface design.

9.3.2 Insolation Control Using Reverse Calculation

It has been described as a practical methodology to control incident solar radiation through calculation, visualization and mapping of quantified insolation over specific surfaces within the model. This enables the analytical tool to feed back into a system of iterative adjustment using reverse calculation in a normal design cycle solving building problems. Several example models have been described in Chapters Six and Chapter Seven to support this technique, which was developed by the author.

9.3.3 Design Influence on Existing Developments

Consideration of available daylight for existing surrounding developments in a period of time created the concept of an envelope growing to an optimum shape in

a complex urban block. This is a flexible application of geometry and daylight responding to right-to-light issues. The technique could preserve a percentage of daylight received by many windows in conjunction with the maximum envelope for any obstructions. It demonstrates the use of reverse computation to generate the optimum form of an envelope in solving a specific tightly defined problem. This technique was originated and devised by the author.

9.3.4 Holistic design paradox

An important architectural consideration follows on from this work – that being the extent to which the introduced method can be applied in the process of building design. Many architects would reject the anti-intuitive approach taken by both the computer and the algorithm it is implementing; arguing that it leaves is no room for creativity or serendipity.

As a flexible volumetric 3D approach, the methodology developed here allows designers to visualise and assess specific criteria to make the best decision in their building design. Such tools aid modern building designers in their pursuit of the ultra-architectural design style aimed at reaching zero (fossil) energy developments.

For example, an architect may want to know to what extent the size and position of windows on a façade in a high latitude location (somewhere like Norway) can affect the energy saved through the use of daylight-linked lighting systems. This technique puts the concept's model in the Norwegian weather condition as well as its actual site, to monitor what are the solar radiation obstructions from self-obstructions to third party obstructions. Then running the cumulative yearly incident solar radiation, shading masks and surface maps will show what the comparative exact amount of solar radiation is, over the concept's surface. Design alternatives can even be introduced by the designer to make proper decisions by running related scripts to show the optimized window sizes which have greater daylight factors.

One of the most significant parts of this technique is the speed of calculation and the graphical model output in three dimensional perspectives, with storable views to look at and decide which parts must be amended before rerunning the program.

9.4 Further Steps

This research also may play a basic role for generative-based design method. The thesis has shown the potential for the generation of building form in Chapter Eight. This potential suggests a broad spectrum of research creativity for building form generation. An attempt could be made to generate optimum possible forms based on weather data and location. One line of research could be to adapt work already done on three-dimensional structures in the Formex method (Nooshin 1996; Nooshin and Disney 2000), Gen Opt (Wetter 2000) and generative algorithms for three-dimensional forms in Bentley's Generative Components (Aish 2003), in order to develop generative-performance-based design which when used by creative designers and engineers will provide for the most expressability and the most extensibility.

REFERENCES

10 References:

(CIE), C. I. d. L. E. ed. 1973. Standardization of Luminance Distribution on Clear Skies. Paris: CIE Publication

Abanomi, W. M. 2005. Environmental Design of Prtotype School Buildings in Hot, Arid Regions with Special Reference to Riyadh, Saudi Arabia. Cardiff University.

Aish, R. 2003. Bentley's Generative Components, A design tool for exploratory architecture. [online]. Available at: <URL: <http://www.bentley.com/en-US/Markets/Building/GenerativeComponents.htm>> [Accessed: 08/07/2003].

Arumi-Noe, F. 1996. Algorithm for the geometric construction of an optimum shading device. Automation in Construction 5(3), pp. 211-217.

Bari, S. 2001. Optimum orientation of domestic solar water heaters for the low latitude countries t. Energy conversion and management 42(10), pp. 1205-1214.

Bartzokas, A. et al. 2003. Sky luminance distribution in central Europe and the Mediterranean area during the winter period. Atmos Solar-Terr Phys 65, pp. 113-129.

bernhard, F. 2003. The SOHO (Solar & Heliospheric Observatory). [online], (30 June). Available at: <URL: <http://sohowww.nascom.nasa.gov/>> [Accessed: 04/02/2004].

Blanco-Muriel, M. et al. 2001. Computing the Solar Vector. Solar Energy 70(5), pp. 431-441.

Boyle, G. 1996. Renewable Energy Power for a Sustainable Future. Milton Keynes: Oxford University Press.

Capeluto, I. G. and Shaviv, E. 2001. On the use of 'solar volume' for determining the urban fabric. Solar Energy 70(3), pp. 275-280.

Carruthers, D. D. et al. 1990. An Evaluation of Formulae for Solar Declination and the Equation of Time. School of Architecture, University Western Australia.

Chauliaguet, C. 1977. *Solar Energy in Buildings. Preface of English edition ed.* Paris: John Wiley & Sons.

Chow, T. T. and Chan, A. L. S. 2004. *Numerical study of desirable solar-collector orientations for the coastal region of South China. Applied Energy* 79(3), pp. 249-260.

Chung, T. M. and Mardaljevic, J. eds. 2004. *Quantifying solar access and daylight availability in dense urban settings. International Housing Conference. Hong Kong:*

Commission Internationale, d. L. E. C. 1973. *S003 Spatial distribution of daylight-CIE standard overcast sky and clear sky. Paris:*

Commission Internationale, d. L. E. C. K., J. D. ed. 1989. *Guide to recommended practice of daylight measurement. Vienna: Commission Internationale, de L'Eclairage CIE S003.*

Cotton, J. F. 1996. *Solid modeling as a tool for constructing solar envelopes. Automation in Construction* 5(3), pp. 185-192.

Diasty, R. E. 1998. *Variable Positioning of the Sun Using Time Duration. Renewable Energy* 14, pp. 185-191.

Dickinson, W. C. and Cheremisinoff, P. N. 1980. *Solar Energy Technology Handbook. 6 ed. Indiana: Marcel Dekker, INC.*

Duffie, J. A. 1974. *Solar Energy Thermal Processes. Wisconsin: John Wiley & Sons.*

Givoni, B. 1994. *Passive and Low Energy Cooling of Building New York: John Wiley.*

Gunerhan, H. and Hepbasli, A. *Determination of the optimum tilt angle of solar collectors for building applications. Building and Environment In Press, Corrected Proof.*

Haghparast, F. 2002. *"ECOTECH"-The Complete Environmental Design Tool and Energy Conscious Design in Architecture. In: the ninth Iranian Researchers Conference in Europe. (UCE) Birmingham, UK.*

Haghparast, F. 2004. *The Optimisation of Stadium Roof Glazing for Cost and Solar Access Using Built Form Generation based on performance-Optimised Solutions to Tightly Defined Design Problems. In: the 21st Conference on Passive and Low Energy Architecture (PLEA). Eindhoven, The Netherlands.*

Hanafi-Rifai, W. 1990. *Environmental design in hot humid countries with special reference to Malaysia. University of Wales, Cardiff.*

Hartley, L. E. and Martinez, L. J. A. 1999. *The optimisation of the angle of inclination of a solar collector to maximise the incident solar radiation. RENEWABLE ENERGY 17(3), pp. 291-309.*

Iqbal, M. 1983. *An Introduction to Solar Radiation. New York, pp. 23-25.*

Kaftan, E. ed. 2001. *The Cellular Method to Design Energy Efficient Shading Form to Accommodate the Dynamic Characteristics of Climate. PLEA. Brazil: The 18th Conference on Passive and Low Energy Architecture.*

Kittler, R. 1994. *Some qualities of scattering functions defining sky radiance distributions. Solar Energy 53(6), pp. 511-526.*

Kittler, R. and Darula, S. 1997. *Prevailing sky conditions: Identifying simple parameters for definition. Lighting Res Technol 29(2), pp. 63-78.*

Kittler, R. and Darula, S. 1998. *Linking sunlight with skylight by sky types and luminous turbidity. Build Res 46(3), pp. 173-188.*

Kittler, R. et al. 1998. *A set of standard skies American- Slovak grant project US-SK 92052.*

Kittler, R. et al. 1997. *A new generation of sky standards. In: Lux Europa Amsterdam: Proceedings of the Eighth European Lighting Conference., pp. 359-373.*

Klein, S. A. 1977. *Calculation of monthly average insolation on tilted surfaces. Solar Energy 19(4), pp. 325-329.*

Kovach, A. and Schmid, J. 1996. *Determination of the energy output losses due to shading of building-integrated photovoltaic arrays using a raytracing technique. Solar Energy 57(2), pp. 117-124.*

Kundu, B. 2002. *Performance analysis and optimization of absorber plates of different geometry for a flat-plate solar collector: a comparative study. Applied Thermal Engineering* 22(9), pp. 999-1012.

Kunz, W. and Rittel, H. W. J. 1972. *Issues as Elements of Information Systems. Berkeley: Department of Architecture, University of California, Berkeley, CA.*

Lam, M. C. 1987. *Sunlight as Formgiver for Architecture. New York: Van Nostard Rainhold.*

Lang, K. R. 2001. *The Cambridge Encyclopedia of the Sun. Arlington, Massachusetts: Cambridge University Press.*

Linacre, E. 1992. *Climate Data and Resources. New York: Routledge.*

Littlefair, P. J. 1991. *Site layout planning for daylight and sunlight: a guide to good practice. Garston: Building Research Establishment.*

Mahdavi, A. 1993. "Open" Simulation Environments: A "Preference-Based" Approach. In: *CAAD Futures. CMU, Pittsburgh, Pennsylvania, USA: Elsevier Science Publishers B.V. pp. 195-214.*

Mahdavi, A. 1996. *SEMPER: A New Computational Environment for Simulation-Based Building Design Assistance. In: International Symposium of CIB W67 (Energy and Mass Flow in the Life Cycle of Buildings). Vienna, Austria. pp. 467-472.*

Mahdavi, A. 1997. *Toward a Simulation-assisted Dynamic Building Control Strategy. In: the Fifth International Building Simulation Association (IBPSA) Conference. pp. 291-294.*

Mahdavi, A. 1999. *A comprehensive computational environment for performance based reasoning in building design and evaluation. Automation in Construction* 8(4), pp. 427-435.

Mahdavi, A. and Berderidou-Kallivoka, L. 1992. *A 'Two-Way' Inference Approach to Daylighting Simulation. In: IESNA Annual Conference. San Diego, CA, . pp. 263-271.*

mahdavi, A. and Berderidou-Kallivoka, L. eds. 1995. A Generative Simulation Tool for Architectural Lighting. The Fourth International Conference of the International Building Performance Simulation Association (IBPSA). Madison, Wisconsin:

Mahdavi, A. et al. eds. 2001. Performance-Based computational design via differential modeling in Building and Two-Stage mapping. the CAAD Futures Conference Eindhoven, the Netherlands:

Mahdavi, A. and Lam, K. P. 1991. Performance Simulation as a Front-End Tool for 'Integrative' Conceptual Design Evaluation. In: J.A. Clark, J.W.M., R.C. Van ed Perre ed. International Building Simulation Association (IBPSA) Conference. pp. 439-445.

Mahdavi, A. et al. 1997. Bi-directional computational design support in the SEMPER environment. Automation in Construction 6(4), pp. 353-373.

Mahdavi, A. and Ries, R. 1998. Towards computational eco-analysis of building designs. Computers & Structures 67(5), pp. 375-387.

Mardaljevic, J. 2005. Quantification of Urban Solar Access. In: Jenks and Dempsey eds. Future Forms and Design for Sustainable Cities. Architectural press (Oxford, UK), pp. 371-392.

Mardaljevic, J. and Rylatt, M. 2003. Irradiation mapping of complex urban environments: an image-based approach. Energy and Buildings 35(1), pp. 27-35.

Markou, M. T. et al. 2005. Sky type classification in Central England during winter. Energy 30(2005), pp. 1667-1674.

Marsh, A. 1997. Performance Analysis and Conceptual Design. PhD, University of western Australia.

Marsh, A. J. ed. 2003. Computer-Optimised Shading Design. Building Simulation. Eindhoven: Eighth International IBPSA Conference.

Marsh, A. J. ed. 2005. The Application of Shading Masks in Building Simulation. Building Simulation. Montreal, Canada:

Meeus, J. 1998. Astronomical Algorithms. Second ed. Richmond, Virginia, USA: Willmann-Bell.

Met Office, U. 2004. Products and services. Met Office. Available at: <URL: <http://www.met-office.gov.uk/index.html>> [Accessed: 2004].

Mohd Azmi bin Hj Mohd Yakup and Malik, A. Q. 2001. Optimum tilt angle and orientation for solar collector in Brunei Darussalam. *Renewable Energy* 24(2), pp. 223-234.

Moon P and Spencer DE 1942. Illumination from a non-uniform sky. *Trans Illum Eng Soc*, pp. 707-726.

Morcos, V. H. 1994. Optimum tilt angle and orientation for solar collectors in Assiut, Egypt. *Renewable Energy* 4(3), pp. 291-298.

NASA. 2003. Surface Meteorology and Solar Energy. NASA's Earth Science Enterprise. Available at: <URL: <http://eosweb.larc.nasa.gov/cgi-bin/sse/sse.cgi?na#s01>> [Accessed: 12/08 2003].

Neville, R. C. 1978. Solar energy collector orientation and tracking mode. *Solar Energy* 20(1), pp. 7-11.

Nooshin, H. 1996. A Technique for surface eneration. In: *Int. Symp. on Conceptual Design of Structures. Stuttgart Inst. fur Konstruktion und Entwurf II*. pp. 331-338.

Nooshin, H. and Disney, P. 2000. Formex Configuration Processing I. *Int. J. Space Structures* 15(1), pp. 1-52.

Page, J. K. 1986. *Prediction of Solar Radiation on Inclined Surfaces*. Sheffield: D. Reidel Publishing Company.

Perez, R. et al. 1990. Modeelling daylight availability and irradiance components from direct and global irradiance. *Solar Energy* 44(5), pp. 271-289.

Perraudeau, M. and Chauvel, P. 1986. One year's measurments of luminous climate in Nantes. In: *International Daylighting Conference*. Long Beach, USA.

Perry, J. and McClintock, M. eds. 1997. *The Challenge of 'Green' Buildings in Asia*, . *International Conference on Building Envelope Systems and Technology Bath: CWCT Service*.

Quaschnig, V. and Hanitsch, R. 1998. Irradiance calculations on shaded surfaces. *Solar Energy* 62(5), pp. 369-375.

Reda, I. and Andreas, A. 2004. Solar position algorithm for solar radiation applications. *Solar Energy* 76, pp. 577-589.

Robinson, D. et al. 2003. Integration Resource Flow Modelling of Urban Neighbourhoods: Project SUNTOOL. In: the Eighth International IBPSA Conference. Eindhoven, Netherlands. pp. 1117-1122.

Robinson, D. and Stone, A. 2004. Solar Radiation Modelling in the Urban Context. *Solar Energy* 77(3), pp. 295-309.

Roy, G. et al. 1995. The Development of Modelling Strategies for Whole Sky Spectrums under Real Conditions for International Use. Sydney: University of Sydney, Murdoch University.

Salmon, C. 1999. Architectural Design for Tropical Regions. New York: John Wiley.

Sayigh, A. A. M. 1979. Solar Energy Application in Buildings. Riyadh: Academic Press, INC. (London) LTD.

Shariah, A. 2002. Optimizing the tilt angle of solar collectors. *Renowable Energy* 26(4), pp. 587-598.

Snow, M. et al. eds. 1999. A GIS Building Integrated PV (BIPV) Simulation Approach International Solar Energy Society (ISES). Jerusalem: Proceeding of the Congress on Photovoltaics (PVs) Modeling for Cities.

Song, L. et al. 2002. Developing an Equal area global grid by small circle subdivision. Santa Barbara, CA, USA: National Center for Geographic Information & Analysis.: Discrete Global Grids. Available at: <URL: <http://www.ncgia.ucsb.edu/globalgrids-book/song-kimmerling-sahr/>> [Accessed: 14 December 2003].

Streete, J. 1996. The Sun-Earth System. Tennessee: University Science Books.

Struub, R. 2005. Sim Solve v3.0. Available at: <URL: <http://computing.ee.ethz.ch/sepp/simusolv-3.0.html>> [Accessed].

Szokolay, S. V. 2004. Introduction to Architectural Science: The Basis of Sustainable Design. London: The Architectural Press, Butterworth-Heinemann Ltd.

Tempczyk, H. 1986. A survey of research and studies on design. DESIGN STUDIES 7(4), pp. 199-215.

Tiris, C. and Tiris, M. 1998. Effect of collector orientation on solar energy availability. Energy Conversion and Management 39(8), pp. 843-852.

Tregenza, P. R. 1999. Standard skies for maritime climates. Lighting Res Technol 31(3), pp. 97-106.

Tregenza, P. R. and Sharples, S. 1995. New Daylight Algorithms. Tregenza, P. R. Univ Sheffield, Sch Architectural Studies, Sheffield S10 2uj, England: IEA Task 21, Subtask C2-New Daylight Algorithms. Available at: <URL: <http://eande.lbl.gov/Task21/BRE-ETSU/contents.html>>> [Accessed: 13/11 2004].

U.S. Department of Energy. 1996. Building Energy Software Tools Directory. the U.S. Department of Energy (DOE). Available at: <URL: http://www.eere.energy.gov/buildings/tools_directory/about.cfm> [Accessed: 08/09 2003].

Vanderplaats, G. N. 2001. DOT Design Optimization Tools Users Manual - Version 5.X. Colorado Springs, USA: Vanderplaats Research & Development. Available at: <URL: <http://www.vrand.com/DOT.html>> [Accessed: 14/12/2003].

Wetter, M. 2000. Design Optimization with GenOpt. Building Energy Simulation User News 21(September/October), pp. 19-28.

Wetter, M. 2004. GenOpt - Generic Optimization Program User Manual Version 2.0.0, Technical Report LBNL-54199. Lawrence Berkeley National Laboratory, Berkeley.

APPENDICES

11 Appendices

11.1 Appendix A - Stadium Design

11.1.1 Introduction

The main dilemma in stadium roof design is to provide rain and sun protection for the audience whilst still allowing adequate solar radiation onto the pitch. Direct sunlight on the pitch is vital in the heart of winter to promote turf growth and the recovery of the playing surface. This is a dilemma for naturally turfed stadia throughout most of northern Europe.

This section presents the results of an example study undertaken by the author and his supervisor into the availability of solar radiation over the playing surface within the proposed Morpha Stadium in Swansea, Wales. The aim of this study was to determine the influence of transparent roof panels on incident solar radiation and the levels of Photosynthetically Active Radiation (PAR) which affects turf growth. The PAR values for a range of configurations of glazed panels were compared with those for an opaque roof, and assessed for the benefit that they might bring to the health of the turfgrass.

Using geometrical optimisation methods based on projections of the playing surface onto the roof area, the optimum location of glazing panels within the proposed roof was determined. This study is included to illustrate the direct and immediate application of some of the ideas developed in this thesis to real design problems.

A geometric model of the stadium was constructed using the Ecotect software. The roof was generated such that the relative area of glazing could be changed algorithmically, allowing for a wider range of options to be considered.

The stadium roof is modelled using a series of roughly rectangular sections – except at the corners where they approached a more triangular shape. The length of each section from the outer edge of the roof to the internal edge could be manipulated by a script by simply multiplying its original length by some fraction based on where the section was in relation to the centre point of the pitch. This way the glazing / roof ratio was altered in each segment by using a roof section projecting a fraction F

inward from the outer edge, and a glazing section projecting a fraction $1-F$ outwards from the inner edge.

Both linear and trigonometric functions were used to generate different glazing ratios in different parts of the roof. Using the azimuth of each inner edge line relative to the pitch centre allowed the results to be biased towards a southern orientation.

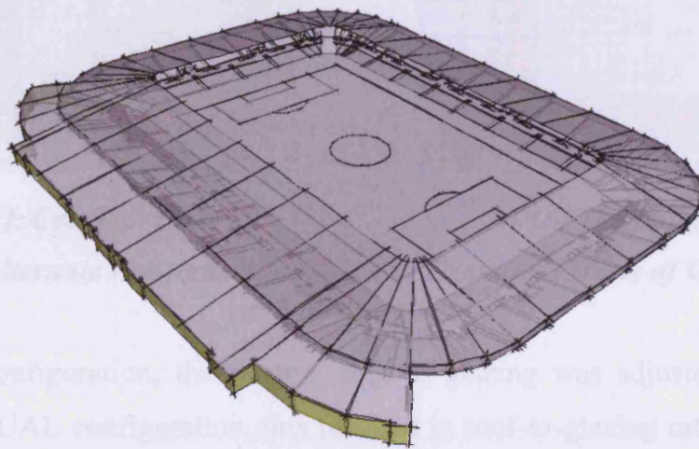
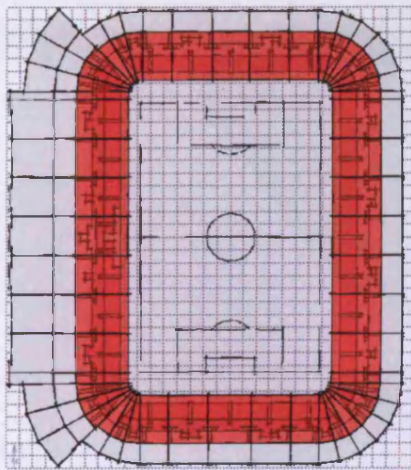


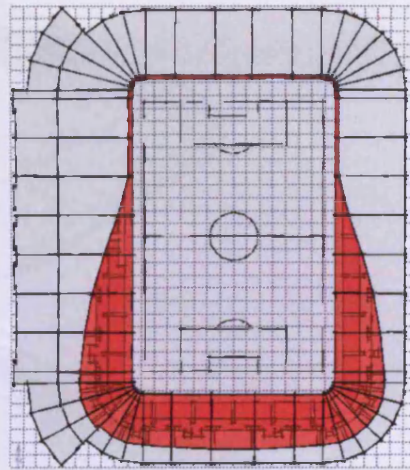
Figure 11-1: The Geometric Model Used for the Solar Analysis.

Therefore, a systematic analysis was carried out using a range of roof-to-glazing ratios. This was initially performed by simply increasing the amount of glazing at the edge of the roof closest to the playing area. However, in order to evaluate the relative effect of direct gains from the Sun against indirect gains from the rest of the sky dome, an additional configuration was tested which biased the area of glazing towards the southern end of the stadium.

Examples of the two configurations, termed EQUAL and BIASED, are shown in Figure 11-12 below.



EQUAL Configuration



BIASED Configuration

Figure11-2: Alternate Configurations Used to Examine Effects of Glazing Area on Pitch Insolation.

Within each configuration, the relative area of glazing was adjusted in 10 stages. Within the EQUAL configuration, this resulted in roof-to-glazing ratios between 0% and 90%, in steps of 10%.

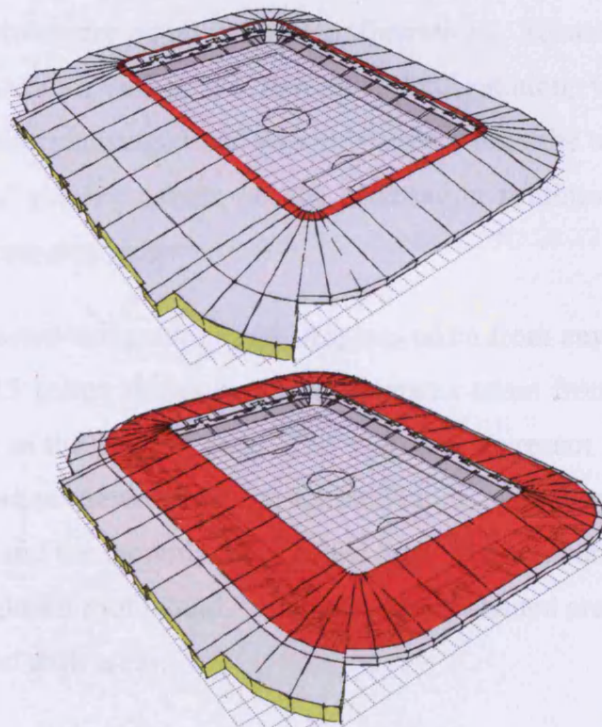


Figure11-3: The two extreme ratios within the EQUAL Configuration.

However, in the BIASED configuration this resulted in roof-to-glazing ratios between 4% and 41% in steps of approximately 4%.

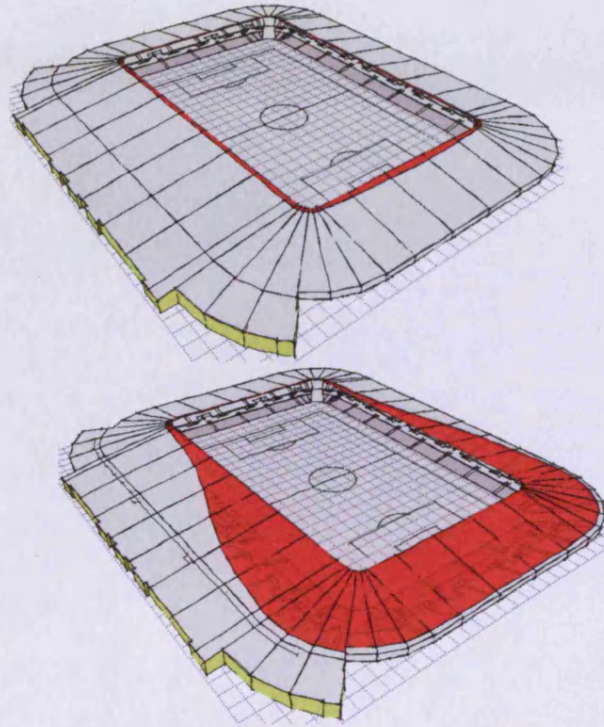
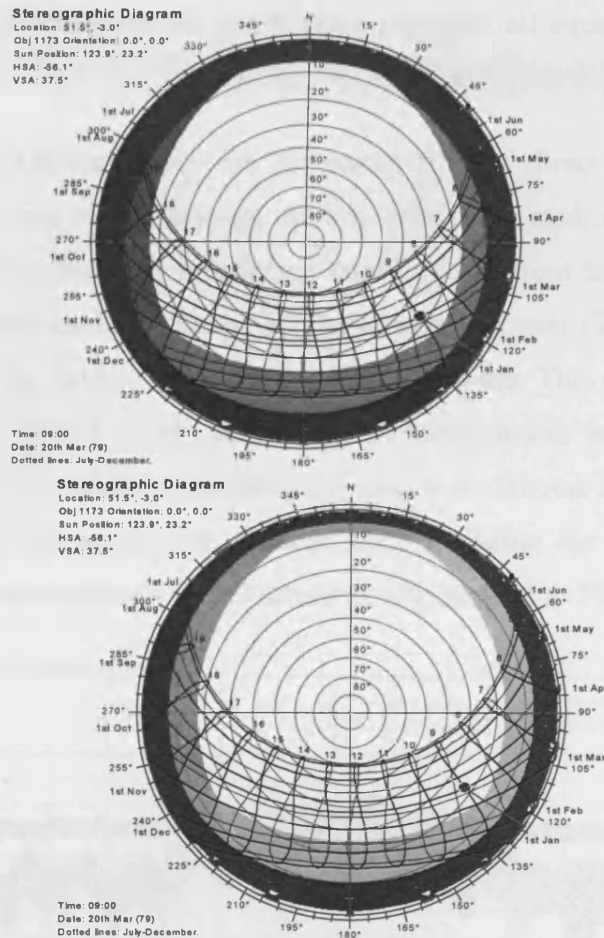


Figure 11-4: The two extreme ratios within the BIASED Configuration

Thus, glazing areas at the southern end of the stadium, where low level direct solar radiation enters in winter, are equal in both configurations. However, the small area of glazing on the northern end in the BIASED Configuration, where only diffuse skylight enters, remains unchanged and was only used within the analysis to ensure a consistent number of glazing panels for the automation routines to act upon. Its effects on the results are negligible.

This can be demonstrated using a Sun-Path diagram taken from any point on the pitch surface. Figure 11-15 below shows two such diagrams taken from the centre of the southern goal mouth in the playing area. The diagrams represent a fish-eye view of the entire sky dome when viewed from the selected point, overlaid with both the areas obstructed by stands and the monthly paths of the Sun. For comparative purposes, the shading from a non-glazed roof would, occupy the entire shaded area in each diagram, over both the light and dark areas.



BIASED Configuration

EQUAL Configuration

Figure 11-5: Overshadow masks generated from the centre of the southern 'D'.

It also clearly shows that the areas where the direct Sun is obstructed in each configuration are the same.

11.1.2 Methodology, Optimisation and Geometry of stadium design

To establish the link between insolation on the playing surface and the geometric form of the roof, the Ecotect software (Marsh 1997) was used to model and analyse the stadium. Importantly, the scripting language capabilities on Ecotect allowed for the generation and manipulation of model geometry as well as direct access to analysis routines and their results. Thus, scripts were created to iteratively perform calculations, modifying the geometry of the model based on calculation results, and then repeating the process until specific criteria were met.

Using such scripts, the starting assumptions and decision-making techniques are fundamental to the final results. Different starting points and decision methods will

likely yield quite different solutions to the same problem, all equally valid based on the test criteria.

The calculation of PAR was based on the summation of direct and diffuse solar radiation values at points on the playing surface within the stadium, accounting for overshadowing and the effects of translucent panels at different locations within the roof. The weather data used was based on a test reference year (TRY) for England-West, encompassing the Bristol, Newport and Swansea areas. This data file contained a full year record of actual hourly recordings of temperature, humidity and solar radiation for the year most closely matching the long-term 20-year average. The data in this file was also compared with detailed data available for Swansea and the averages were found to correlate well, as shown in Figure 11-6 to Figure 11-10 below.

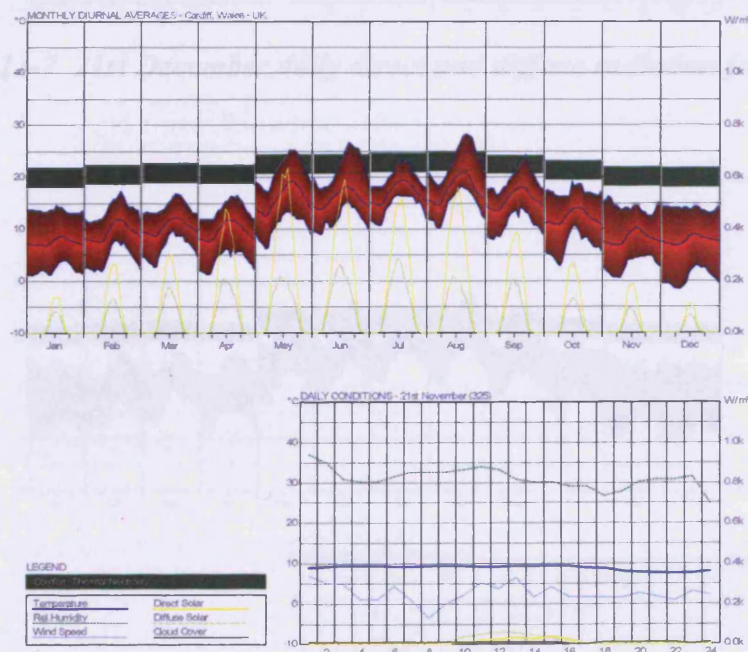


Figure 11-6 21st November daily direct and diffuse radiation for Wales

Figure 11-5 21st January daily direct and diffuse radiation for Wales

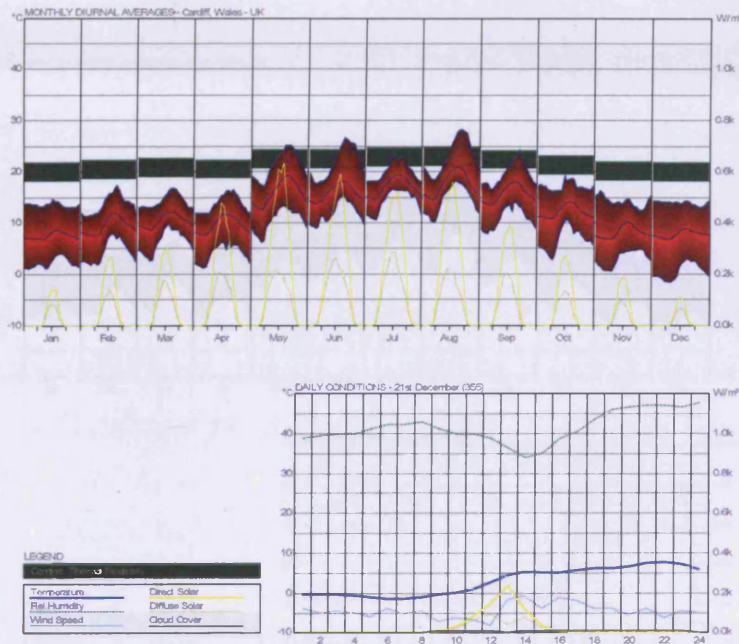


Figure 11-7 21st December daily direct and diffuse radiation for Wales

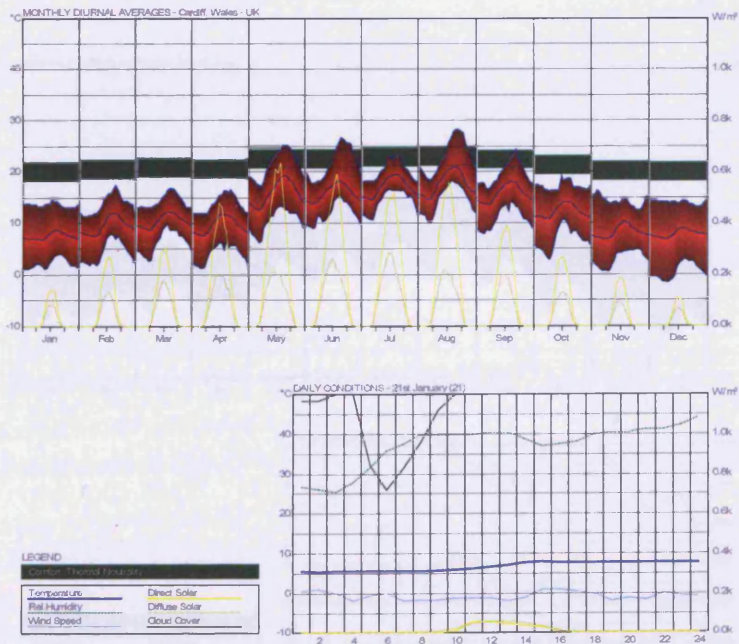


Figure 11-8 21st January daily direct and diffuse radiation for Wales

11.1.3 The Impact of Radiation on Crop

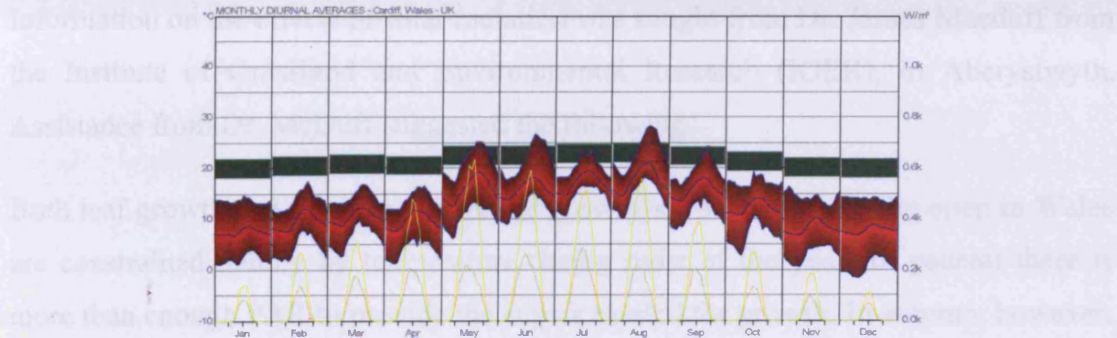


Figure 11-9 21st February daily direct and diffuse radiation for Wales

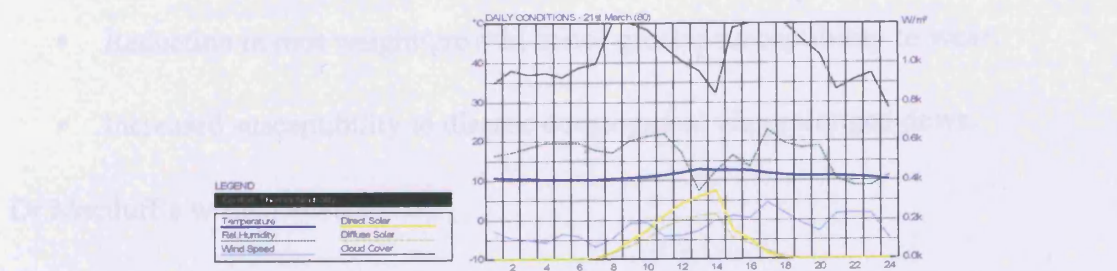
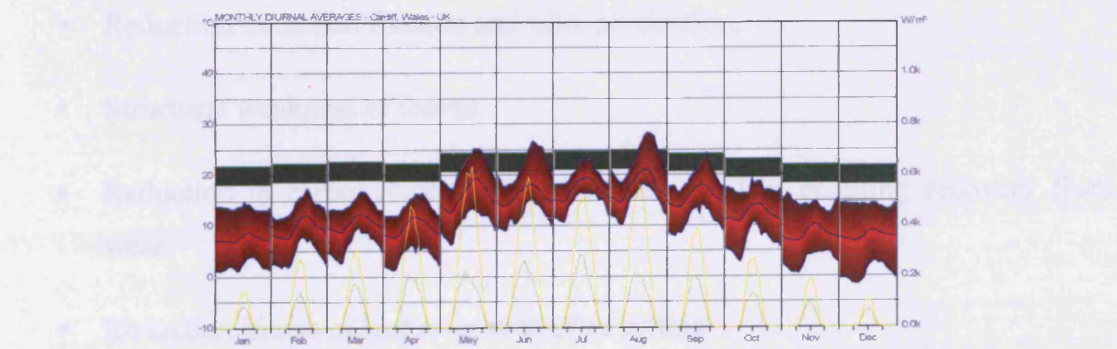


Figure 11-10 21st March daily direct and diffuse radiation for Wales

11.1.3 *The Impact of Shading on Turf*

Information on the effects of solar radiation was sought from Dr. James Macduff from the Institute of Grassland and Environmental Research (IGER), in Aberystwyth. Assistance from Dr. McDuff suggested the following.

Both leaf growth and tillering (horizontal growth) of turfgrasses in the open in Wales are constrained mainly by temperature during most of the year. In general there is more than enough PAR to provide the sugars needed for growth. In autumn, however, the relatively high temperatures and rapidly falling natural light supply means that grass can suffer from a deficit of light - respiratory losses of carbon are not compensated for and the turf is unable to recover from wear. Recovery from wear during mid-winter is generally inhibited by very low temperatures and by low light levels where the temperature is sufficiently high to enable growth.

Where the turf is exposed to prolonged shading, as in many stadia, the following deleterious effects occur throughout the year:

- Reduction in carbon fixation and tiller production.
- Structural weakness of leaves.
- Reduction in carbohydrate reserve content of plant enabling recovery from wear.
- Reduction in rate of leaf re-growth after cutting.
- Reduction in root weight/growth: hence greater susceptibility to wear.
- Increased susceptibility to disease development via prolonged dews.

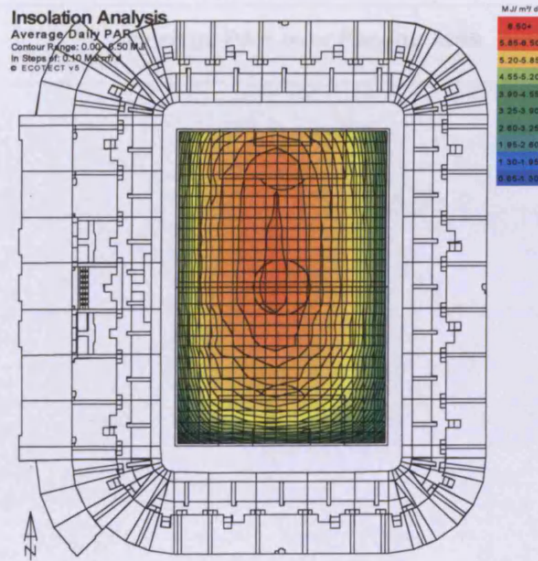
Dr Macduff's written advice was:

“Measures to minimize shading are therefore highly advisable. It should also be borne in mind that in the future as autumn and winter temperatures increase under global warming, the potential for grass growth during the winter will also increase, as will etiolation and net loss of carbon by respiration when the light levels are too low. Hence measures to increase winter light levels will become even more important.”

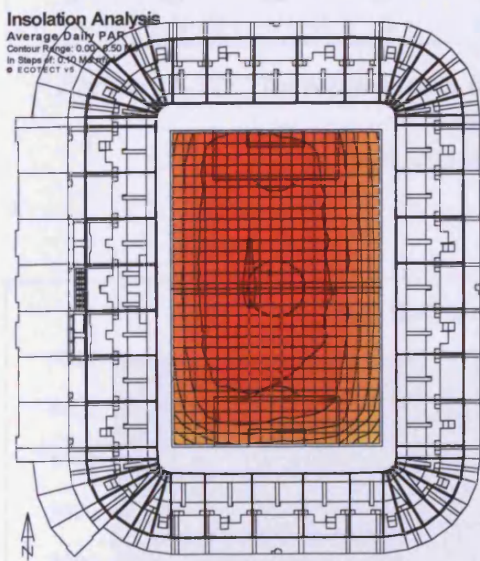
“In the absence of wear (i.e. for turf subject to no play whatsoever during winter) we have recommended minimum winter PAR values of 1 MJ m⁻² day⁻¹ as target ‘turf maintenance’ values over winter. However, where turf is subject to wear associated with a normal event schedule a figure of 3 MJ m⁻² day⁻¹ has been recommended if recovery from wear is to occur throughout the winter period, assuming temperatures are sufficiently high to support growth. This latter value exceeds the corresponding available natural light in the open, hence cannot be achieved inside stadia without recourse to artificial lighting. Some loss of pitch condition over the playing season is therefore inevitable in all stadia.”

11.1.4 Stadium Calculation Results

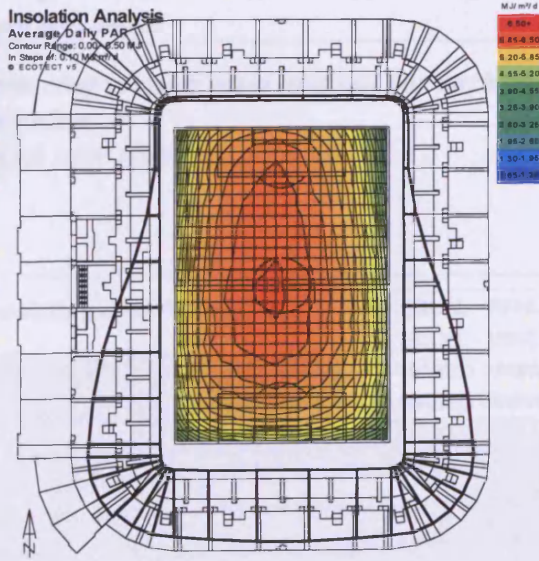
Figure 11-11 below presents an example of the comparative results using the 3 configurations.



No-Glazing Configuration



EQUAL Configuration (80%)



BIASED Configuration (41%)

Figure 11-11: The Distribution of Annual Average Incident Solar Radiation over the Playing Surface.

From this data, charts relating average values to relative glazing ratio were generated. The purpose of these charts are to illustrate the rate of diminishing returns with increased glazing area.

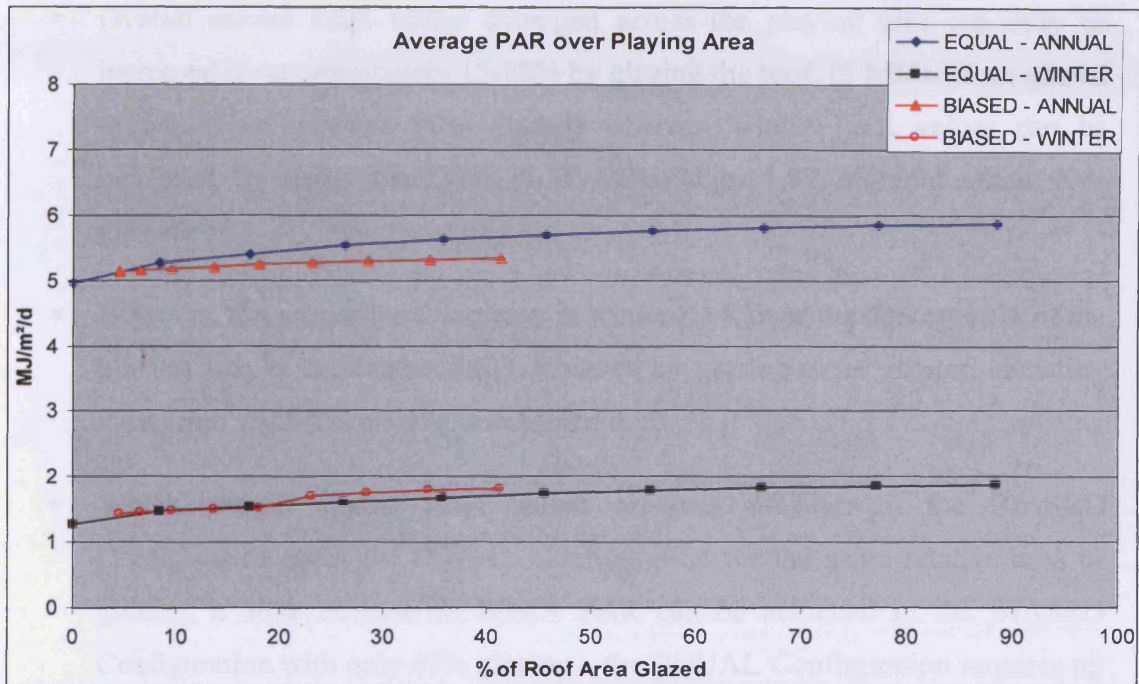


Figure 11-12: The relationship between roof glazing ratio and par for each configuration, both annually and over winter.

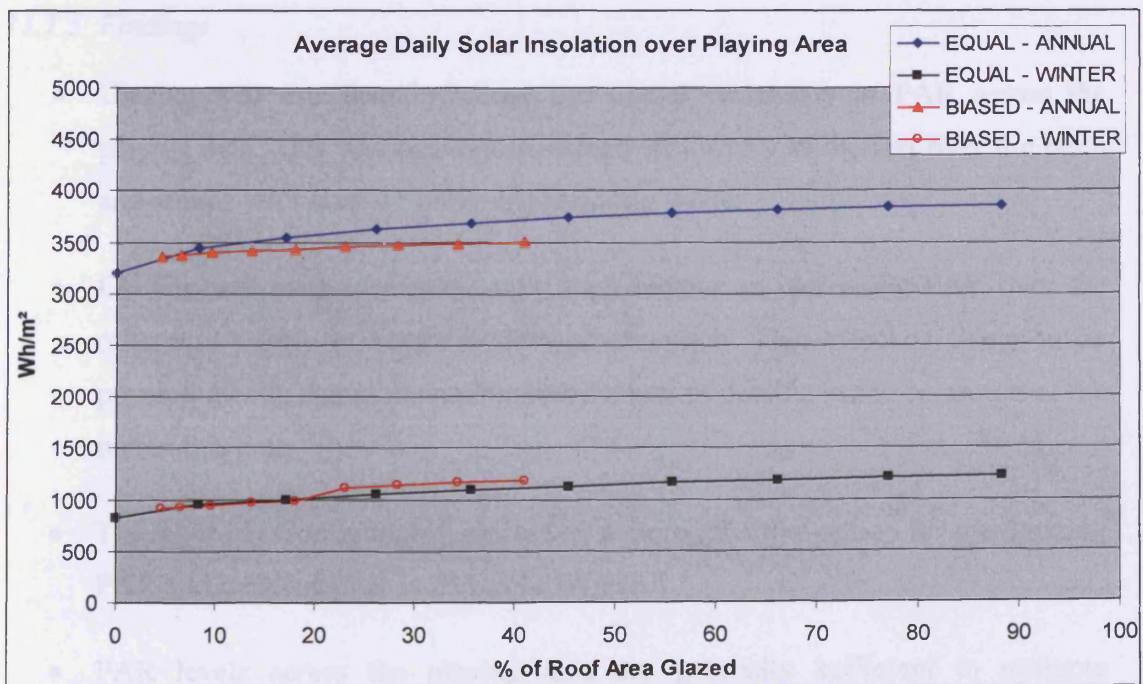


Figure 11-13: The relationship between roof glazing ratio and incident solar radiation for each configuration, both annually and over winter.

The graphs in Figure 11-12 and Figure 11-13 show that:

- Overall annual PAR values averaged across the playing area can only be increased by approximately 15-18% by glazing the roof, (5 MJ/m²/d un-glazed to 5.8 MJ/m²/d when 90% glazed) whereas Winter PAR values can be increased by more than 30% (1.27 MJ/m²/d to 1.87 MJ/m²/d when 90% glazed).
- However, the proportional increase in winter PAR over the darkest 20% of the playing area at the southern end achieved by glazing is far greater, elevating PAR from < 0.5 MJ/m²/d to > 1 MJ/m²/d.
- Whilst overall annual PAR values are not as high in the BIASED Configuration as in the EQUAL Configuration for the same relative area of glazing, a 30% increase in Winter PAR can be achieved in the BIASED Configuration with only 40% glazing – the EQUAL Configuration requires up to 80% of the roof area glazed to achieve the same result.

This indicates the relative prominence of direct solar gains over diffuse gains in Winter within the weather data for this area.

11.1.5 Findings

- Glazing will significantly reduce the spatial variability in PAR across the playing area. This will result in increased uniformity of the turf over the pitch and reduce ‘end effects’, particularly during winter.
- Glazing will have a proportionally high impact on increasing PAR over the otherwise poorly lit southern 20% of the pitch. This effect is likely to be physiologically significant and lessen the rate of decline in the condition of the turf in this area.
- The BIASED Configuration represents a more effective option for maximizing PAR and incident solar radiation in Winter.
- PAR levels across the playing area are generally sufficient to promote recovery of the pitch from normal wear during spring and summer, but not during the winter, a situation common to most stadia.

11.1.6 Detailed Optimisation of Roof Glazing

The requirement was to determine the optimum location and area of roof glazing to maximise incident solar radiation (insolation) falling on the playing surface, thus maximising grass growth. The stadium model shows the proposed unglazed roof area together with the total annual distribution of solar radiation over the pitch.

To do this, the roof was divided into segments running from the perimeter inwards. The amount of glazing within each segment was controlled within an analysis script developed by the author's supervisor. This was done by specifying a depth value on each side of all roof segments, ensuring a continuous edge running around the stadium.

The first issue was the determination of a suitable metric for insolation values. Taking the total annual insolation would bias the result towards Summer, when solar radiation is significantly greater than in Winter and when grass growth is not really a problem. Thus the insolation period needed to consider when the playing surface was under most stress – at times of high usage rates and low radiation levels.

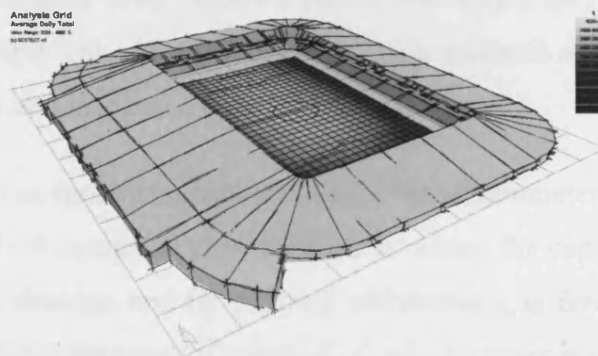


Figure 11-14: Stadium model showing the distribution of solar radiation over the playing surface with an unglazed roof.

Additionally, stress levels are not usually uniform over all areas of a playing surface. Traditionally it is the southern end of a pitch that suffers most in the UK as it is in shade for the longest period in winter. This can be accommodated by summing up only the southern half of the playing surface, or even the southern-most quarter.

The specific insolation period chosen and area of pitch area over which the calculation is done will both directly influence the resulting glazed area of the roof. However, there is no available guidance on whether, for example, to take only the three months of winter, or the coldest three months, or even the coldest seven weeks.

Similarly, why not the southern-most third of the pitch instead of the southern-most quarter.

The second issue is the definition of what is optimum. If maximum insolation is the only criteria, then the glazing area simply resolves to the entire roof, as shown in Figure 2-1.

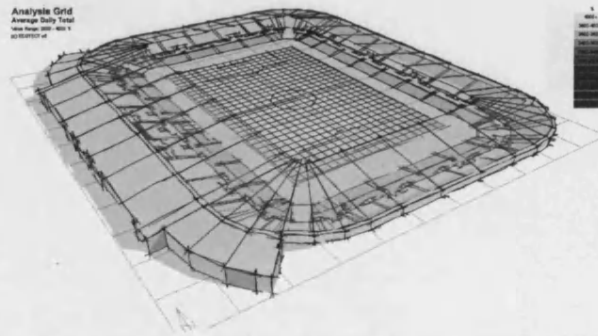


Figure 11-15: If incident solar radiation is the only criteria, then the entire roof glazed is the 'optimum' solution.

The obvious constraints to offset this are material and maintenance costs. These need only be expressed as ratios between the costs of the opaque and glazed materials. Additionally, maintenance costs require a period over which they are to be calculated. The script then simply calculates the areas of each material and looks for the point where the total cost and insolation curves meet.

However, here too the specific values chosen for these parameters significantly affect the result. Figure 11-16 compares two situations in which the capital cost of glazing is twice that of metal decking and its ongoing maintenance is five times higher. The image on the left shows the result if a period of only 10 years is considered whilst the image on the right considers a period of 50 years.

11.2 Appendix B– Papers’ Summary Presented in Conferences Based on the Thesis Investigation

- 1- Farzin Haghparast (2002), “ECOTECT”-The Complete Environmental Design Tool and Energy Conscious Design in Architecture. The 9th Iranian Researchers Conference in Europe, (UCE) Birmingham, UK**

ABSTRACT

A range of conceptual environmental design software is currently under development by Dr. Andrew Marsh at the welsh school of Architecture. This software is quite unique in that it is targeted primarily at architects and designers for use during the earliest most conceptual stages of design. The software allows the designer to interactively test the thermal, lighting, acoustic and passive performance of a design as it develops, from concept sketch studies through to final design validation.

What is interesting about this software is that it is particularly suited to design in hot-dry, hot-steam, and all the environments, providing a wide range of solar and overshadowing analysis features as well the visual display of thermal mass effects within spaces.

Part of my research will be to utilize and adapt some of these tools to the specific conditions of Iran. This will involve validating many of the algorithms used against Iranian data and tailoring the user interface to meet the requirements of Iranian architects. This is possible, as I will be able to work with the software author during their development.

I would therefore like to present the software in its current form, discussing its relevance to design practice in Iran and how this adaptation may be possible.

Key words: sun control, Passive design, Acoustic design, Lighting, Climatic design in Iran

2- Farzin Haghparast (2003), The Development of Computer-Optimised Solutions to Tightly defined Design Problems, Welsh School of Architecture, First Research Student Conference, Cardiff, UK

ABSTRACT

Although simulation is increasingly being used as part of building systems design, the full potential of simulation is usually not fully realised. To improve system performance, designers generally guess different values of system parameters and then redo the simulation many times. This is inefficient and labour intensive. Also, if the number of parameters being varied exceeds two or three, the designer can be overwhelmed in trying to understand the non-linear interactions of the parameters. However, techniques exist that allow automatic, multidimensional optimization of a simulation model, leading to better design with less effort.

It is argued in this paper that computer simulation is well suited to answering very tightly defined design questions. Thus, iterative computer simulations can then be used in the same way the designer uses iterative analysis to provide optimised solutions. All that is needed is a way for a simulation tool to generate a new potential design solution based on the results of a previous analysis.

3- Farzin Haghparast (2004), The Optimisation of Stadium Roof Glazing for Cost and Solar Access Using Built Form Generation based on performance-Optimised Solutions to Tightly Defined Design Problems, The 21st conference on Passive and Low Energy Architecture (PLEA) Eindhoven, The Netherlands

ABSTRACT

Computational simulation is typically used towards the end of the building design process, serving mainly as a design validation tool. In such situations it is applied to well developed design proposals where the majority of the design parameters are known or have been determined by the design team. At conceptual design stage, where even the basic form of the building has not yet been finalised, designers typically rely more upon the guidance of experienced consultants. The sheer number of unknown parameters at this stage are considered to render detailed computational simulation of limited use.

However, with the development of parametric optimisation techniques, there is now significant opportunity for the use of computational simulation during concept design. Whilst the focus of most optimisation research has been on multiple simple numeric design parameters, if these same techniques can be applied with actual building geometry as a parameter, then the potential for form generation based on performance criteria is possible.

Obviously no currently available optimisation method is going to generate a viable building design from a range of performance criteria. However, such a method may be able to generate the optimum site envelope that complies with complex right-to-light restrictions, or the optimum stadium roof shape to maximise solar gains on the playing surface.

The research work presented here has attempted both of these examples. This paper argues that optimised forms based on tightly defined design problems can provide critical information for the designer to integrate into their developing ideas, even at the earliest conceptual stages.

Keywords: problem, optimisation, decision

4- Farzin Haghparast (2004), Built Form Generation Based on Performance-Optimised Solutions to Tightly defined Design Problems, Presented for the Canadian Conference in Building Energy (eSim), British Columbia University, Vancouver, Canada (Unpublished)

ABSTRACT

Whilst simulation is increasingly being used as part of the building design process, its potential as a design aid is usually not fully realised. To improve the potential performance of a design, designers generally guess some starting values for parameters and then conduct a series of iterative simulations until the required criteria are met. This is relatively inefficient and labour intensive. Also, if the number of parameters being varied exceeds two or three, the designer can be overwhelmed in trying to understand any non-linear interactions between them.

Mathematical techniques exist that allow for automatic, multi-dimensional optimisation of simulation models, leading to better design with less effort. However, current optimisation systems operate best with simple numerical parameters. The research work presented here looks at the use of actual building geometry as a parameter, and is therefore investigating the generation, manipulation and optimisation of building form.

It is argued in this paper that optimised forms based on very tightly defined design problems can provide important information for the designer at the earliest stages of the design process. All that is needed is a way for a simulation tool to generate a new potential design solution based on the results of a previous analysis.

5- Farzin Haghparast (2004), Site Obstructions and the Optimisation of Solar Collector Angles, International Conference Energy and security in the Changing World, Tehran, Iran

ABSTRACT

There has been much previous research into the optimisation of solar collector angles, however the full impact of obstructions and complex site overshadowing is rarely considered. In an increasingly built-up urban environment such issues are critical to the effective utilisation of photovoltaics and water/space heating systems at the point of use.

This paper demonstrates a technique for solar collector optimisation that fully accounts for complex overshadowing situations, as well as both dynamic shading systems, such as that due to deciduous vegetation, and complex load-matching requirements in which the optimisation is biased towards a specific range of dates and times. The basis for this technique is presented along with some quantified examples of the increased efficiencies possible.

6- Farzin Haghparast (2005), The Role of Incident Solar Radiation in Performance Analysis and Form Generation in Buildings, Welsh School of Architecture, Second Research Student Conference, Cardiff, UK

ABSTRACT

Solar energy, as the world's most plentiful and permanent source of energy, needs to be considered much more seriously. The fossil fuel crisis and current thinking about sustainability makes the consideration of solar radiation usage as an energy source increasingly important. This paper argues that a consideration of incident solar radiation is not only a useful performance analysis tool but also provides a basis for form generation at all stages of the building design process.

7- Farzin Haghparast (2005), The Spatial Mapping of Incident Solar Radiation, 13th Multi-disciplinary Iranian Researches Conference in Europe, University of Leeds, UK

ABSTRACT

In a dense urban environment, complex overshadowing causes significant variation in the distribution of incident solar radiation (insolation) over the facades of most buildings. However surface treatments, glazing selection and shading designs tend to be uniformly applied. This paper argues that an appropriate consideration of surface insolation can lead to significant economies, especially in complex projects where there is self-shading. A technique is presented for calculating and displaying distributed cumulative insolation over the facades of building models in overshadowed sites. This clearly shows the distribution of solar stresses on each façade at different times of the day and year. Such information can then be used by the designer to more appropriately apply glazing or optimise the use of solar control glass and shading devices in different areas. A number of examples are used to illustrate the application of these techniques and where potential savings in design costs can be made. The paper also shows how these techniques can be used to assess the potential for building-integrated photovoltaics, assist in the landscape planning of outdoor spaces and optimise the location of solar collectors.

